SNOW STORAGE MODELLING IN THE LAKE PUKAKI CATCHMENT, NEW ZEALAND: AN INVESTIGATION OF ENHANCEMENTS TO THE SNOWSIM MODEL

A thesis submitted in partial fulfilment of the requirements for the degree of Master of Science by

TIM KERR

Department of Geography

University of Canterbury

2005

Contents

List of figures

List of tables

List of symbols

a = dry/wet parameter used in melt factor determination

CSC = clear sky coefficient

d = distance between the location of interest and the climate station

E = evapotranspiration

f = melt factor

$f_{\max}$ = maximum melt factor

$f_{max,i}$ = initial maximum melt factor

f_{min} = minimum melt factor

h = difference in elevation between the location of interest and that determined from the climate station elevations

i = time step

j = climate station number

l = precipitation equation constant

L_f = latent heat of fusion, the energy required to melt ice

M = melt water

M_i = snowmelt on day i.

M_{ice} = annual ice melt

M_{lti} = long term annual ice melt

M_s = annual snowmelt

$M_{s,i}$ = melt from shortwave radiation on day i

N = number of snowmelt years

n = number of time steps

n = total number of observations

P = precipitation

P_{mean} = average precipitation

P_r = precipitation falling as rain

P_x = precipitation at a distance x from the western 1200 m contour line

$P_{x,y}$ = precipitation at grid location (x,y)of interest

P_z = precipitation at elevation zone z.

Q = Lake inflows

Q_E = latent heat flux exchange derived from melting, crystallisation, condensation and sublimation

Q_G = conductive heat energy flux exchanged with the surrounding snow pack

Q_H = sensible heat flux exchanged between the snow and the surrounding air

Q_L = long wave radiation energy flux derived from any surrounding body of mass (including the surrounding atmosphere) and/or given off by the snow pack itself

Q_M = energy flux for melt of the snow pack

Q_P = energy flux exchanged between the snow and newly fallen precipitation that is at a different temperature to the snowmelt surface

Q_S = shortwave radiation energy flux derived from the sun and reflected from the snow pack

$Q_{s(max),i}$ = total maximum short wave energy on day *i*

t = time, in days, since the last snowfall

T_i = positive air temperature at time step *i*

$\overline{T}_{15\,\mathrm{min}}$ = 15 minute average temperature

$\overline{T}_{\mathrm{min,max}}$ = average of maximum and minimum temperatures

V_{ci} = computed runoff volume during snowmelt year i

V_{oi} = observed runoff volume during snowmelt year i

x = distance from the western 1200 m contour line

y_c = computed discharge

$\overline{y}_c$ = mean computed discharge

y_o = observed discharge

$\overline{y}_o$ = mean observed discharge

$\overline{y}_{od}$ = mean daily observed discharge for each day of the year derived from the calibration period

z_j = climate station data on day *j*

$z_{x,y}$ = value at location of interest

α = albedo

β = a smoothing constant used in inverse distance weighting

ΔI = long term change in ice storage

ρ = density of water

Acknowledgements

Top of the list of acknowledgement has to be my two sponsors: Meridian Energy Ltd and the Tertiary Education Commission. As well as providing the resources for life, their support added a level of value and worth to the project that helped justify the endeavour. To that end, the regular communication with Rod Feller, my industry mentor of Meridian Energy, and meetings with Associate Professor Ian Owens, my supervisor and academic mentor ensured I had plenty of encouragement and direction in my undertakings.

Through the course of the year a variety of data sources have been dredged at little or no cost to myself and often at considerable expense of effort to the supplier. These include MCo, Meridian Energy, NIWA, Alpine Guides Mt Cook, Landcare and Hawea Cryology Data Archives (a.k.a. Trevor Chinn). At NIWA, Andrew Tait, Roddy Henderson, Ross Woods, Jochen Schmidt and Ian Halstead were particularly helpful with excellent advice and data support.

Brian Anderson and Steven Thompson both deserve a special mention for allowing me to pick their brains (repeatedly) on precipitation distribution.

The majority of time during the year has been spent in front of a computer, which in itself requires a great deal of support for programme updates, data backup and the like. This was delivered with patience, professionalism, and plenty of good humour by the computer genii of the University Of Canterbury Department Of Geography: John Thyne, Paul Bealing, Graham Furniss, and Steve Sykes.

On a more personal front, another year of self absorbed study has been endured by my long suffering partner Clare to whom I am once again indebted.

Abstract

The quantity of seasonal snow stored in the Lake Pukaki catchment, New Zealand has a significant impact on the country's economy through its influence on hydroelectricity generation, tourism, agriculture and conservation. SnowSim is a snow storage model developed for New Zealand conditions that may be used to quantify the catchment's frozen water resource and the melt water derived from that resource. Through implementation on a geographic information system, SnowSim has been applied and optimised to the Lake Pukaki catchment. The optimal parameters found were: temperature-elevation lapse rate of 0.005 $^{o}C\ m^{-1}$, snow/rain temperature threshold of 2.5 ^{o}C, and a melt to temperature relationship factor ranging from 1 to 6 mm $^{o}C^{-1}\ d^{-1}$. The melt to temperature relationship factor is significantly reduced from that previously used for a New Zealand wide application of SnowSim. Use of a daily measured lapse rate was found to provide no improvement to the model, considered to be because of the spatial variability of lapse rates. Inclusion of a radiation component also provided no improvement in the model. This is contrary to the experience found in similar model applications in other regions of the world. The lower relative importance of radiation melt (with regard to total melt) in the region compared to continental locations may explain this result. The use of a new precipitation distribution system did improve model results. Daily precipitation measurements were related to a new annual average precipitation surface prior to interpolating them across the region, without any elevation to precipitation relationship. Model free water results required an offset adjustment to bring them into line with measured lake inflows limiting the application of the model to estimation of seasonal variation, relative magnitudes and event frequencies of snow storage. Over four years of data a model output quality criterion of 0.61 (where a value of 1 is a perfect model) was returned. This increased to 0.76 for monthly values indicating a high quality of output at the seasonal scale. Model parameters and output quality are in line with those found using comparable models for various applications around the world. The variety of outputs available from the model provide a valuable resource for applications in the electricity, tourism, conservation and agriculture industries as well as for climate, glacier, snow and mountain research.

1 Introduction

1.1 Background

The storage of seasonal snow in New Zealand's Lake Pukaki catchment has an impact on a wide variety of arenas: from the landing of a tourist ski plane, to the boiling of a jug many thousands of kilometres away, from the fine woollen fibres of an Italian suit, to the survival of the endangered Black Stilt. Accurate knowledge of the variation in storage of that seasonal snow is important for the management and understanding within each of these fields. This thesis examines the optimisation and modification of a snow storage model, SnowSim, to enable daily snow storage quantity estimations for the Lake Pukaki catchment.
This chapter provides a brief overview of snow storage modelling, followed by a description of the aims and objectives of this research. Finally, an outline of the structure of the thesis itself is given.

1.2 Snow storage modelling

Common snow storage information requirements are melt water runoff, snow covered area and seasonal snow storage volume. These are most accurately determined from direct measurement at a high spatial and temporal scale. Such measurements are seldom available. Modelling of snow storage from limited input data provides a means of estimation of the required information without the need for extensive and expensive data gathering facilities. Numerous snow storage models have been developed around the world (see Table 1) for exactly this reason. The differences between the various models are the required inputs, the generated outputs and the region of applicability. Generally each model is developed to best represent the most important snow storage processes in the region for which they were developed. To enable estimation of snow storage in New Zealand's South Island hydro-electric catchments, a snow storage model called SnowSim has been developed (Fitzharris and Garr 1995). SnowSim enables snow storage estimation based on limited spatial climate data, includes snow accumulation and snow ablation modelling throughout the year, and provides for severe precipitation variation in the area of interest. These factors are not all commonly included in models derived for continental applications.

Table 1. Snow storage model examples, including country of origin, and intended application (adapted from WMO 1986).

Name	*Country of origin*	*Application*	*Required Inputs*
CEQUEAU (Charbonneau et al. 1977)	Canada	Hydropower Flood warning Drought warning	Temperature, precipitation, snowfall, discharge
ERM (Turcan 1981)	Czechoslovakia	Water management Reservoir operation	Temperature, precipitation, discharge
HBV (Bergström 1975)	Sweden	Flood warning Hydropower	Temperature, precipitation, evapotranspiration, discharge
IHDM (Calver 1988)	UK	Land use and climate change effect investigation Ungauged catchment prediction	
NAM-II (Gotleib 1980)	Denmark	Flood warning Water supply Hydropower	Temperature, precipitation, discharge
NWSRFS (Burnash et al. 1973)	USA	Flood warning Water supply Low flow warning Water management	Temperature, precipitation, discharge
PRMS (Leavesley et al. 1983)	USA	Flood control Irrigation Water supply Prediction of effects of land use	Temperature, precipitation, solar radiation
SnowSim (Fitzharris and Garr 1995)	New Zealand	Hydropower	Temperature, precipitation
SRM (Martinec 1975)	Switzerland	Hydropower Irrigation Water supply Reservoir operation	Temperature, precipitation, snow cover, discharge
SSARR (Anderson 1973)	USA	River system multi-use operation	Temperature, precipitation, discharge
Tank (Sugawara 1979)	Japan	River system multi-use operation	Temperature, evapotranspiration, precipitation, discharge
UBC (Quick and Pipes 1976)	Canada	Reservoir operation Flood warning	Temperature, precipitation, discharge

1.3 Aims and objectives

With improved technology, longer data records, and continued related research, it is of value to review SnowSim to assess whether changes to the model may enable improved output. It is not uncommon for model complexity to be limited by the time required to undertake calculations, and/or by storage requirements for recording information. As computer speeds and memory storage increase, the level of model complexity may also increase with no loss in processing time or cost. Utilising this extra available computing power may enable improved model output accuracy. Geographic Information Systems (GIS) provide a powerful computer application base for undertaking spatial modelling. Designed specifically for use on spatial data sets with common spatial manipulation procedures inherent in the application platform, GIS allow for data calculations and visualisation without in depth programming knowledge. Calibration of the model may be improved using recently obtained high altitude climate and snow measurements. A historic lack of climate records in New Zealand's mountainous regions has to some extent been alleviated in the Mt Cook region through the installation of five new climate stations over the last ten years. The new data available from these sites may enable improved estimation of climate variables throughout the region. Snowmelt modelling around the world has continued to develop since SnowSim originated. While this research has generally been carried out in continental regions, some of the results may be able to be applied to SnowSim to provide further improved model accuracy.

The aim of this thesis is to review SnowSim in light of recent research, high altitude climate and snow measurements and GIS technology to establish whether improved results may be derived for the Lake Pukaki catchment.

1.4 Thesis structure

The following chapter outlines the Lake Pukaki catchment; its location, history, and the importance to New Zealand of snowmelt in the catchment. Chapter three, "Previous work", outlines snowmelt modelling methods and provides a discussion of the history of snowmelt measurements in New Zealand and the Lake Pukaki catchment in particular. A detailed description of SnowSim is then provided. "SnowSim modification and verification methods", the fourth chapter, provides details of the methods used to investigate SnowSim modifications, presents what modifications are to be trialled, and sets out how the results of those modifications are analysed. Results of optimising SnowSim to both a point site and the entire catchment are provided in the fifth chapter together with an analysis of how each parameter affects the model outputs. This provides a detailed insight into the strengths and

weaknesses of the model. The sixth chapter presents the results of the trialled modifications. Further sensitivity analysis of new parameters required as part of the modifications is described here as well. In the seventh chapter, the performance of SnowSim at the point and catchment scale is discussed with presentation of the results of applying the best performing model to several years of data. The final “Conclusion” chapter summarises the findings of the research and discusses the limitations, applications and potential future developments of the model.

2 The Lake Pukaki catchment

2.1 Introduction

The Lake Pukaki catchment is important to New Zealand for its contribution to the country's electricity supply, tourism and agricultural production. The large seasonal fluctuation in snow and snowmelt in the catchment has a serious impact on all of these industries. Improved knowledge of the snow storage and snowmelt quantities in the catchment will enable improved management of these industries, ensuring more efficient operations and maximising returns. Successful snow storage modelling helps increase understanding of snow processes and glaciation as well as enabling investigation into climate – snow storage linkages. With increasing interest in global climate change, these fields of research are becoming of greater importance in the scientific arena.

This chapter describes the Lake Pukaki catchment and the impact of snow and snowmelt upon the use of the catchment. The location, climate, geology, flora and fauna will all be described in turn, with discussion of their interaction with snow storage. The human use of the region both historic and current is then reviewed. Detail is given to the agricultural, tourist and hydro-electric generation use of the catchment.

2.2 Location

The Lake Pukaki Catchment is situated in the west of Canterbury, South Island, New Zealand at 170°10' E, 43°48' S (Figure 1). The axis of the catchment runs roughly north-south with the north-western boundary on the Main Divide of the Southern Alps and the southern edge in the Mackenzie Basin. The catchment area is 1359 km^2 with a length of 79 km and a width of 22 km. The elevation of the catchment averages 1260 m, ranging from the lake level at 524 m up to 3754 m, the height of Aoraki/Mt Cook, the highest peak in New Zealand.

The upper catchment contains 133 glaciers, including the Tasman, Murchison, Mueller and Hooker glaciers, New Zealand's 1st, 2nd, 6th, 7th largest glaciers respectively (Chinn 2001). Lake Pukaki itself covers an area of 168 km^2 (one eighth of the catchment area) and has a maximum depth of 99 m close to its south western shore. It was originally formed behind a terminal moraine (Wallace 2001) and has twice been raised, (1952 and 1976) for flood control and improved storage for hydro electric generation (Sheridan 1995).

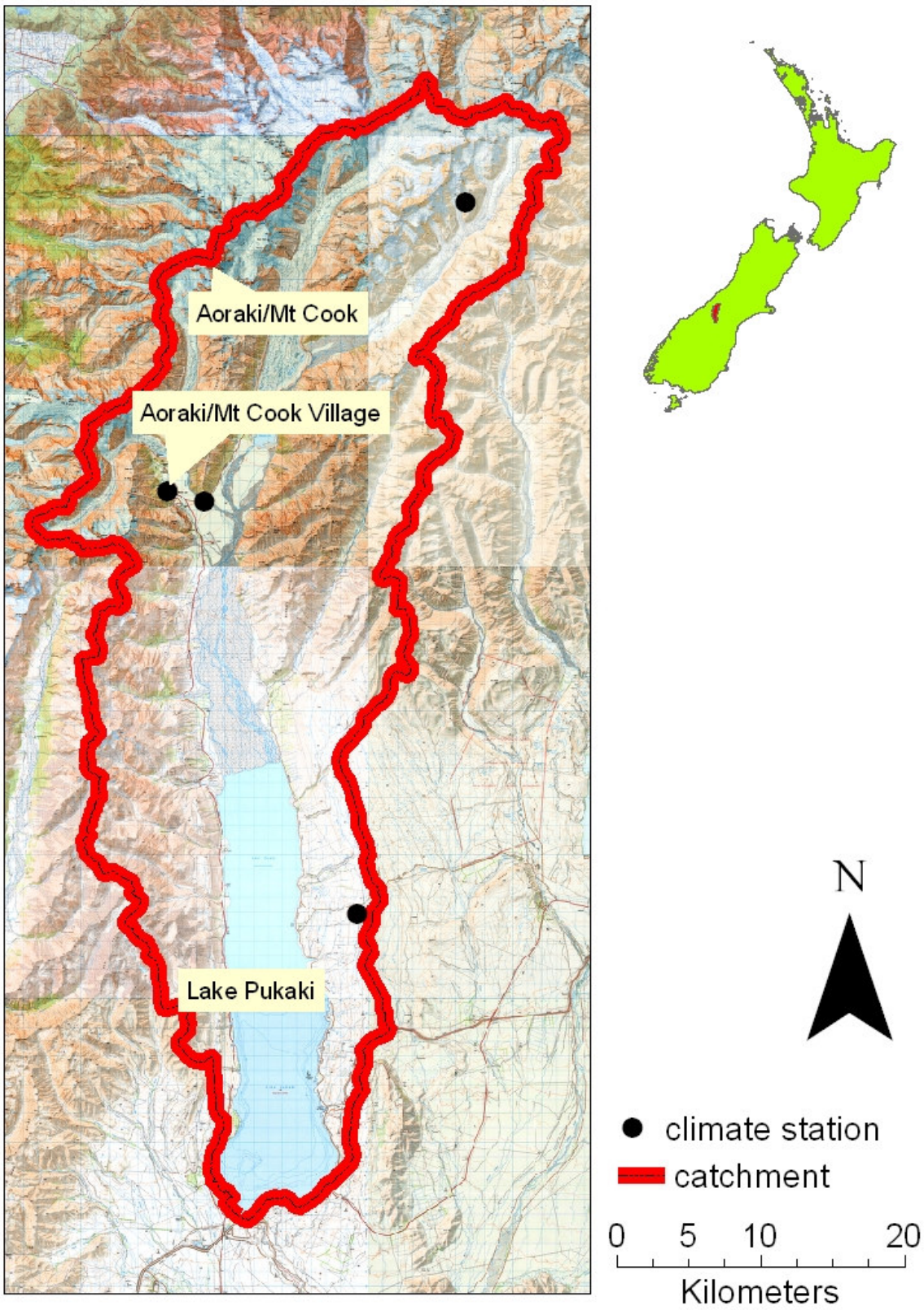

Figure 1. Lake Pukaki catchment location.

2.3 Climate

The climate of the catchment is primarily influenced by its position adjacent and east of the main divide of the Southern Alps, which themselves lie astride the Southern Hemisphere westerly wind belt in a maritime setting. High precipitation approaching 10 m per year water equivalent (Henderson and Thompson 1999) created by spill over from the west dominates the north and western catchment with a reduction in precipitation away from the divide. In contrast, the south and eastern regions of the catchment are characterised by high sunshine hours, and low rainfall (Ryan 1987) with just 860 mm of rain falling on average per year at Guide Hill on the eastern side of Lake Pukaki (Tomlinson and Sanson 1994).Temperatures vary throughout the catchment according to altitude, with the mountain tops remaining below zero degrees Celsius for the majority of the year. Seasonal variation occurs throughout the catchment, though it is more pronounced in the lower eastern portion of the catchment. Snow can fall in the catchment at any time of the year but accumulation of snow from one storm to another is more common in the winter months from April until October. This climate has resulted in seasonal snow and perennial ice being important components of the catchment's environment. With the difficulty of measuring precipitation in the mountainous regions, modelling is required to enable estimation of daily and seasonal variations in snow and rainfall throughout the catchment.

2.4 Geomorphology

The dominant rock type within the catchment is Torlesse greywacke with overlying post-glacial alluvium (Suggate 1978). This arrangement is a result of two major processes, uplift and erosion. The uplift is from the Pacific tectonic plate moving up against the Australian plate at the Alpine Fault just 20 km west of the catchment. The uplift is estimated at 10-20 mm per year (Coates 2002). Erosion transforms the uplifted greywacke into alluvium and spreads it across the lower catchment through primarily fluvial processes and rock avalanching (Whitehouse 1988). Glaciation's role in erosion has resulted in distinctive landforms throughout the catchment. The southern end of the lake is dammed by a terminal moraine originating from the Tekapo glacial advance with terminal moraines from two earlier advances directly behind indicating the Lake has been in its current position for some time. The lower eastern boundary of the catchment is formed by a medial moraine from when the Tasman and Tekapo glaciers combined into a single lobe during the major Balmoral advance (Wallace 2001). Recessional moraines are evident on the eastern side of the Tasman River, whilst numerous trim lines can be seen on valley walls throughout the catchment. The

currently existing 133 glaciers (Chinn 2001) continue to erode the underlying rock forming characteristic arêtes, horns and cirques. The related over steepened slopes result in extensive rock fall and formation of large talus slopes with rivers and glaciers transporting debris to lower regions (Whitehouse 1988). This in turn produces the classic glacial outwash plains of the Tasman, Hooker and Murchison river flats. The major impact of glaciation within the catchment deems it prudent to have a full understanding its glacial systems, both to improve understanding as to how the catchment has been shaped, and to predict future glacial effects. The accurate modelling of snow processes is fundamental to understand this glaciation as it is the positive balance of snow accumulation against snowmelt that is the first step in forming glacial ice (Paterson 1994).

2.5 Flora and fauna

The flora and fauna of the Lake Pukaki catchment may be divided into four broad zones based on land cover types (DLS 1986):

1. Alpine
2. Forest
3. Tussock/grasslands
4. River/wetland

The areas of these land cover types are shown in Figure 2. The Alpine and Tussock/grassland zones are by far the largest of the zones, being 38% and 37% of catchment area respectively, followed by the River/wetland zone (18%) and just 7% in the Forest zone.

The highest of these, the Alpine zone, has large tracts of non-vegetated cover, herb fields, short tussock land, and sub alpine scrub. Thar, Chamois, Kea and Rock Wren frequent these zones, though arguably the Rock Wren is the only true alpine inhabitant, living under the snow in rock crevices through winter (Moon 1992).

Though much smaller than the alpine regions, the Forest zone is important as a habitat for a variety of native forest birds like the Grey Warbler (Riroriro) and Kereru (Wood Pigeon). Wilding pines and forest plantations in the farmed areas are becoming an increasingly large component of the Forest zone, though the fauna is less prolific in these habitats.

The Tussock/grassland zone, which includes scrub covered regions as well as the tussock and grassed farmland, forms the significant portion of the agricultural regions. Sheep and rabbits are the dominant animals in this zone. Invertebrates, such as grasshoppers, moths, and flies though found throughout the catchment, are particularly common in the Tussock/grassland zone.

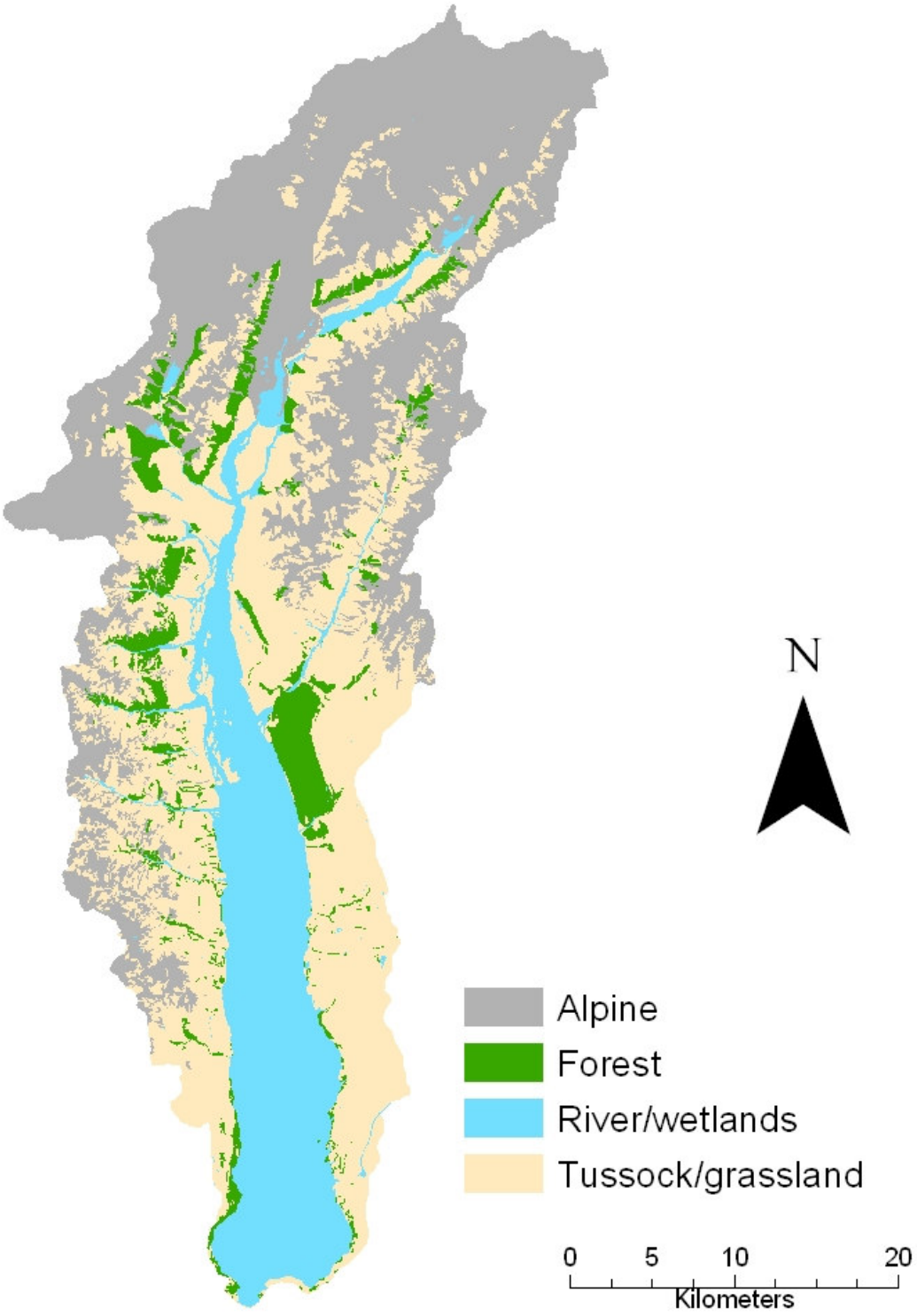

Figure 2. Major land cover types of the Lake Pukaki catchment (data derived from the Land Cover Database Version 2 of the Ministry of Environment).

The remaining River/wetland zone is colonised by rapidly spreading and growing species of vegetation such as Lupin, Willow and Foxglove, the first to take hold after frequent flooding events. These areas are important ecologically to the myriad of birds that make this zone their home including the rare Black Stilt and Wrybilled Plover. Decline in some species in similar areas throughout the South Island has been attributed to increased hydro-electric and irrigation development (Heather and Robertson 1996). Within the water bodies themselves the glacial flour renders the larger rivers and Lake Pukaki itself low in life though the non glacial and spring fed tributaries thrive with life.

For each of these zones, snow cover and snowmelt has a different but important impact. A long season of snow cover in the Alpine zone ensures a short growing season for the hardy plants that have endured the winter. The forest covered regions are limited to areas that can obtain enough moisture for growth, yet are not in flood nor avalanche zones, nor too cold to prevent growth. The large Tussock/grassland areas require moisture input during the warmer growing months. This is provided by the melting of the seasonal snow pack which ensures a continual release of water, rather than a flood/drought scenario that occurs when rainfall is the only moisture provider. The River/wetland zone contains unstable river channels caused by high sediment loading and high flow variations, in turn derived from the glacial and snowmelt processes occurring up stream. In return the flora within each zone has an impact on the snow itself. For example, in the alpine zone, the vegetative cover has little impact on snow transport and melt processes whereas within the bush covered zone the opposite is true (Swanson 1970).

2.6 Land use

Maori tradition credits the creation of Lake Pukaki to Rakaihautu, rangatira of the Uruao waka which brought the Waitaha people to the South Island (Reed and Calman 2004), probably in the 13th century (King 2003). As shown by a Moa butchering site on the eastern shore of Lake Pukaki (McKinnon 1997) it is likely that Moa hunting in the Lake Pukaki district occurred from about this time until their eventual extinction. The arrival of the Waitaha resulted in an increased frequency of bush fires leading to a transformation of the flora (and the accompanying fauna) in the catchment from a fern-scrub land to extensive tussock lands (McKinnon 1997). Ngai Tahu migrated south in the 18th century from the east coast of the North Island and through war and intermarriage became the dominant people of the South and Stewart Islands (McKinnon 1997) though it is likely that the Lake Pukaki region would have been visited only seasonally for food gathering. The Lake Pukaki

catchment was sold by Ngai Tahu to the British government in 1848 as part of the major South Island "Kemp" purchase. However the inclusion of the Lake Pukaki catchment in the purchase is a point of contention (Watangi Tribunal 1991). Despite the land having changed ownership for all practical purposes to the European settlers in 1848, the European "discovery" of the catchment is often attributed to James Mackenzie seven years later. Mackenzie used the area to move flocks of stolen sheep from Canterbury to Otago (Marr 2001). Shortly after Mackenzie's arrest the area up to the head of the lake was surveyed (Von Haast 1948) and pastoral leases were taken up for sheep farming (Sheridan 1995). This signalled the beginning of a permanent population in the area. Widespread ecological changes soon followed with the influx of European flora and fauna and the accompanying farm management practices, one of which was even more frequent burn offs.

Following the discovery of gold in Otago, the Canterbury Provincial government offered a reward for the discovery of a Canterbury gold field. Subsequently the provincial geologist, Sir Julius von Haast, accompanied by Sir Arthur Dudley Dobson made a geological inspection of the Mt Cook region in 1862. No gold (the mineral of primary interest) was found, but he did report the outstanding scenic qualities and vast glaciated terrain of the region (Von Haast 1948). In 1873 the New Zealand Governor, Sir George Bowen visited the Mt Cook area. This visit was publicised by newspapers and can be thought of as the origins of tourism to the area. The Mt Cook area was made a reserve by the government in 1885. Soon a coach service and accommodation was being provided at the location of the current Mt Cook village specifically for tourism. By 1921 Harry Wigley and his Mount Cook Company had taken over the Hermitage (the tourist accommodation). The company proceeded to expand its operations, taking full control of the reserve, recreation, accommodation and transport in the area (Wigley 1979). By 1942 when the company relinquished its lease back to the government, the Mt Cook area had become a holiday resort of international standing (Pawson 2001).

Today Aoraki/Mt Cook National Park contains the upper third of the catchment. This park was gazetted in 1953 (DLS 1986) with the majority of the remainder of the catchment being farmed as sheep or sheep and beef stations.

2.6.1 Tourism and recreation

The Aoraki/Mt Cook National Park at the head of the catchment is used extensively for tourism and recreation. Climbing, skiing, hiking and sight seeing are some of the activities regularly enjoyed within the park. Aoraki/Mt Cook Village situated near the junction of the Mueller and Hooker valleys caters for the tourist market with accommodation, restaurant,

information and guiding services. A small support community for these services also exists at the village which includes staff accommodation and a primary school.
Outside the park two airstrips cater for scenic flights and mountain access. Ski equipped fixed wing aeroplanes and helicopters operate from both these airstrips. Domestic flights from around the country arrive and depart at the larger Mt Cook airstrip, situated at the junction between the Tasman and Hooker valleys. The second air strip is situated further south as part of a tourist complex that includes accommodation and restaurant facilities. Walking tracks exist in the vicinity of the Aoraki/Mt Cook Village. These provide access to the Hooker Valley, the Tasman Valley, the Sealy Range and Mt Sebastapol.
One private and sixteen public mountain huts are scattered around the National Park. These are used by climbers, trampers and skiers throughout the year for accommodation and shelter.
The scenic qualities of the park can be attributed to the steepness of the terrain, and the associated glaciation which in turn is reliant on a positive seasonal snow balance. Many of the activities in the park are directly dependent on snow accumulation. Ski landings of aeroplanes on the Tasman Glacier, a major tourist draw card, and something of a New Zealand tourism icon, relies on a smooth crevasse free landing site being available. Low snow years can restrict the landing sites of these planes. The skiing and climbing is also directly reliant on snow accumulation or melt. Skiers require good snow cover without dangerous avalanche conditions, whereas climbers may require high snowfalls to keep crevasses well bridged, or alternatively, low snow to keep rock climbs snow free. Regular avalanche and snow condition information is provided by the park authorities to enable safe recreation in the park.
Modelling of snow cover and snowmelt enables regular assessment of snow conditions, valuable for avalanche forecasting, recreational planning, and operational management of tourist activities.

2.6.2 Farming

The tussock lands of the catchment are now farmed as part of 15 stations, a mix of leasehold and freehold properties (Sheridan 1995). Most of the stations are dedicated to production of fine merino wool which is of international quality and used in manufacture of quality Italian suits among other things (Carter and MacGibbon 2003). Cattle and deer are also run on the stations, and some forestry and general agriculture occurs.
The seasonal variation of snow cover has a large impact on farm management in the region. Stock must be kept in regions where heavy snowfalls will not affect them, while snowmelt is crucial to ensure grass growth for stock feed. Every few winters a severe snow storm causes severe stock losses, though the losses have reduced with the advent of improved weather

forecasting. Floods also occasionally cause havoc, especially during combined rainfall and snowmelt periods. Improved snowmelt modelling would assist with flood forecasting to help reduce their impacts. The use of irrigation has the potential to greatly improve production in the relatively dry regions of the Mackenzie country. Lake Pukaki is the obvious source of the required water. This provides further impetus to manage the Lake in as efficient manner as possible. Snowmelt modelling can enhance knowledge of melt water volumes and occurrences to enable this improved lake management.

2.6.3 Hydroelectricity

Lake Pukaki was incorporated into the Upper Waitaki Power Scheme between 1970 and 1977. A canal feeds water from Lake Tekapo into Lake Pukaki via the Tekapo A and B power stations. The Tekapo B power station is on Lake Pukaki's eastern shore. A control gate at the southern end of the lake then feeds the outflow into another canal. This canal is joined by one from Lake Ohau before passing through the Ohau A, B and C power stations and so feeding Lake Benmore. Lake Benmore is the first of three Lakes constituting the Lower Waitaki power scheme.

To enhance the controllable storage capacity of Lake Pukaki it was raised by 37 m during the power scheme construction. This has enabled 14 m of the lake water height to be controllable (Martin 1998). As a result Lake Pukaki became the largest single controllable storage reservoir for New Zealand's hydro-electric generation (see Figure 3).

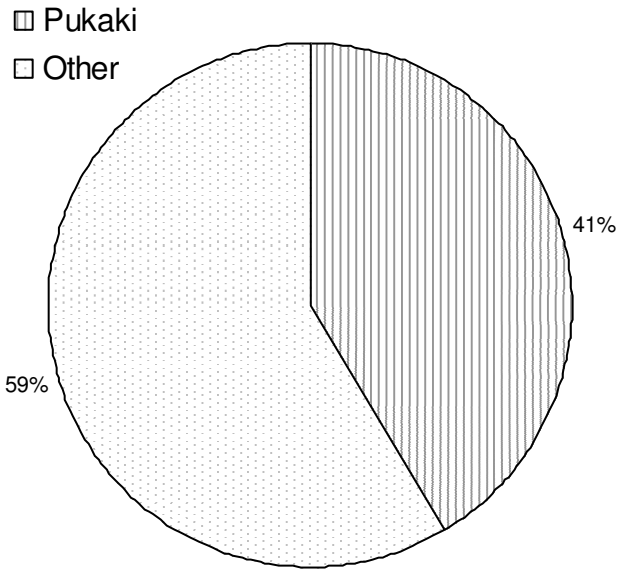

Figure 3. 1999 – 2002 average contribution of Lake Pukaki to national controllable hydro-electric energy storage (data: M-Co).

The inflow to Lake Pukaki is strongly seasonal because of the impact of snow accumulation and melt in the upper catchment. Whenever the lake is overfull and water is required to be released down the flood channels without going through the power scheme's canals, a loss of potential income occurs. At the other end of the scale, whenever electricity cannot be generated because of low lake levels, the higher cost of alternative electricity generation (as well as increased pricing from market pressures) results in a nation wide economic impact and a loss of consumer confidence in electricity. Improved knowledge of snow storage variation enables more efficient lake management, therefore reducing the risk of these high and low lake level scenarios.

3 Previous work

3.1 Introduction

This chapter reviews snow storage modelling, that is, the estimation of change in snow quantity on the ground from accumulation and ablation processes. The spectrum of modelling systems is described from empirically through to physically derived methods. The lumped and distributed options of model application are then reviewed. The benefits and limitations of each approach are discussed with particular reference to application to the Lake Pukaki catchment. This is followed by a review of snowmelt research in New Zealand with special reference to the development and application of SnowSim, an empirical distributed model.

3.2 Overview

Snow storage modelling can be divided into two broad categories, empirical and physical. In reality these categories are at either end of a spectrum so that most models have contributions from both approaches. An empirical model utilises statistical relationships between inputs and outputs. A physically based model describes the physical processes that relate inputs to outputs. In turn, these models can be applied in a lumped or distributed mode. A lumped model describes catchment processes with single "catchment average" values. A distributed model divides a catchment into sections and carries out model calculations for each section. A lumped model can be considered a single section distributed model, or equally, a distributed model can be considered a series of small lumped models. The two more common ways of sub dividing an area of interest for snowmelt modelling is into elevation zones, or into grid squares. This broad model classification system is outlined in Figure 4.

3.2.1 Empirically based models

It is not infrequent to find a relationship exists between a required model output and an available model input, even though the reason for the relationship is complex or not well understood. For instance, the amount of snowmelt that occurs on any one day may be related to the day number of the year. It is not the date that affects snowmelt, but the relationship between date and available melt energy (among other things), which is a result of years being arranged to encompass a complete cycle of seasons. It is not necessary to understand the underlying reason for the input-output linkage for the relationship to be useful in a model. Admittedly though, a basic understanding may be of assistance in anticipating situations where the relationship may not hold. For instance, if a 200 day year was used as the basis for

a date system, the relationship between date and snowmelt would no longer hold, as the date from year to year would not correspond to similar climatic conditions.

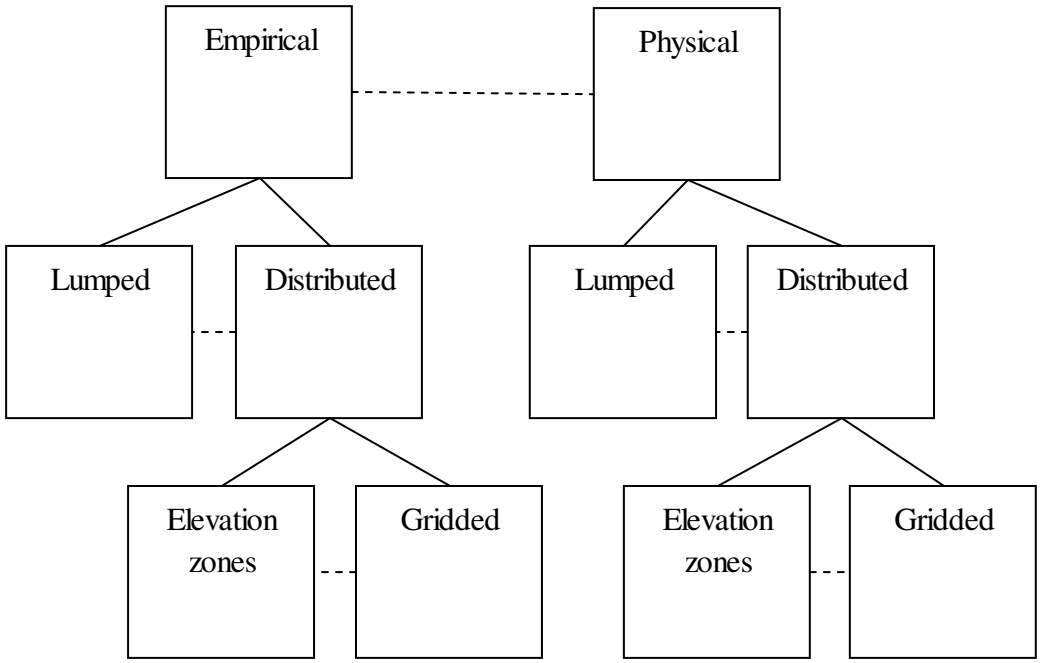

Figure 4. Model classification categories.

Empirical snow accumulation models commonly utilise measurements from precipitation gauges as an index. The assumption is that snow accumulation across a region is proportional to the amount of precipitation that is measured at one or more locations. This requires the relative components of snow storage to remain constant both spatially and temporally. Re-freezing of liquid water, avalanches, slush flows, snow drift and glacial flow are all snow accumulation factors not accounted for by precipitation measurements. These factors all vary in space and time, for instance snow drift is dependent on wind direction and strength which in turn is strongly dependent on terrain (spatial variation) and synoptic condition (temporal variation). Utilising an appropriate modelling period and area of interest that are both sufficiently large is necessary to ensure the variations of the non-precipitation accumulation factors average out to an acceptable level. Precipitation measurements are usually derived from rain gauges but may also be snow measurement devices e.g. ultrasound sensors, snow pillows, weighing bucket rain gauges and snow course depth and density measurements. Each system of precipitation gauging has limitations. Rain gauges may return low measurements during windy conditions. Non heated rain gauges can fail during freezing temperatures or be over capped during snowfalls. Snow depth measurement devices do not capture rainfall events, whilst a snow pillow will only record rainfall if no resultant runoff occurs. When used

as an index, these measurement errors are effectively extrapolated across the region of interest highlighting the reliance of empirical models on the quality and integrity of input data.
Perhaps the most common empirical snowmelt model is a temperature-index system. This relates snowmelt to air temperature. The higher the temperature is above zero, the greater the melt. While this is a good approximation, in reality the relationship has been found to vary with season, altitude (Kirkbride 1995) location (Hock 2003), and synoptic condition (Neale 1996; Cutler 2002). Table 2 shows the range of temperature-index factors found by various authors. Despite these limitations, the temperature-index system is used extensively as the basis of snowmelt models throughout the world (WMO 1986). A temperature-index model considers temperature at a regular time scale and apportions snowmelt accordingly. The general form of a temperature-index calculation is commonly written as:

$$\sum_{i=1}^{n} M = f \sum_{i=1}^{n} T_i \qquad \textbf{(1)}$$

Where
M = melt water
f = a melt factor
T_i = positive air temperature at time step i
n = number of time steps

A temperature-index model is most accurate when the relative importance of the various melt factors remain constant (Lang and Braun 1988). The larger the time step and the greater the area involved, the closer this assumption is to reality. As a compromise between model accuracy and output usefulness, temperature-index models are frequently operated at a daily level and referred to as degree-day models. At a daily level, a temperature-index model will not accurately account for variations in season, and synoptic condition, both of which, through various mechanisms, affect the relative importance of the melt energy components. For this reason temperature-index models often include secondary indices (time of year being a common one) to account for these changes.
Spatially, variations in melt energy resulting from different topography, latitude, meteorology or elevation are not well represented by the degree-day system. For this reason temperature-index models need to be tuned to the application area of interest to enable optimum results. This can be seen by the wide variety of degree-day factors for different regions of the world and even for different areas within New Zealand as shown in Table 2. Despite these shortcomings, temperature-index models can enable simple implementation and have a low

input data requirement. The size of the Lake Pukaki catchment and the limited number of climate stations that exist in the area render the temperature-index approach suitable for modelling of the general snowmelt situation in the catchment.

A second empirical relationship that is frequently used as part of snow storage models is that between snowmelt runoff and the depletion of snow covered area. The snowmelt runoff model (SRM)(Seidel and Martinec 2004) combines this approach with a temperature-index system. This model has been used extensively throughout the world with success (e.g. Baumgartner et al. 2000; Qobilov et al. 2000; Gómez-Landsea and Rango 2002). The snow covered area parameter is frequently derived from remote sensing products enabling successful operation in remote regions with few (if any) climate stations. This is the model's major advantage. The disadvantages are that snow covered area measurement are not always available, and that a clear consistent relationship between snow covered area depletion and catchment discharge does not always exist. In the Lake Pukaki catchment, where cloud cover is frequent in the mountainous snow covered regions, obtaining snow covered area estimates is very difficult (Fitzharris and McAlevey 1999). In New Zealand's mountains, the snow line created during storm cycles is usually above the mountain's base. This results in a stepped relationship between snow storage and elevation which is not seasonally consistent. Snow covered area is thus not sufficient to assess snow water equivalent quantities in these regions (Fitzharris 1978). Use of the SRM model within the Lake Pukaki catchment was trialled by Bowden (1994) with poor results, considered to be partly because of the poor snow covered area estimation and poor precipitation distribution estimation.

Both these empirical models are primarily concerned with snowmelt. While the SRM can estimate snow accumulation from increased snow covered area, it is runoff from snow area depletion that is the primary output. Likewise, temperature-index models estimate melt, not accumulation. It is not uncommon for snow storage models to use peak snow water equivalent measurements to initialise the model avoiding the need to model precipitation through the accumulation period (e.g. Hock 1999; Pellicciotti 2004), the assumption being that snow accumulation during the snowmelt season is negligible. This may be a fair assumption in many regions of the world, but in high alpine regions of New Zealand, snowfall can occur at any time of year and snow pack measurements (for finding peak values) are very rare. As a result both accumulation and ablation processes need to be modelled.

Table 2. Parameters found for various models.

Application	*Citation*	*Area*	*Temp.-index-factor (mm $^{o}C^{-1}$ d^{-1})*	*Snow/rain temp. threshold (^{o}C)*	*Lapse rate (^{o}C m^{-1})*
Snowline	(Barringer 1989)	Remarkables, New Zealand	2.9, 3.6	0 – 0.9	variable
Snow storage	(Moore and Owens 1984b)	Ski Basin, New Zealand	4, 6, 8		0.0065
Glacial ablation	(Kirkbride 1995)	Tasman Glacier, New Zealand	1.8 – 7.4		0.006
Glacier mass balance	(Anderson 2004)	Franz Josef Glacier, New Zealand	7.1 (ice) 4.5 (snow)	1	0.005
Snow storage	(Fitzharris and Garr 1995)	Hydro-electric "macro" catchment, New Zealand	3 - 8	2.5	0.007
Snow storage	(McAlevey 1998)	New Zealand	3 - 12	2.5	0.007
Snowmelt runoff	(Martinec and Rango 1986)	Various	3.5 - 6	0.75 – 3	0.0065
Snow storage	(Anderton 1974)	Lake Pukaki catchment, New Zealand		2.25	0.0075
Snow measurement analysis	(Archer 1970)	Ben Ohau mountains, New Zealand	1.08, 1.15*		
Snow/ice melt	(Payer et al. 2003)	Luggye, Bhutan	6 – 8		0.004 – 0.0045
Snow/ice melt	(Pellicciotti 2004)	Haut Glacier d'Arolla, Switzerland	0.05#		variable
Snowmelt	(Cazorzi and Dalla-Fontana 1996)	Dolomites, Italy	1 – 8	0.5	variable
Snow/ice melt	(Hock 1999)	Storglaciären, Sweden	4.4 (snow) 6.3 (ice)		0.0055

*Maximum daily temperatures were used by Archer for the degree-day factor estimation.

#Model included a radiation parameterization not accounted for by the temperature-index factor.

3.2.2 Physically based models

Describing the particular snow storage processes is the basis of physical modelling. Ideally a full consideration of precipitation, snow distribution, metamorphism, and melt processes is undertaken. This requires knowledge of all aspects of the atmosphere, the snow pack - atmosphere interface, as well as the snow pack itself. This may include (but is not limited to): humidity, air stability, wind, topography, air temperature, air pressure, precipitation, snow pack structure, solar radiation, air transmissivity, cloud cover, cloud type, surface roughness, surface albedo and the interactions of all of these variables with each other. Consideration of all of these factors is a formidable task, so it is common to select a subset that describes the majority of snow storage influences, and even then to only consider general snow accumulation and snowmelt, not mass movement.

For estimation of snow accumulation, physically based models need to consider precipitation, re-freezing of liquid water, avalanches, slush flows, snow drift, glacial movement and the spatial distribution of all these factors. While modelling of complete snow accumulation processes is uncommon, various models exist that account for some of the more important processes. Arguably the most common type of snow accumulation model is the numerical weather model used for weather forecasting and climate prediction. Primarily concerned with atmospheric processes these models have been increasingly integrated with land surface models to provide land-atmosphere linkage modelling. An example of this is the RAMS model which includes the SSNOWD model that keeps account of snow accumulation from the atmospheric processes from one day to the next (Cotton et al. 2003). As computing speeds and storage evolve, so too does the complexity of the models. With the importance of albedo on climate, especially in northern latitudes, it is likely that accurate snow accumulation modelling will become increasingly a focus of development with these models. For instance, in reviewing CLASS, another land surface model, Pomeroy et al. (1998) considered snow interception by tree canopies, wind drifting and sublimation to be important processes in need of inclusion to improve the snow accumulation modelling. At a different scale, in New Zealand the important influence of topography on precipitation has been modelled by Sinclair (1994) through consideration of vertical velocity of air, condensation level, humidity and topography.

The other side of the snow modelling coin from snow accumulation and movement is snowmelt. A common approach to physically based snowmelt modelling is to divide the

energy flux used in snowmelt into its various components as outlined in the generalised energy balance equation:

$$Q_M = \pm Q_L \pm Q_S \pm Q_H \pm Q_E \pm Q_G \pm Q_P \quad \textbf{(2)}$$

Where

Q_M = energy flux for melt of the snow pack

Q_L = long wave radiation energy flux derived from any surrounding body of mass (including the surrounding atmosphere) and/or given off by the snow pack itself

Q_S = shortwave radiation energy flux derived from the sun and reflected from the snow pack

Q_E = latent heat flux exchange derived from melting, crystallisation, condensation and sublimation

Q_H = sensible heat flux exchanged between the snow and the surrounding air

Q_G = conductive heat energy flux exchanged with the surrounding snow pack

Q_P = energy flux exchanged between the snow and newly fallen precipitation that is at a different temperature to the snowmelt surface

All these values can be positive or negative depending on whether they provide a net increase or decrease in the energy available for melting.

The energy available for melt can then be simply converted to snow water equivalent through consideration of the latent heat of fusion and density of ice as described by:

$$M = \frac{1000\, Q_M}{\rho L_f} \quad \textbf{(3)}$$

Where

M = melt water (mm)

Q_M = melt energy flux (J m^{-2})

ρ = density of water (1000 kg m^{-3})

L_f = latent heat of fusion of ice (0.335 MJ kg^{-1})

Each of the energy balance components can be calculated with varying levels of complexity. Application of the energy balance to assess snowmelt has been applied successfully to point sites where well instrumented climate stations are located that gather all the required data (e.g. Braithwaite 1990; Ishikawa et al. 1992; Kelliher et al. 1996; Neale 1996; Bintanja and Reijmer 2001; Cutler 2002; Oerlemans and Klok 2002) as well as part of distributed models for catchment processes (e.g. Baker et al. 1982; Hogg 1982; Hay and Fizharris 1988; Arnold

et al. 1996; Hock and Noetzli 1997; Brock et al. 2000b; Wagnon et al. 2001). The two main disadvantages to this approach are the variety of measurements required to complete the balance equation, and the difficulty in relating point site measurements of some of these parameters to different locations, particularly wind, roughness length and humidity. In the Southern Alps, New Zealand, wind and humidity appear to play an important part in snowmelt as part of sensible and latent energy fluxes (Moore and Owens 1984a; Neale and Fitzharris 1997) yet measurement of these parameters is limited and with mountainous terrain having a large effect on these parameters, it is difficult to assess how measured values relate to catchment wide values. The Hooker River catchment within the Lake Pukaki catchment has been modelled by Islam (2001) utilising a "modified UBC" physically based lumped model and meteorological measurements from the Mt Cook Village climate station. By comparing modelled stream flow to measured stream flow the relationship between climate station measurements and catchment zone averages were found. While the results were promising, precipitation distribution estimation was once again considered a shortcoming. This may be following from the model having been derived for operation in a Western Canadian region with quite a different precipitation regime, at least in terms of magnitude.

The physically based approach generally is more accurate than empirical models, especially at short time scales (sub – daily) and near well instrumented sites. During non-average climatic conditions, a physically based model captures the anomalies, whereas an empirical model often will not.

3.2.3 Lumped or distributed models

Lumped models carry out one set of model calculations per area of interest. The model parameters are scaled in such a way as to be representative of the area of interest as a whole. Distributed models carry out model calculations for subsections of the area of interest. A common method of dividing an area of interest is into elevation zones, or into grid squares. Determining appropriate parameter values for each subsection requires estimation of a parameter's distribution. Temperature, vapour pressure and precipitation are commonly distributed by relating their values to elevation. See Table 2 for a list of temperature lapse rates used by various temperature-index models. Estimation of spatial variation of radiation parameters can be achieved through knowledge of topography and time of application together with surface albedo. The complexity in modelling the spatial variation of wind fields in alpine terrain renders inclusion of physically based turbulent exchange melt fluxes problematic (Marsh 1999) though this may be resolved by using multiple climate recorders, each representative of a subsection. While temperature-index models have improved results

with larger areas-of-interest, using distributed processing can enable inclusion of spatially variable effects because of relatively well understood temperature distribution. The use of a distributed application effectively moves the problem of estimating basin characteristic parameters, to that of estimating accurate parameter distribution systems.

3.2.4 Hybrid models

One component of the physically based approach which requires little data input is global radiation. This can be derived from consideration of topography and time. No on-site instrumentation is required. For this reason, this variable has been included as an enhancement to traditional degree-day models and has resulted in improved modelled to measured relationships (e.g. Kustas and Rango 1994; Cazorzi and Dalla-Fontana 1996; Hock 1999). A common approach is to use a radiation calculation as an index for the daily and seasonal variation in the melt-temperature relationship. While this is not a true physically based approach, it is relating variations in melt to a physical process. Indeed, after comparing different model approaches, Hock (1999) found that the addition of potential solar radiation improved model outputs, but that the inclusion of measured cloud cover effects provided no further improvement. This indicates that the short wave radiation component of the melt model is actually operating as an index to melt processes not limited to short wave radiation i.e. indexing melt processes that are not influenced by cloud cover.

3.3 Snow measurement and modelling in the Lake Pukaki catchment

The earliest measurements of snow and ice in the Lake Pukaki catchment were made by von Haast when he mapped glacier termini as part of his geological survey in 1862 (Von Haast 1948). A more extensive glacier inspection programme was carried out by von Lendenfeld in 1884 during his preparation of the first map of the glaciers (Von Lendenfeld 1884). The government surveyor, Broderick, made further studies of the snow and ice of the catchment including estimating the snow field size of some of the region's glaciers and measuring the flow rate of the lower regions of the Tasman and Mueller glaciers (Broderick 1891; Broderick 1906). Subsequent repeat surveys of transects first surveyed by Broderick (e.g. Skinner 1964; Broadbent 1974; Claridge 1983; Kirkbride 1995; Hochstein et al. 1998) have enabled an assessment of the retreat and down wasting of the Tasman, Mueller, Hooker and Murchison glaciers, and an estimation of the contribution of long term ice melt to river flow. In 1957 three years of an extensive snow and ice measurement programme was begun on the Tasman Glacier. Ablation and accumulation was measured at various sites throughout the glacier

requiring 10 m auger holes to be drilled in the upper Tasman névé (Goldthwaite and McKellar 1962). The Ministry of Works began regular assessment of the snow pack at the head of the Tasman Glacier in 1965 until 1973 (Anderton 1975) in preparation of further hydro-electric development in the upper Waitaki basin. At the same time a seasonal snow study of the Twin Stream area was carried out with an altitude profile of snow depth, snow density and air temperature prepared (Archer 1970). The next large snow storage study in the catchment (as opposed to glaciological investigations) was made by Ruddell in 1994 as part of his doctoral research on the glaciers of the area (Ruddell 1995). Permanent climate stations and snow courses in the Pukaki Catchment were established following the 1992 national electricity crisis. One of these climate stations is situated at altitude within the catchment providing continual measurements of the snow using snow depth and snow weight sensors. The two snow courses in the catchment are monitored four times a year providing snow depth and density measurements (Halstead et al. 2003). A short term snowmelt study was carried out near Mueller hut in the catchment in 1995 recording melt water quantities as well as solar radiation, temperature, humidity and wind speed (Neale 1996).This exercise was repeated in the Tasman glacier névé by Cutler (2002). Currently researchers are investigating cores from the névé with a view to measuring past climatic conditions (Morgenstern and Thomson 2003). The first snowmelt model for the catchment was prepared by Anderton (1974) in anticipation of future demands on water in New Zealand. The model was prepared by classifying days into snowfall, snowmelt or no change according to interpretation of synoptic maps and augmented by lake inflow data. A snow storage index resulted that provided a relative measure of the seasonal snow storage in the catchment. It was not until 1992 and a national electricity energy crisis that focus was again directed to the snow fields of the Lake Pukaki region (Fitzharris 1992). This resulted in another snow storage model “SnowSim”, though, rather than being catchment specific, it applied to a large general South Island hydro-electric “macro-catchment” (Fitzharris and Garr 1995). This model and later variants have been used operationally by hydro-electric companies that operate in this region and for water resource analysis for regional councils. A second initiative to modelling lake inflows following the 1992 electricity crisis was undertaken using the UBC hydrological model (Peters 1996). Yearly flow estimates were satisfactory, while seasonal flow estimates were of variable quality. Yet another attempt at modelling the snowmelt in the region was carried out by Bowden (1994), this time using the Snow Runoff Model. Results were again disappointing and considered to be due to the difficulty in obtaining accurate snow covered area estimates as well as precipitation distribution inaccuracies. Using the new high altitude climate station

data, yet another snow modelling system intended for operational use was prepared for the Ohau, Pukaki and Tekapo catchments (Thompson 1997). This model follows the SnowSim methodology and is tuned to each catchment's runoff data. The SnowSim model was further refined by McAlevey (1998) to produce national snow storage information at a 1 km by 1 km grid scale. Lastly the Hooker catchment, within the Pukaki catchment, was modelled using a "modified UBC" snowmelt–runoff model prior to applying the same model to the ungauged Waiho Catchment on the West Coast (Islam 2001). A summary of the snow storage models applied to the region is given in Table 3.

Table 3. Snowmelt models applied to the Lake Pukaki catchment.

Model name/use	***Citation***	***Area of application***
Anderton model	(Anderton 1974)	Lake Pukaki catchment, New Zealand
Snowmelt Runoff Model	(Bowden 1994)	Lake Pukaki catchment, New Zealand
SnowSim	(Fitzharris and Garr 1995)	Hydro-electric "macro" catchment, South Island
UBC	(Peters 1996)	Catchments for; Lakes Pukaki, Ohau, Tekapo, New Zealand
Thompson model	(Thompson 1997)	Catchments for; Lakes Pukaki, Ohau, Tekapo, New Zealand
SnowSim – McAlevey	(McAlevey 1998)	New Zealand
UBC	(Islam 2001)	Waiho, Hooker, Whataroa catchments, New Zealand

3.4 SnowSim

SnowSim combines daily assessment of snow accumulation and melt from point site temperature and precipitation measurements to provide daily area average snow storage estimation. Detail of the model processes are provided below.

3.4.1 Snow accumulation

Snow accumulation assessment is made on a daily basis by estimating precipitation at each grid cell and assuming that precipitation falls as snow wherever the estimated temperature is less than a rain/snow threshold.

Precipitation estimation

Estimation of precipitation quantity by SnowSim is achieved by considering climate station rainfall measurements in the general area. The initial version of SnowSim divided the area of interest into 300 m elevation zones and lapsed area averaged rainfall (from a select set of climate stations) against elevation for each elevation zone.

The precipitation to elevation relationship was:

$$P_z = P_{mean} \exp^{lh} \quad \textbf{(4)}$$

P_z = the precipitation at elevation zone z.

P_{mean} = the average catchment precipitation determined from climate station data

h = the difference in elevation between the elevation zone of interest and the average climate station elevation

l = a constant tuned to ensure the modelled annual average precipitation matched the long term water balance.

This relationship is shown in Figure 5 as a relative measure of precipitation, where P_{mean} has been set to 1.

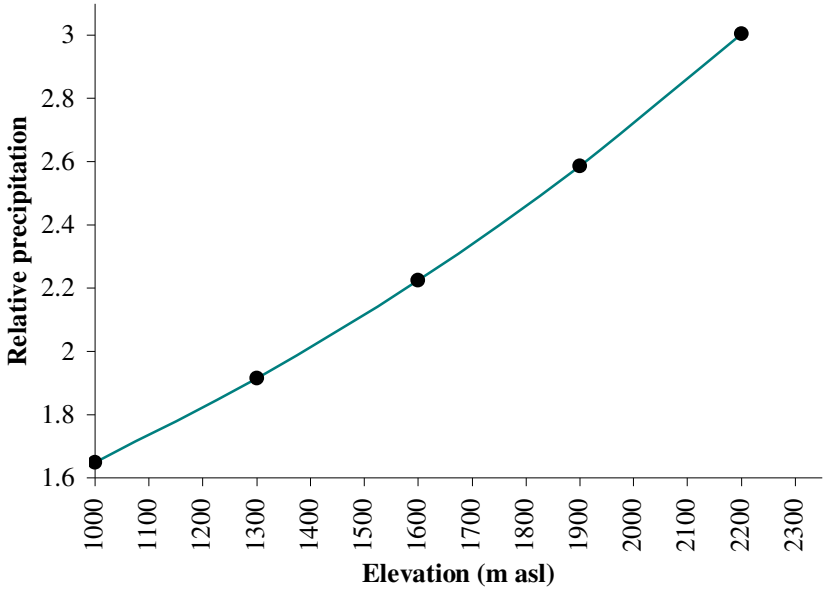

Figure 5. Original SnowSim relative precipitation-elevation relationship.

When SnowSim was converted to a 1km grid based model by McAlevey (1998), the elevation-precipitation relationship was modified:

- each grid square had a different "l" coefficient dependent on how the interpolated annual average precipitation for that grid square (from the selected climate stations) related to the NZ Meteorological Service 1951-80 annual average rainfall surface (NZMS 1985).
- The average precipitation P_{mean} for a grid square was established by interpolating climate station data using an inverse distance weighted algorithm

- The *h* factor was established by finding the difference between the elevation for the grid square of interest and the interpolated climate station elevation, again using an inverse distance weighted algorithm

The original SnowSim precipitation distribution showed no east-west precipitation gradient except in that the higher elevation regions were generally further west. The precipitation distribution used in New Zealand SnowSim (McAlevey 1998) was modified to show a marked east-west gradient, though still retaining a subtle elevation-precipitation component. Precipitation distribution surfaces for the original SnowSim and the New Zealand SnowSim are shown in Figure 6.

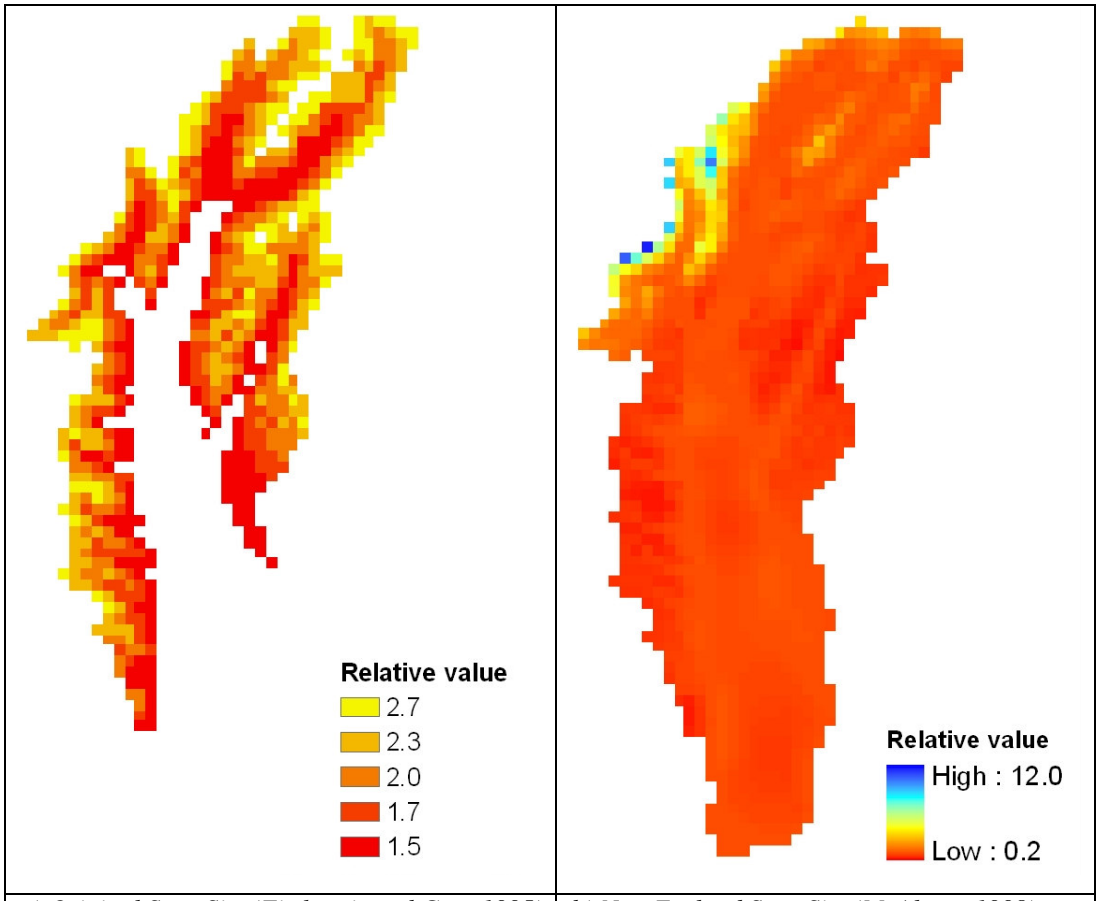

a) Original SnowSim (Fitzharris and Garr 1995) | *b) New Zealand SnowSim (McAlevey 1998)*

Figure 6. Relative precipitation distribution in the Lake Pukaki catchment as modelled by a) Original SnowSim, b) New Zealand SnowSim.

The value of each surface point is how much the regionally averaged precipitation (original SnowSim), or interpolated precipitation (New Zealand SnowSim), needs to be multiplied by to give the final estimated precipitation at that point. Note that for the original SnowSim, only areas between 850 m and 2350 m are included, as that was the considered seasonal snow zone to which the model was applied. Note also that with the original SnowSim, five discrete relative values occur, one for each of the elevation zones that were used, whereas the New Zealand SnowSim application applied to 1 km x 1 km grid locations.

Daily temperature

The value used by SnowSim for the daily temperature at a climate station is the mean of the daily maximum and minimum temperatures. Following analysis of 10 minute records, this mean temperature has been found to overestimate the true daily average temperature depending on the time of year (Cazorzi and Dalla-Fonatana 1986). This leads to threshold temperatures being set lower than intended, and tuned threshold temperatures appearing higher than physically derived values.

Snow/Rain temperature threshold

The precipitation type (rain or snow) has a significant effect on snowmelt model outputs (WMO 1986). The SnowSim model has the threshold temperature set to 2.5 ^{o}C following tuning of the model to match the long term water balance (Fitzharris and Garr 1995). By way of comparison, Barringer (1989) tuned a degree-day model for The Remarkables, New Zealand, using modelled and measured snowline altitudes resulting in a snow/rain threshold of 0.9 ^{o}C. Barringer's model utilised a rain/snow proportion function where at 0.9 ^{o}C mostly rain but some snow fell, and at 0 ^{o}C, all precipitation fell as snow. Moore and Owens (1984b) tuned their degree-day model of snow storage in the Craigeburn Range and found a snow/rain threshold of 2.1 – 2.2 ^{o}C when utilising low elevation temperature measurements, and 1.2 ^{o}C when using high elevation temperature measurements (see Table 2). This rain/snow temperature threshold can have a significant impact on model results, in that a single degree of difference may mean over 100 m altitude difference in the snow line, which in turn, for the Lake Pukaki Catchment could mean over 50 km^2 of additional snow cover (for land between 1000 and 2000 m). A review of Swiss data shows that the transition from rain to snow may occur anywhere between -1 ^{o}C and +7 ^{o}C, with 50% of precipitation falling as snow below 1 ^{o}C as measured by a 10 min interval automatic climate station at 1590 m at Dorf, Paltz (Braun 1991). The difference in snow/rain threshold between various authors would indicate that the value is spatially and temporally variable, but that the difficulty in estimating a representative value requires its setting through model tuning. Care should be taken to ensure that the resulting temperature is reasonable in a physical sense. The SnowSim method of using a single temperature to switch between snow and rain would lead the critical threshold to be ideally set at the temperature at which precipitation is split 50% between rain and snow.

Temperature lapse rate

To determine the temperature at the various elevation zones, SnowSim lapses climate station temperature data to sea level, interpolates the data to all zones (or grids) and then lapses the temperature to the average elevation of the zone. The lapse rate used is 0.007 ^{o}C m^{-1}.

Barringer (1989) utilised three climate stations at different elevations to measure lapse rates in The Remarkables, New Zealand and found that the lapse rate varied from day to day and was rarely linear through the three elevation points. Lapse rates used by various authors are shown in Table 2. The spatial and temporal variability in lapse rates results in a set lapse rate as being necessarily an approximation of the true process. Care is therefore required to ensure that the value chosen is as close a representation of the average conditions within the area of interest as possible.

3.4.2 Snowmelt

Snowmelt estimation is achieved by relating melt rates to estimated air temperature and the day of the year. Only on days when the temperature is estimated as being above zero degrees Celsius is melt considered. The relationship, given by the "Melt factor", is varied depending on the time of year and the elevation. McAlevey (1998) modified the SnowSim melt factor parameterisation to include a consideration for change in albedo of the snow following Woo and Dubreuil (1985) and to extend the range of the possible melt factor up to 12 mm ^{o}C d^{-1} as the snow year progresses. This change in parameterisation leads to a maximum melt at the end of the snow year, with a step change to the minimum melt at the beginning of the melt year one day later. The melt factor parameterisation is given by:

$$f = f_{\min} + \frac{f_{\max} - f_{\min}}{e^{(2.5-0.2at)} + 1} \quad \textbf{(5)}$$

Where:

f = melt factor

f_{min} = minimum melt factor (3 mm ^{o}C^{-1} d^{-1})

$f_{\max}$ = $f_{max,i}$ for days 1 to 250 (where day 1 is 1st of April)

$f_{max,i}$ +1 for days 250 to 280 (Dec 6th to Jan 6th)

$f_{max,i}$ +2 for days 280 to 300 (Jan 6th to Jan 26th)

$f_{max,i}$ +4 for days 300+ (Jan 26th to Mar 31st)

$f_{max,i}$ = initial maximum melt factor (8 mm ^{o}C d^{-1})

a = 1 for a dry day, 2 for a day when rainfall is estimated to have fallen

t = time, in days, since the last snowfall

The melt factor variation with time, with different values for the α and t variables, is shown in Figure 7. The dot represents the melt factor on a wet day, five days after a snowfall. The top of the bars represent the possible melt factor on a wet day, 10 days after a snowfall. The bottom of the bars represents the possible melt factor on a dry day, 1 day after a snowfall.

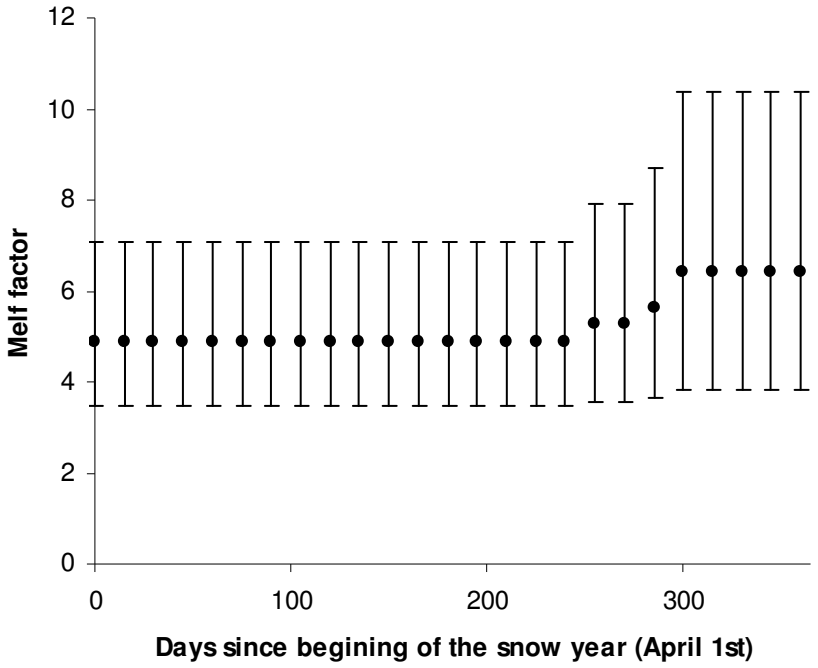

Figure 7. Change in possible melt factor with time as modelled by McAlevey (1998) showing potential values under different conditions.

3.4.3 Snow storage

Snow storage for any day is found by adding snow accumulation and snowmelt from the beginning of the current snow year up to the day of interest. A snow year is defined as being from 1st April (when seasonal snow will be close to an annual minimum) through to 31st March of the following year. In this way the "year" begins with zero seasonal storage. This is an approximation of reality as evidenced by seasonal snow enduring in the upper catchment from one season to the next. This is necessary for the creation of glaciers. To avoid inclusion of glacial effects, the original SnowSim model considered snow storage as being seasonal for the elevation bands below 2050 m, which is near the regional end-of-season snowline. In fact the elevation of the glacial seasonal snowline is spatially variable and, for the Lake Pukaki catchment at least, declines steeply from 2300 m in the east of the catchment to 1800 m in the west of the catchment (Chinn and Whitehouse 1980).

3.4.4 SnowSim applications

The first application of SnowSim was to provide an indication of the past variability and a quantification of seasonal snow in the hydro-electric "macro" catchment of the South Island (Fitzharris and Garr 1995). The snow storage was found to build from about May to a maximum of on average 366 mm SWE in October, then to decline at a slightly faster rate than

it accumulated until May when any net annual accumulation is considered as input to the region's glaciers. From year to year this scenario was found to be highly variable both in timing and in magnitude, with no general trend between 1930 and 1993. A derivative of SnowSim was shortly thereafter included in a catchment scale snow-storage estimation system for hydro-electric operation with the addition of discharge measurements. The inclusion of the snow storage processes improved storm flow predictions compared to excluding it (Thompson 1997). SnowSim has also been used to provide stochastic forecasts of summer inflows to hydro-lakes through consideration of how the current snow storage volumes match historic differences between snow storage and summer flow (Fitzharris 1997). By way of understanding snowmelt processes, SnowSim has been used at a point scale, comparing output to measured and physically based models (Neale 1996; Cutler 2002). The physically based models returned an improved result compared to SnowSim especially during strong warm wind conditions, when snowmelt was severely under estimated by SnowSim. SnowSim was substantially reviewed by McAlevey (1998) providing national gridded outputs of snow storage and providing a tool to estimate variation in snow cover for different climate conditions as part of a general climate change study. De Latour (1999) then used SnowSim outputs at the macro catchment scale to assess snow-storage to synoptic situation linkages. SnowSim enabled a clear identification of the importance of south westerly conditions in increasing snow storage, especially where the wind is related to a Tasman Sea anticyclone. More recently SnowSim has been utilised to provide historic maps of snow cover for regions of New Zealand as part of the NIWA climate mapping programme (Tait, pers.comm.) and to provide seasonal snow cover "accounts" for the New Zealand government (Fitzharris 2004).

Table 4. Applications of SnowSim.

Purpose	*Citation*
Quantification of seasonal snow storage	(Fitzharris and Garr 1995)
Historic variability of snow storage	(Fitzharris and Garr 1995)
Hydro-electric water storage monitoring and forecasting	(Thompson 1997)
Point scale snowmelt research	(Neale 1996; Cutler 2002)
Climate change forecasting	(McAlevey 1998)
Snow storage – synoptic condition linkages	(De Latour 1999)
Snow cover mapping	(Tait, Pers.comm.)
National seasonal snow account	(Fitzharris 2004)

3.5 Summary

Snow storage modelling techniques vary around the world according to conditions, available inputs and applications. The most accurate models operate at a point scale utilising extensive measurements to describe the physical processes involved in snow gain and melt. Empirical models relating precipitation to snow accumulation and temperature to snowmelt provide useful outputs where inputs are restricted and output accuracy is not critical. The temperature-index component of snow storage models can be enhanced with solar radiation calculations without any increased data input requirements. SnowSim is a combined precipitation and temperature-index model derived for New Zealand conditions which has been applied both operationally for hydro-electricity generation and for research in a variety of fields.

4 SnowSim modification and verification methods

4.1 Introduction

Four distinct steps were taken in modifying SnowSim. Firstly, SnowSim was set up on a geographic information system platform and restricted to the Lake Pukaki catchment. Secondly, the model parameters were tuned to optimize performance when compared to measured data. Thirdly, modifications to SnowSim following consideration of current snowmelt modelling research were implemented and tested. Lastly, the optimized, modified model was verified against measured data.

Unless otherwise referenced, New Zealand SnowSim refers to the version that was prepared by McAlevey (1998). This version is New Zealand wide and has variations on climate interpolation techniques to the original SnowSim of Fitzharris and Garr (1995) as outlined in the previous chapter.

4.2 Geographic information system model implementation

SnowSim has been prepared as a custom computer application in the past. This has enabled ease of operation but has required knowledge of the underlying computer languages for modification. As computer speed, storage capacities and operating systems have developed, it is necessary to continually update the original applications to ensure optimal performance and avoid obsolescence. As the capabilities of Geographic Information Systems grow, they become increasingly attractive as a platform to solve spatial problems. The extensive use of Geographic Information Systems at an operator level (as opposed a programmer level) ensures a broad understanding of their use and an extensive user community. Many of the tasks required for spatial data set manipulation (not least of which is visual representation) are handled by the application ensuring simple algorithm implementation. As a high level application, the responsibility of providing backward compatibility upon application version upgrades is borne by the software manufacturer. Geographic Information Systems and the ArcGIS application in particular (version 8.3 at the time of writing) have been chosen as the platform for the SnowSim model prepared as part of this research. This is arguably an industry standard GIS platform used throughout the world. ArcGIS provides facilities to view spatial databases, often referred to as layers (maps, line drawings etc) and functions for these layers to be manipulated, both within themselves and with each other. SnowSim has been implemented by utilising these functions to carry out the required calculations of climate station measurements to provide maps of parameters, as well as combining these maps

together in such a way as to provide a variety of outputs. To enable repeated and automatic operation of functions, a scripting process is provided by ArcGIS. A series of GIS functions can be written to a text file (script), which may then be "run" by the GIS, allowing several functions to operate sequentially on pre-prepared data. In this manner, SnowSim can operate on large sets of data without user intervention. By repeat use of the same script, variations in input data can be analysed for its effect on the output. ArcGIS uses a scripting language called Arc Macro Language (AML) which is an enhanced version of the command line operation of ArcGIS. In preparing scripts, the desired sequence of GIS functions was trialled manually until the correct operation was achieved. This sequence was then transferred to the AML script for repeat use.

Flow charts have been used throughout this chapter to assist with describing algorithm processes and implementation. A key to the various flow chart components is provided for reference in Figure 8.

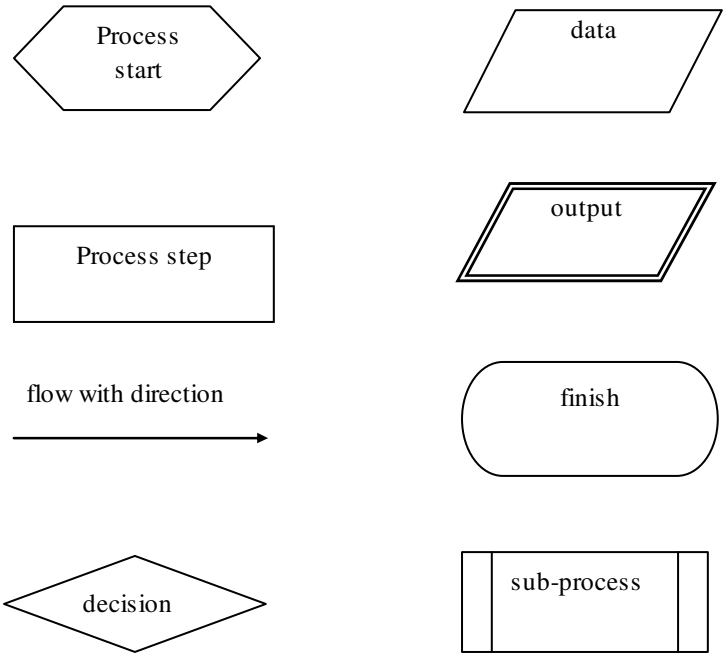

Figure 8. Key to flow chart symbol shapes.

4.2.1 AML script structure

The structure of the AML script was prepared to ensure various components of SnowSim were independent of each other, whilst enabling operation of SnowSim on daily data from one day to many years. This was achieved by dividing model components into modules, and calling each module in turn for each day of consideration. The main script initialises data, operates each module in turn for every day of interest and then finishes, as outlined in Figure 9. This structure provides the potential to apply the model for any number of consecutive days at any time of the

year. While it would be normal to operate the model for an entire snow year (from April 1st to 31st March), it may be desirable to run the model for a few days part way through a season with pre-prepared initial snow storage layers.

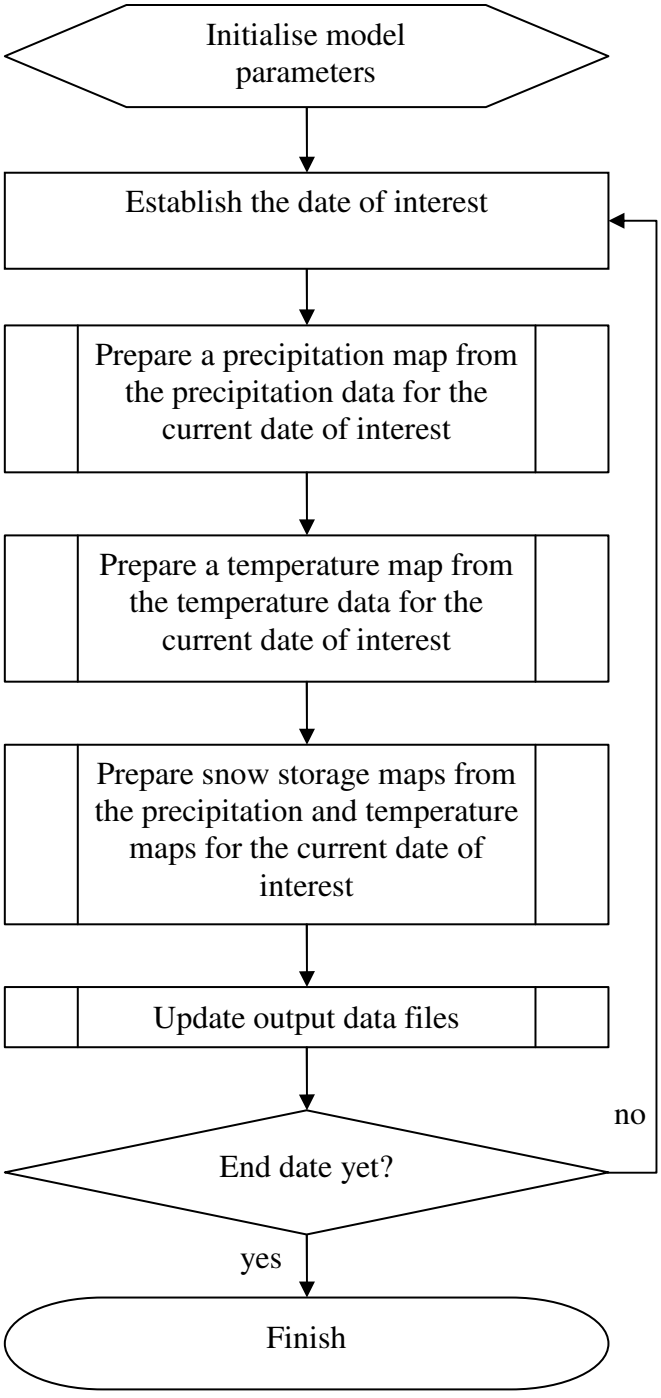

Figure 9. Flowchart of AML script processes.

4.2.2 Initial data

Data, as used in a GIS, can take a number of different forms. Point data consists of position references to a location. For compatibility with other data sets, position references usually adhere to a standard referencing system, for instance latitude and longitude, or New Zealand Map Grid. All data sets plotted using the same position reference system will have the same relative positions as occur in true physical space. A data set may be made up of a number of different position references, but the set will adhere to a single reference system. As well as position references, a data set may contain attributes for each position. Attributes may consist of a number (e.g. climate station ID number), or a physical description, (e.g. “rain gauge”) or any combination of data types. As well as point data, line and polygon data may be held as a data set. These formats are merely more complex forms of the point data in that multiple position references are needed for each data item. For a line, each vertex requires position information, though attribute data is held for the entire line rather than for each vertex. Likewise for a polygon, the position reference of each polygon is stored together with the attribute information of the entire polygon, not the lines that contain the polygon, nor the vertices at the polygon corners. Another data set type is the raster type. Raster data assigns values to every possible position reference within a boundary (or sets of boundaries). The number of position references is determined by the extent and resolution of the raster. A 1 km x 1 km resolution would indicate that a data value is held for every location on a 1 km x 1 km grid within the extents of the data set. Raster data sets are generally more memory intensive than point, line or polygon data, because of the greater amount of data stored. However, interaction between raster data sets provides a powerful means of exploring spatial data that is not as easily obtained through point, line or polygon data. For implementation of SnowSim, extensive use of the raster format is used. For compatibility to reference data (e.g. digital topographical maps) the New Zealand Map Grid was selected as the reference system of choice. As a compromise between detail and efficiency, a standard grid resolution of 1km x 1km was selected. This was initially selected to conform to satellite imagery data that was intended to be included in the analysis, but that was later discarded. The extent of the data sets vary depending on their use. For climate interpolation, the extent of data is set to 75 km beyond the catchment boundary. For calculations of catchment properties, the extent of each data set was set to a rectangular box that wholly included the catchment. Each raster data set has been aligned to ensure the grids exactly match each other. This ensures that inter raster calculations do not cross grid boundaries.

Much of the information used in SnowSim does not change during model operation. This information is prepared ahead of time and identified by the AML script as part of the data initialisation. A list of the various spatial data sets used in the model is outlined in Table 5. These include a spatial definition of the rectangle that wholly contains the catchment (*aoi* and *aoi_grid*), and just the catchment itself (*catchment*). Digital elevation models of the catchment and the South Island (*dem_aoi_1k*, *dem_si_1k*), point data for rain gauge and temperature measurement sites (*pukaki_p_cs*, *pukaki_t_cs*) and a raster for the "*l*" coefficient within the catchment as needed for the precipitation interpolation system.

Table 5. Fixed spatial data sets used within SnowSim.

Name	***Spatial data type***	***Description***
aoi	Polygon coverage, with the map projection set to the New Zealand Map Grid	Area of interest delineation
aoi_grid	Binary raster	A binary raster of *aoi* with 1000m by 1000m cell size with the map projection set to the New Zealand Map Grid
dem_aoi_1k	Continuous data raster, extent, grid size and projection as per *aoi_grid*	Digital elevation model for the area of interest. Derived from the LINZ 25 m DEM
si_dem_1k	Continuous data raster, grid size and projection as per *aoi_grid*	Digital elevation model for the South Island. Derived from the LINZ 25 m DEM
catchment	Binary raster, extent, grid size and projection as per *aoi_grid*	The area of the Lake Pukaki catchment.
pukaki_p_cs	Point coverage, projection as per *aoi_grid*	Climate station locations as held in the NIWA climate station data base that record daily precipitation
pukaki_t_cs	Point coverage, projection as per *aoi_grid*	Climate station locations as held in the NIWA climate station data base that record daily temperature values
pukaki_l	Continuous data raster, extent, grid size and projection as per *aoi_grid*	"*l*" coefficients used in interpolating precipitation

As well as spatial data sets, there are various parameters required for model calculations. These were set as per those used in New Zealand SnowSim, as outlined in Table 6.

Table 6. Parameters used for New Zealand SnowSim (McAlevey 1998).

Parameter	*SnowSim*
Snow/rain temperature threshold	2.5 ^{o}C
Minimum melt factor	3 mm $^{o}C^{-1}$
Initial maximum melt factor	8 mm $^{o}C^{-1}$
Temperature lapse rate	0.007 ^{o}C m^{-1}

4.2.3 Climate stations

To delineate a region within which climate station data is to be considered, a buffer zone of 75 km was created around the Lake Pukaki catchment. A compromise between too large a zone, which would include data from climate stations in areas experiencing quite different weather conditions to the catchment, and too small a zone, which would limit the available data, was made in selecting 75 km as being appropriate. All currently operating climate stations with daily precipitation records were identified from the NIWA climate station database and their positions together with names, identification numbers and elevations were saved as a GIS data file called "*Pukaki_p_cs*". Likewise all currently operating climate stations with daily temperature records were identified and their positions together with names, identification numbers and elevations were saved as a GIS data file called "*Pukaki_t_cs*". These stations included six stations operated by NIWA for Meridian Energy specifically for hydro-lake management.

4.2.4 Climate station data

Daily mean temperature and total precipitation data for the selected climate stations were downloaded from the NIWA climate database for days from 1st April 2000 until 31st March 2004. These data were reformatted into DBASE data files, each containing 6 months data of either precipitation or mean temperature. Each column (item) in a data file contained a different day's data (column headings were dates), while each row (record) contained a different climate station's data (row headings were "station ID"). All entries with unknown data were allocated the value "999.99".

4.2.5 Precipitation

To determine daily precipitation, equation (4) (section 3.4.1) must be solved in a distributed manner. This is done by using the New Zealand SnowSim (McAlevey 1998) interpretation of the parameters:

$$P_{x,y} = P_{mean} \exp^{lh} \quad \textbf{(6)}$$

Where:

$P_{x,y}$ is the precipitation at grid location (x,y) of interest

P_{mean} is the average catchment precipitation determined from interpolating climate station precipitation data using an inverse distance weighting (IDW) algorithm

h is the difference in elevation between the grid location of interest (derived from the digital elevation model) and the value at the grid square found by interpolating the climate station elevations (again using an IDW algorithm).

l is a constant tuned to ensure the modelled annual average precipitation at the grid location of interest matches the annual average precipitation as determined by the New Zealand Meteorological Service 1951-80 annual average rainfall surface (NZMS 1985).

The "*l*" coefficient is a spatially variable parameter which is required for precipitation interpolation (see section 3.4.1). The "*l*" value was found for each grid square by:

- Creating a "climate station elevation difference" surface by interpolating the elevations of the climate stations using the IDW function available in ArcGIS, then subtracting this grid from the digital elevation model of the area (*dem_aoi_1k*). This surface is then a grid of "*h*" values
- Creating an "annual average precipitation" surface by interpolating the annual average precipitation values for the climate stations, again using the IDW function. This surface is then a grid of "P_{mean}" values
- Using the NZ Meteorological Service Annual average rainfall raster surface (NZMS 1985) as the "P_z" grid.
- Solving equation (6) for "*l*" using the NZMS annual average rain surface 1951-80 (NZMS 1985) and applying this equation in "Map algebra"[1] to prepare a grid of "*l*" values.

$$l = \frac{\ln(P_{x,y} / P_{mean})}{h} \qquad (7)$$

[1] *When performing arithmetic on spatial data sets, calculations may be carried out on data within a data set, or between data sets, depending on the context. In generating the grid of "l" values, equation 7 was calculated for each grid square using precipitation and elevation data for the same grid square position on the respective grids.*

Wherever "*h*" approached 0 (resulting from the interpolated climate station altitude being identical to the DEM) "*l*" tended to infinity. This resulted in discontinuities in the "*l*" grid which were removed. This was done by, firstly, limiting "*l*" values to be between -0.002 and 0.002 (reclassifying values outside this range to "NODATA") as per Equation 8:

$$\begin{Bmatrix} l < -0.02, & l = NODATA \\ -0.02 < l < 0.02, & l \\ l > 0.02, & l = NODATA \end{Bmatrix} \quad \textbf{(8)}$$

and secondly, by applying a "focal mean" function operating with a focus of 5 x 5 grid squares repeatedly (5 times) until all NODATA values had been removed. The focal mean function operates on each cell in turn, calculating the mean of the 25 grid cells around the cell of interest and setting the result to that grid square. Applying a focal mean has the effect of making extreme values closer to the average of the grid values in the immediate neighbourhood. NODATA values are ignored when calculating the focal mean. The resultant "*l*" surface was retained for daily precipitation estimation and stored as "*pukaki_l*".
The derivation of the daily precipitation estimation surface was carried out in the "Precipitation" module of the SnowSim AML script (see Figure 10 for an outline of the module's processes). The precipitation surface for each day is saved as a raster data file.

4.2.6 Temperature

New Zealand SnowSim uses a three step temperature interpolation technique.
Step one generates a "general" temperature trend from 22 South Island climate stations' data using a neural network (the temperature data having being lapsed to sea level). This identified latitudinal variations in temperature.
Step two establishes a "local" trend using IDW of the difference between climate station data and the "general" trend. This identifies variations in temperature caused by the synoptic situation and large scale topographic features.
The IDW formula used is:

$$z_{x,y} = \frac{\sum_{j=1}^{n} z_j d_{x,y,j}^{-\beta}}{\sum_{j=1}^{n} d_{x,y,j}^{-\beta}} \quad \textbf{(9)}$$

Where:

$z_{x,y}$ is the value location of interest

z_j is the climate station data

d is the distance between the location of interest and the climate station

j is the climate station number

β is a smoothing constant. This was set to 3 (McAlevey 1998).

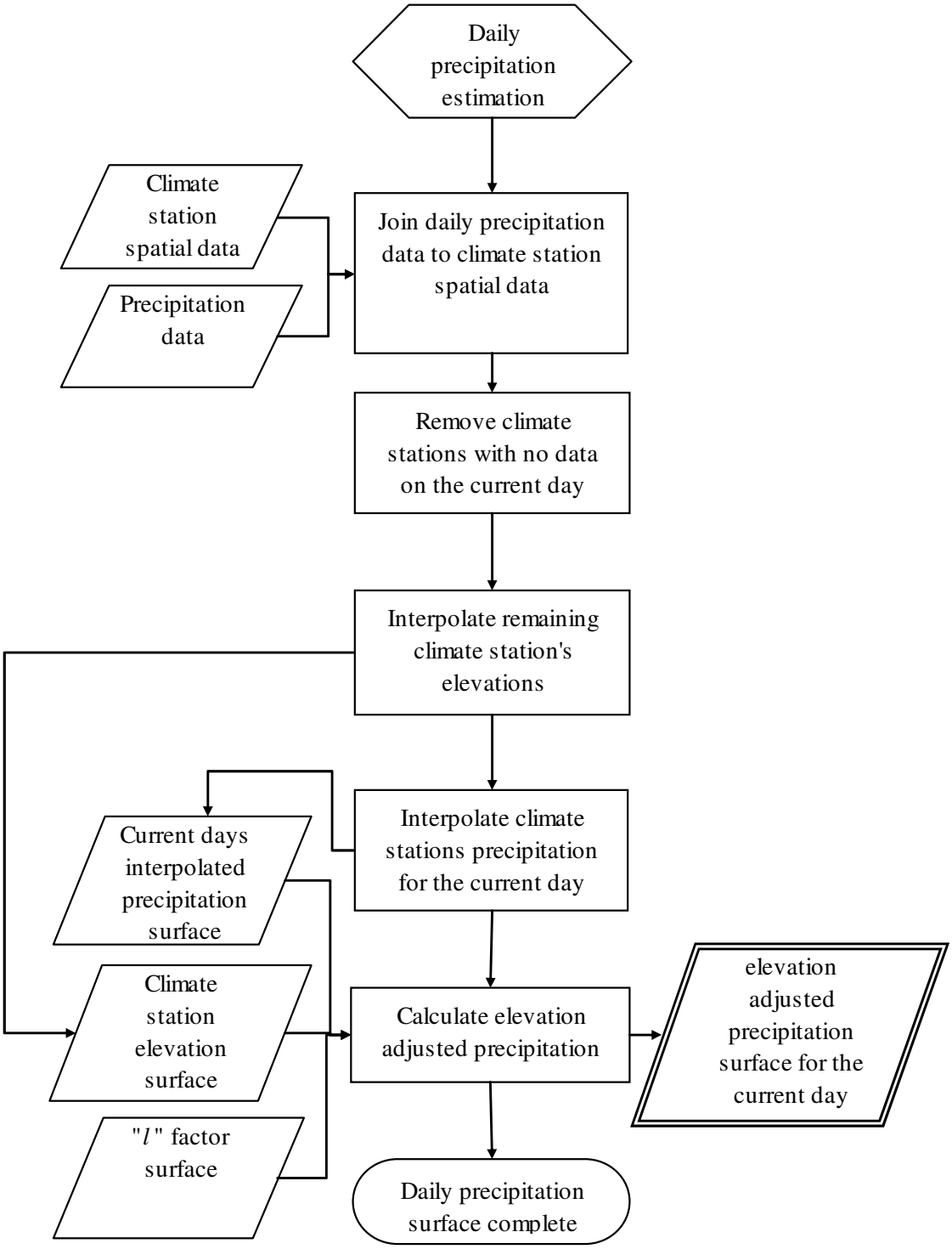

Figure 10. Precipitation estimation process.

The third step lapses the sum of the general and local trends to the height of the location of interest using a lapse rate of 0.007 ^{o}C m^{-1}.

For implementation in ArcGIS the "general" trend was not determined, as this is considered to be inherently included in the "local" trend, and exclusion of it greatly simplifies the implementation. The "local" trend was determined using the GIS in-built IDW interpolation method. This interpolation was carried out on the climate station temperature values, lapsed to sea level, rather than the difference between the lapsed climate station values and the "general" trend as was implemented by McAlevey (1998). The resulting interpolated sea level temperature surface was then lapsed back to true ground level resulting in the required daily temperature estimation surface. The process is outlined in Figure 11.

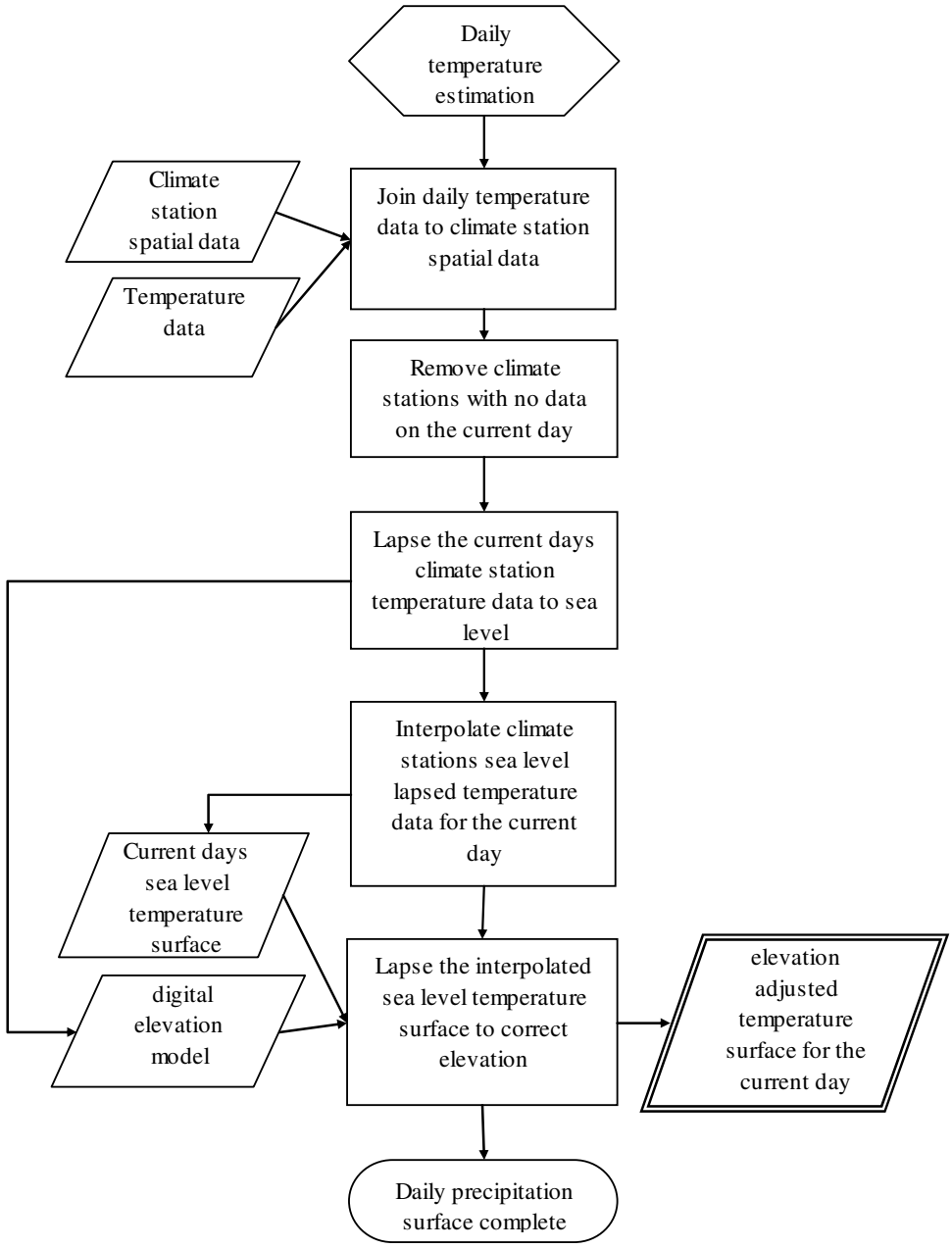

Figure 11. Temperature estimation process.

4.2.7 Snow storage

Snow storage is estimated by finding the snow accumulation and snow ablation each day to provide a net change in snow storage. The cumulative total thus provides the snow storage quantity since the beginning of the snow year (1st of April). These calculations are done in a spatial manner within the GIS.

Daily snow accumulation is found by identifying the grid squares that were estimated to be at a temperature below the snow/rain temperature threshold. Precipitation that occurred in these regions was then considered to be snowfall, thus providing daily snow accumulation estimation as outlined in Figure 12.

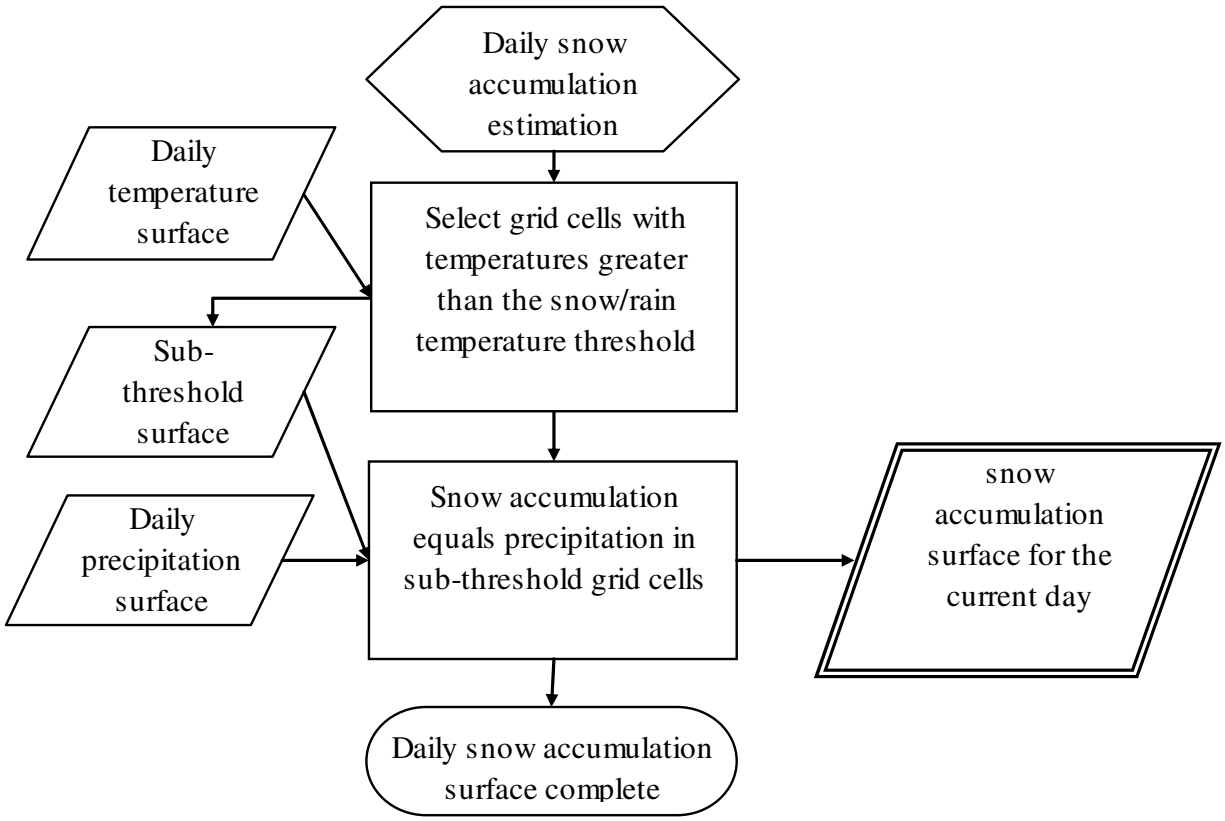

Figure 12. Snow accumulation process.

Daily snow ablation was found by identifying the grid points that were estimated to be at a temperature greater than 0 ^{o}C. Ablation was then calculated using equation (5) (Section 3.4.2). This process is outlined in Figure 13.

The daily change in snow storage is found by subtracting the daily ablation from the daily accumulation at each grid cell. Total snow storage is found by adding the current days change in snow storage to the previous day's total, and reclassifying all negative total snow storage values to zero. These calculations are carried out spatially, so that the total snow storage result is an estimation of snow storage at each grid point. To convert this to a single number

signifying the total catchment snow storage for a day, all the snow storage values for the grid points within the catchment are summed. This is achieved in ArcGIS through the use of the *Focalsum* function. The *Focalsum* function totals grid cells within a defined area (the catchment) and outputs the resulting number to a text file. Note that the output is in millimetres of snow water equivalent per square kilometre per day, which can be converted to cubic metres per second or potential giga-watt-hours, depending on requirements. The snow storage estimation process is outlined in Figure 14.

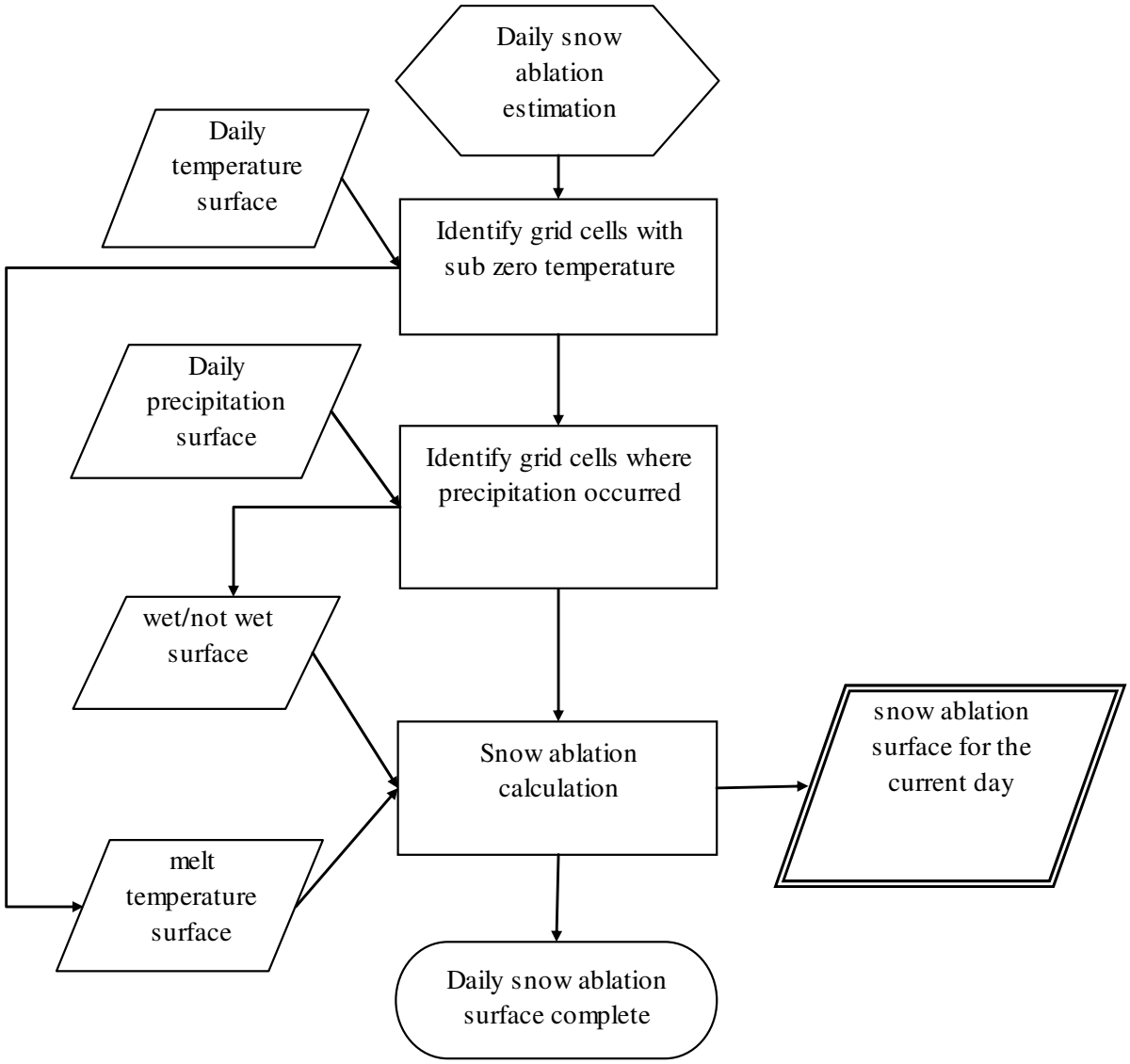

Figure 13. Snow ablation estimation process.

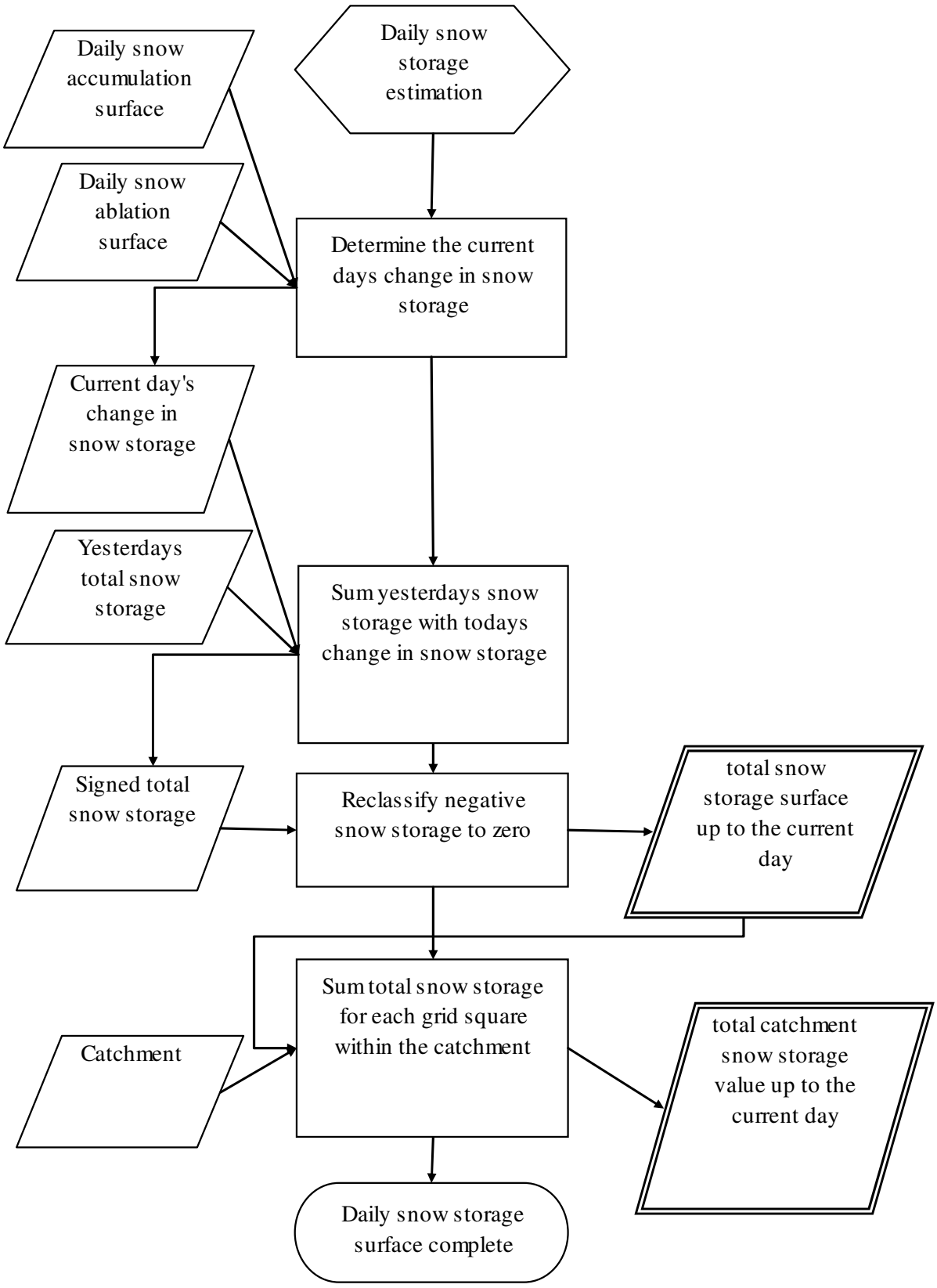

Figure 14. Snow storage estimation process.

4.3 SnowSim modifications

Three methods of model modification are described in this section. The first describes a technique to use measured lapse rates within the model. The second describes the use of a

new precipitation distribution system, while the third sets out the methods taken to include a radiation component in the model

4.3.1 Lapse rate calculation

Lapse rates are spatially and temporally variable as shown in Table 2, section 3.2.1. With the availability of temperature data from high elevation climate stations near the Lake Pukaki catchment, the use of daily measured lapse rates within SnowSim (as opposed to a constant estimated annual average) is now a possibility. The temperature data from the Panorama Climate station (1509 masl) and the Mt Cook climate station (765 m asl) were used to this effect. The Panorama climate station is situated north and east of the Lake Pukaki catchment in the adjacent Lake Tekapo catchment as shown in Figure 15.

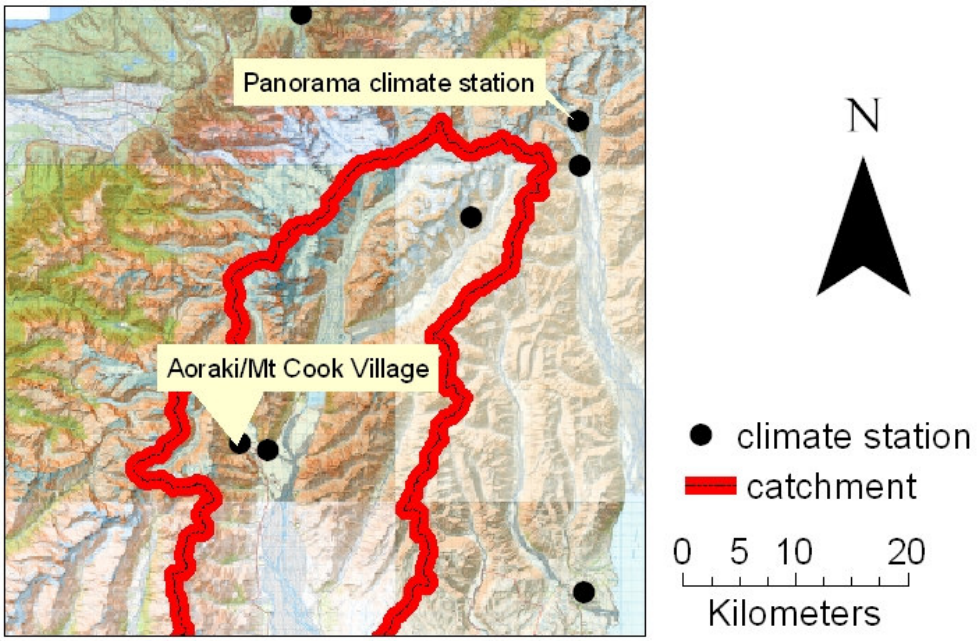

Figure 15. Location diagram showing the position of the Panorama climate station with respect the Lake Pukaki catchment.

Rose Ridge climate station (1940 m) data were not used, even though it is within the catchment, as the data are used for verification. A relationship between the annual average Panorama-to-Mt Cook lapse rate and the optimised lapse rate for interpolating the Rose Ridge climate station temperature was found. For each day of analysis, the lapse rate, as measured from the two stations (Panorama and Mt Cook) is scaled using that relationship to provide a Rose Ridge lapse rate. This in turn was used in the temperature interpolation process in place of the constant default lapse rate. The resulting modelled temperatures were compared to the

measured temperatures at Rose Ridge using the NTD criterion (see section 4.5 below) to determine whether the temperature modelling was improved.

4.3.2 Precipitation estimation

Estimating the quantity of precipitation in the mountainous regions of the Lake Pukaki catchment is problematic because of the lack of data for the area. The assumption that there is a significant elevation-precipitation linkage does not appear to be well founded for a region strongly influenced by orographic rainfall from a single general direction. The proximity of a location in relation to the precipitation barrier is a more appropriate generalisation of precipitation distribution. Such distributions have been found in various mountainous regions of the world (e.g. Alam 1972; Skaar 1972; Givone and Meignien 1990) and for various transects through New Zealand's Southern Alps (McSaveney et al. 1978; Griffiths and McSaveney 1983; Henderson and Thompson 1999). In view of this, the precipitation estimation system of SnowSim is to be modified by removing the elevation component. This simplifies precipitation estimation by relating daily precipitation measurements to a regional annual average precipitation surface only. This is done by:

- Establish what proportion of the long term annual average precipitation the current day's measurement is at each climate station
- Interpolate these proportions using inverse distance weighting to the entire catchment
- Multiply the interpolated proportions by the annual average precipitation surface

This method assumes every precipitation event has a distribution that is related to the annual average. The strong influence of westerly precipitation events on the annual precipitation surface means that for westerly events the annual precipitation surface is likely to be a close approximation. It is in the less common easterly and southerly events that this distribution technique may be less accurate.

The method also relies on the accuracy of the annual average precipitation surface. New Zealand SnowSim utilised the NZMS 1951-80 annual average rainfall surface (NZMS 1985) as the reference surface (McAlevey 1998). However, when compared to measurements from the Rakaia (McSaveney et al. 1978) and Franz Josef (Anderson 2004) regions, the surface appears inaccurate in the upper regions of the alpine catchments. By estimating the annual average precipitation in the upper Pukaki catchment and assuming similarity of distribution to the Rakaia catchment, just 60 km to the north east and in a similar position east of the main divide, a new annual average precipitation surface has been prepared for the Lake Pukaki catchment.

Annual average precipitation estimates for Tasman névé and the Rose Ridge Climate Station were prepared by relating short term measurements to Franz Josef Climate Station measurements over the same periods, ensuring a correlation existed, finding the magnitude of the relationship, and then applying this relationship to the Franz Josef annual average precipitation value. The precipitation measurements were related to Franz Josef as it had the highest correlation of any long term rain gauge site to the Tasman névé and Rose Ridge measurements. The position of Franz Josef with respect the catchment is shown in Figure 16.

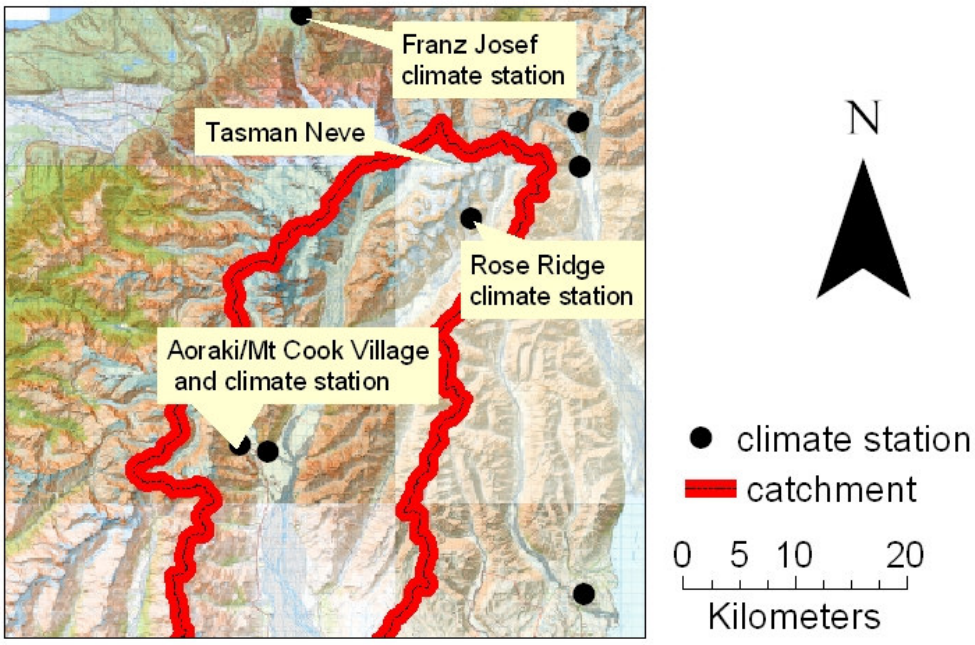

Figure 16. Position of Franz Josef with respect the Lake Pukaki catchment, the Tasman névé and the Rose Ridge climate station.

For the Tasman névé, snow pack measurements from Anderton (1975) for the winter of 1971 and 1972 were used. This is based on the assumption that in winter little ablation or rainfall occurs, so that the change in snow pack (in snow water equivalence) is a close measure of precipitation. For Rose Ridge, a summer rainfall period between December 2002 and March 2003 was used. During this time little snow is likely to fall, and the rainfall record is likely to be a close approximation to the total precipitation.

The Tasman névé and Rose Ridge annual average precipitation estimates (see Table 7) vary by 3042 mm and 1988 mm respectively from the NZMS surface demonstrating the inaccuracy of that surface. Following review of South Island precipitation regions (Salinger 1979; Thompson 1985; Sturman 1986; Ryan 1987) (see Figure 17) a line 33 km from the western 1200 m contour was selected as dividing the catchment into two distinct precipitation zones as shown in Figure 18.

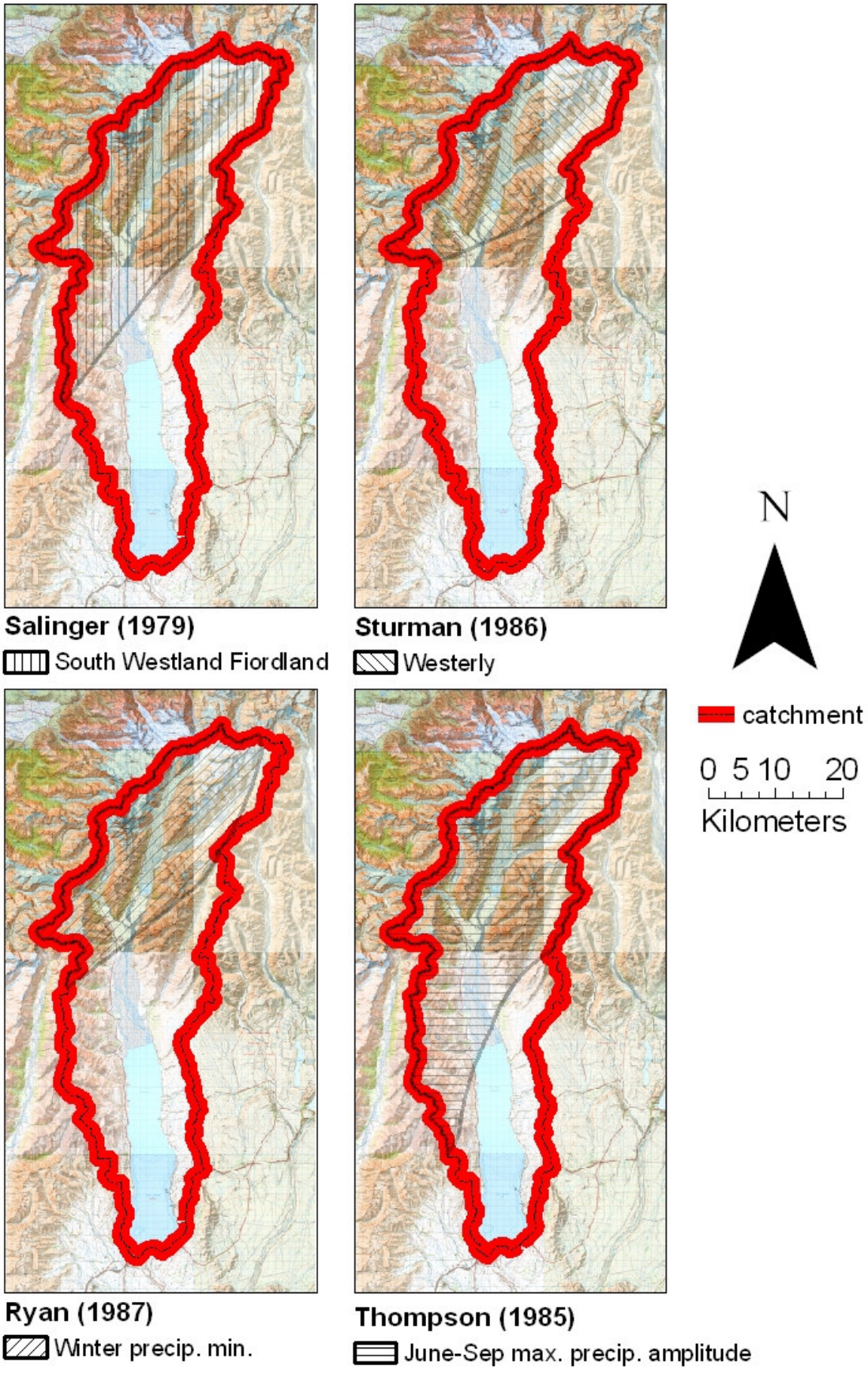

Figure 17. Suggested climate zone divisions in the Lake Pukaki Catchment.

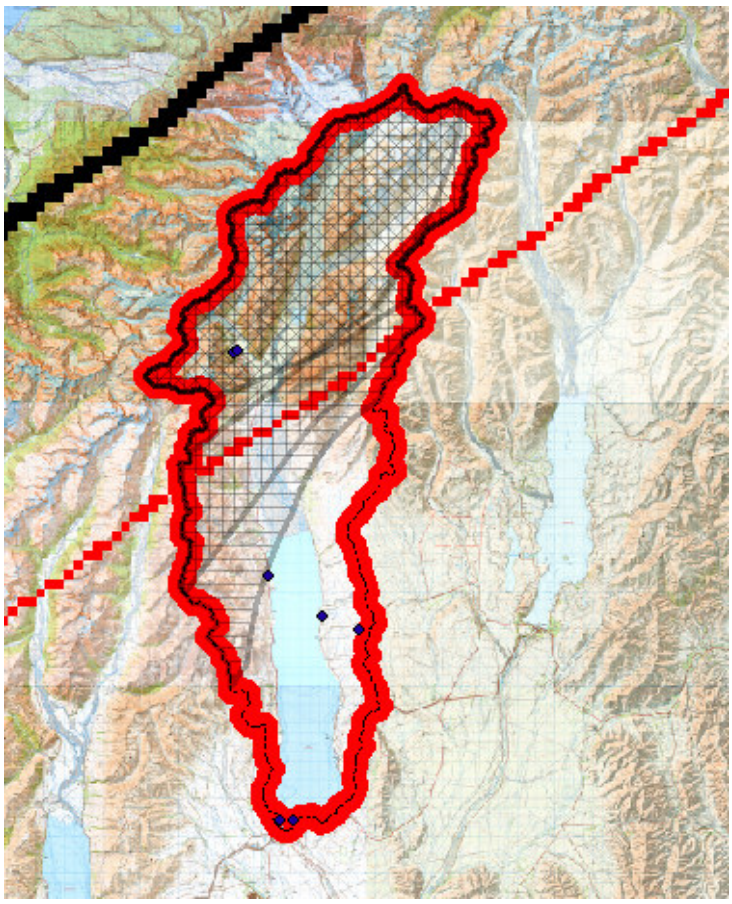

Figure 18. Division of the Lake Pukaki catchment based on differing precipitation zones (various hatching) using a line (red line) 33 km from the western 1200 m contour (black line). The blue dots show the positions of rain gauge sites within the catchment used to prepare the NZMS 1951-80 annual average rain surface.

A new annual average precipitation surface was prepared that combines the NZ Met. Service surface for the lower catchment (that part of the catchment beyond 33 km from the western 1200 m contour) with an exponential surface relating distance from the western 1200 m contour to precipitation magnitude, as suggested by McSaveney et al. (1978), and similar to that proposed by Thompson and Adams (1979) using the following equation:

$$P_x = 28500e^{\frac{-x}{12.5}} \quad \textbf{(10)}$$

Where

P_x = precipitation at a distance x from the western 1200 m contour line

x = distance from the western 1200 m contour line

The western 1200 m contour base line runs south-west to north-east along the western side of the Southern Alps roughly parallel to the alpine fault. It is considered by McSaveney et al. (1978) to provide the optimum base line for precipitation measurement, though Henderson

and Thompson (1999) have suggested the Alpine Fault as an alternative. The curve was found by finding the exponential line of best fit to pass through the plotted data points of the Mt Cook village annual average rainfall, the estimated annual average precipitation at Tasman névé, the estimated annual average precipitation at the Rose Ridge climate station and the annual average rainfall at 33 km from the western 1200 m contour as found from the NZMS annual average rainfall surface (Table 7) as shown in Figure 19.

Table 7. Annual average precipitation estimations for various locations in the upper Pukaki Catchment.

Location	***Annual Average Precipitation (mm)***	***Distance to western 1200 m contour (km)***
NZMS at 33 Km from 1200 m western contour	2000	33
The Hermitage, Mt Cook	3985	24
Hooker Flats, Mt Cook	3877	24
Rose Ridge	5627	20
Tasman névé	8619	15

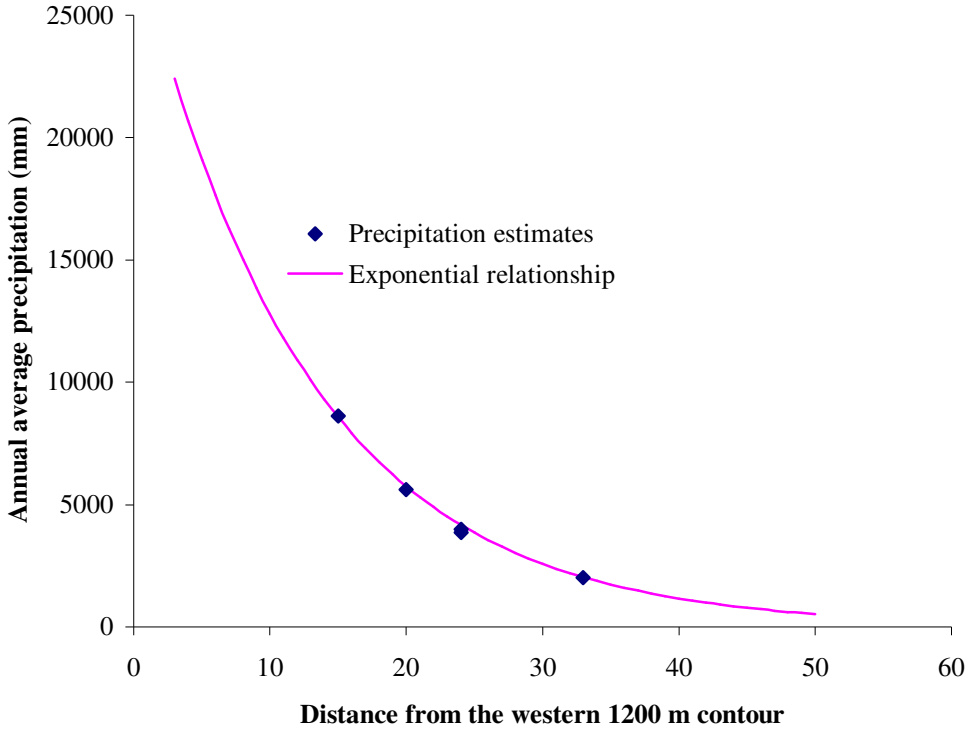

Figure 19. Exponential line of best fit for precipitation in the upper Lake Pukaki catchment.

The surface was prepared using the following process:

From the 1 km NZ DEM all heights within 50 m of 1200 m were highlighted. A line was manually digitised on-screen to follow this western 1200 m contour, from Hollyford in the south to Reefton in the north. This line was buffered at 1 km intervals to 70 km and converted

to a 1 km grid. Precipitation values were calculated for the 1200 m contour buffer grid using the exponential relationship (equation (10)) and saved as a precipitation grid. The upper catchment exponential surface was then combined with the lower catchment NZMS surface to provide the new Lake Pukaki catchment precipitation surface as shown in Figure 20.

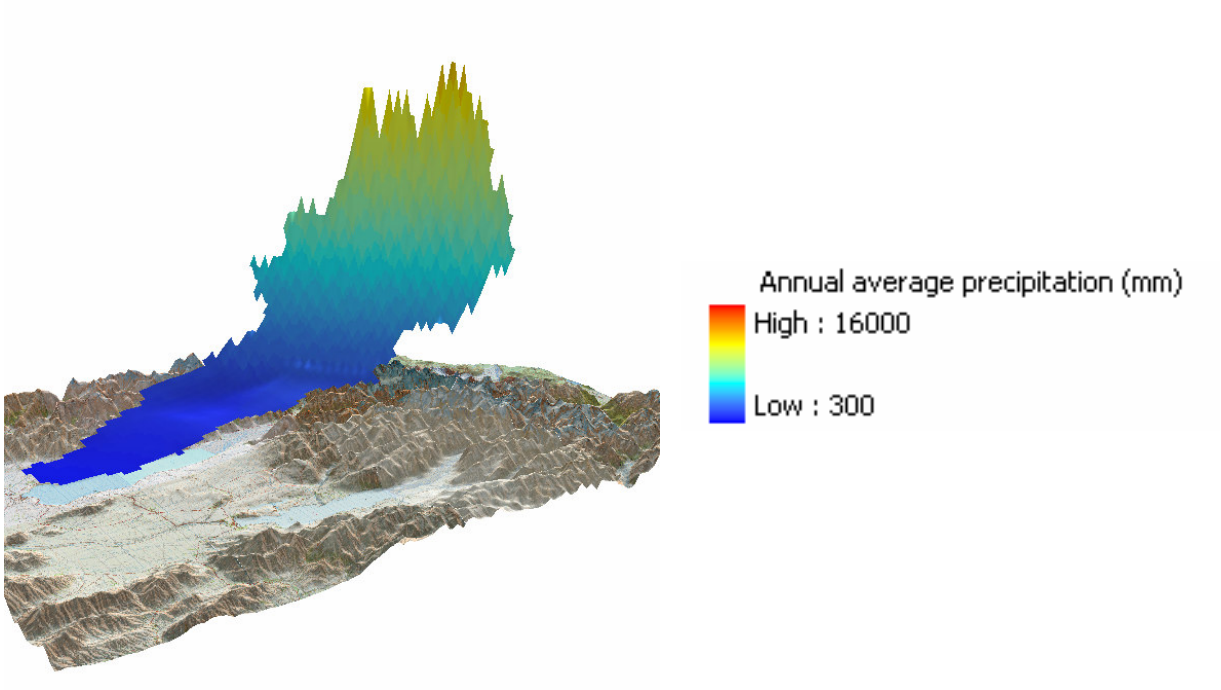

Figure 20. New annual average precipitation surface.

By way of verification, the estimated average total yearly precipitation volume can be compared to long term annual lake inflows through the use of the water balance equation (Anderton 1974):

$$P = Q + E - \Delta I \qquad \textbf{(11)}$$

Where

P = precipitation

Q = Lake inflows

E = Evapotranspiration

ΔI = long term change in ice storage

The annual average evapotranspiration for the catchment has been estimated as 400 mm a^{-1} (Anderton 1974) and 522 mm a^{-1} by Fitzharris and Garr (1995), whereas McKerchar and Pearson suggest 700 mm a^{-1} for areas with greater than 800mm a^{-1} rain and negligible ground water loss (McKerchar and Pearson 1997), this leads to an annual evapotranspiration estimate for the catchment of 0.75 ± 0.2 km^3 a^{-1}. The annual average runoff into Lake Pukaki is

estimated at 124 m^3s^{-1} (McKerchar and Pearson 1997), which equates to 3.9 km^3 a^{-1}. The long term change in ice storage is estimated by Purdie (1996) as being 7.3 m^3s^{-1} or 6% of annual flows (Purdie and Fitzharris 1999), which relates to 0.23 km^3 a^{-1}. The long term annual average catchment precipitation volume is therefore estimated using equation (11) as being between 4.22 km^3 a^{-1} and 4.62 km^3 a^{-1}. These values are shown in Table 8.

Table 8. Estimated water balance components.

Parameter	***Source***	***Annual average total (km^3)***
Evapotranspiration (*E*)	(Anderton 1974; Fitzharris and Garr 1995; McKerchar and Pearson 1997)	0.75 ± 0.2
Annual average lake inflow (*Q*)	(McKerchar and Pearson 1997)	3.9
Ice berg calving	(Purdie 1996)	0.03
Long term ice melt (ΔI)	(Purdie 1996; Purdie and Fitzharris 1999)	0.23
Annual average precipitation (*P*)		4.42 ± 0.2

The annual average precipitation total volumes for a variety of precipitation surfaces that have been applied to the Lake Pukaki catchment are compared in Table 9.

Table 9. Annual average precipitation totals for the Lake Pukaki catchment for different annual average precipitation distributions.

Surface Citation	***Annual average precipitation total (km^3 a^{-1})***	***Estimated annual average precipitation at Tasman névé (mm)***	***Estimated annual average precipitation at Rose Ridge (mm)***
(Thompson 1997)	5.39	13484	7252
(Thompson and Adams 1979)	4.71	6116	4872
(NZMS 1985)	5.46	11661	7615
(Anderton 1974)	5.81	6545	7463
(Fitzharris and Garr 1995)	N/A	N/A	4873
(Leathwick et al. 1998)	4.87	7366	5602
This thesis	4.44	8584	5754

The annual average precipitation volume for the new surface provides the closest match to the estimated annual average precipitation volume derived from the water balance components. It was therefore considered the best surface to use for precipitation interpolation within SnowSim.

4.3.3 Radiation component

The ability to determine maximum potential solar radiation without the need for climatic measurements provides a means of including further physically based snowmelt parameters to the snowmelt calculations. The cost is in computational efficiency, not in data availability. Increased computer capabilities have made this a possibility. Such a variation on the basic temperature-index model has been implemented with success (e.g. Kustas and Rango 1994; Cazorzi and Dalla-Fontana 1996; Hock 1999; Pellicciotti 2004). The approach taken for enhancing SnowSim is to split the snowmelt into two additive components, one dependent on temperature, and one dependent on radiation. The snowmelt can then be estimated by:

$$M_i = fT_i + M_{s,i} \quad \textbf{(12)}$$

Where

M_i = snowmelt on day i (mm).

f = melt factor (mm $^{o}C^{-1}$ d^{-1}).

T_i = positive temperature on day i (^{o}C).

$M_{s,i}$ = melt from shortwave radiation on day i (mm).

The shortwave radiation melt flux is estimated from the daily maximum total potential shortwave radiation energy ($Q_{S(max),i}$), by considering surface albedo (α) and a clear sky coefficient (CSC):

$$M_{s,i} = \frac{1000\ CSC(1-\alpha)Q_{S(\max),i}}{\rho L_f} \quad \textbf{(13)}$$

Where:

$M_{s,i}$= melt from shortwave radiation on day i (mm)

$Q_{s(max),i}$= total maximum short wave energy on day i (kJ m^{-2})

CSC = clear sky coefficient

α = albedo

ρ = density of water (1000 kg m^{-3})

L_f = latent heat of fusion, the energy required to melt ice (334 kJ kg^{-1})

The clear sky coefficient was established by tuning the model and was kept constant both spatially and temporally. The potential exists to parameterise this constant based on historic and/or current cloud cover measurements, obtainable from satellite imagery.

Albedo is estimated following Woo and Dubreil (1985) with the addition of a wet/dry parameter following McAlevey (1998)

$$\alpha_i = \alpha_{\max} - \{[\alpha_{\max} - \alpha_{\min}]/[\exp(b_1 + b_2 tw) + 1]\} \quad \textbf{(14)}$$

Where:

α_i = the albedo on day *i*

α_{max} = albedo for new fallen snow

α_{min} = albedo for old snow

b_1 and b_2 = empirical constants are taken to be 2.46 and –0.26 respectively following Woo and Dubreil (1985) for "relatively clean" snow.

t is time in days since the snow fell

w is an adjustment for wet or dry surface, 1 for dry, 2 for wet following McAlevey (1998).

Figure 21 shows how the albedo parameter is set to change since the last snowfall, including the variation that wet or dry conditions have on the albedo parameter (new snow albedo has been set to 0.8, old snow albedo has been set to 0.6).

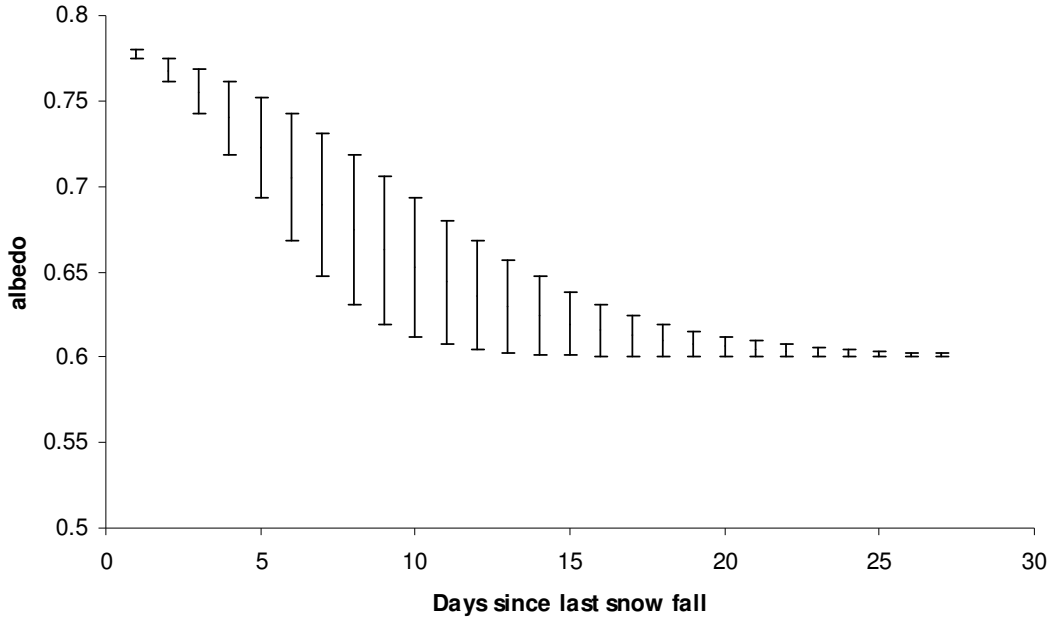

Figure 21. Change in albedo with time since the last snowfall. Maximum values are for dry conditions, minimum values are for wet conditions.

Shortwave radiation is comprised of direct and diffuse radiation. Direct radiation is that radiation which comes straight from the sun. Diffuse radiation is that portion of incoming radiation that is reflected off the atmosphere or surrounding land prior to arriving at the point of interest.

Direct and diffuse radiation can be estimated by considering the angle of the sun and the slope and aspect of the terrain (Swift 1976; Dozier 1980; Munro and Young 1982; e.g. Duguay 1993; Dubayah and Rich 1995; e.g. Varley et al. 1996) Calculations are necessarily approximations of reality to ensure computational efficiency. The position of the sun can be determined through astronomical calculations whereby the location of the point of interest with respect to the sun can be determined by its latitude, longitude, date and time of day. This is required to determine the path length of the solar beam through the earth's atmosphere. At high sun-earth angles, the path length is short, whereas at low sun angles (i.e. near the horizon) the path length is long plus there is increased refraction (further increasing the effective path length). Slope and aspect of a point of interest can be determined through consideration of elevation, and the elevation of the surrounding area. This can be achieved through in-built GIS functions applied to the digital elevation model of the region.

Two Arc Macro Language scripts prepared by Kumar et al. (1997) and updated by Zimmerman (2001) were used to determine the maximum potential solar radiation factor. These scripts consider topography and sun angle at regular intervals (set to hourly between sunrise and sunset) to calculate the potential maximum solar radiation for the day of interest. A "solar constant" is used for the solar flux at the earth's atmosphere/space boundary, and an average transmittance of 0.8 for a vertical solar beam through the earth's atmosphere is assumed. In reality, the makeup of the atmosphere affects the transmittance, and the variations in the earth's orbit around the sun, together with sun spot cycles affect the solar constant. Ignoring these variations is acceptable considering increased simplicity and computational efficiency for a small loss in accuracy. The diffuse radiation calculation considers direct radiation and the slope of the terrain, but does not consider wall effects of the surrounding terrain, again for computational efficiency at the loss of a level of accuracy considered acceptable.

By including the radiation component in the melt calculation, the need to vary the melt factor through the season has been removed. The step change of the melt factor at the beginning of the snow year in the McAlevey SnowSim indicates the melt factor parameter had become removed from any likely physical condition. Linking melt variation to maximum potential solar radiation is an attempt to restore a likely physical linkage in the model. A second advantage of including the radiation parameter is the ease with which it can be spatially distributed. This enables conditions of slope and aspect to be accounted for, something of which a purely temperature based melt index is incapable. In very steep topography this can be of importance especially if sub catchment and spatial outputs are to be utilised.

4.4 Model tuning

For optimal model operation in the Lake Pukaki catchment, the various model parameters require tuning. With each modification to SnowSim, the parameters were retuned to find optimal output. The change in model performance following modification using tuned parameters provided the basis on whether the modification was an improvement or not. The parameters requiring tuning varied with the inclusion of the radiation component as set out in Table 10.

Table 10. Parameters requiring tuning depending on model version.

Parameters requiring tuning	*Without radiation component*	*With radiation component*
Snow/rain temperature threshold	✓	✓
Minimum temperature melt factor	✓	✓
Maximum temperature melt factor	✓	n/a
Clear sky coefficient	n/a	✓
New snow albedo	n/a	✓
Old snow albedo	n/a	✓

For each model version the likely physical limits of parameters were determined and then the model was run with various combinations of the parameters. Optimal parameters were then selected by comparison of model outputs against two independent sets of measurements:

1. The model output for daily snow water equivalent at the grid square overlying the Rose Ridge Climate Station point location was compared to that measured at Rose Ridge for the 2002 snow year.
2. The model output for total daily catchment rain plus melt (free water) was compared to the measured lake inflows for the 2002 snow year. To remove the influence of channel propagation delays, 14 day running means were used for both the model output and lake inflow data.

For both sets of data the NTD criterion as set out in Section 4.5 below, was used to determine the quality of model output.

Following optimization, further model outputs were generated while varying a single parameter at a time. Graphical and numerical criteria were used to compare the model outputs. In this way the sensitivity of the model to each parameter was explored both in general terms and with regard specific aspects of the snow storage season.

4.4.1 Rose Ridge measurement comparison

The Rose Ridge climate station includes ultrasound snow depth sensors, a snow pillow, and a weighing bucket rain gauge. The data from these instruments enable an estimation of the daily snow water equivalent of the snow pack. The four-times-a–year snow survey at the site enables relating the point site measurement to the local average. In using these data for tuning the model an assumption is made that the measurements can be related to the nearest 1 km by 1 km grid square model output. To this end, the DEM for the model was artificially modified to ensure that the elevation, aspect and slope of the Rose Ridge grid square, were the same as at the actual Rose Ridge climate station site.

A graph of daily snow water equivalent for 2002 was prepared from the Rose Ridge data. Daily model output of snow water equivalent for the Rose Ridge grid square was plotted over the measured data. The magnitude and timing of the differences between the modelled and measured data provided an indication of the parameters that required adjusting. Large variations at the beginning of the winter indicate snow accumulation processes are not well modelled whereas large variations at the end of the summer indicate that snowmelt processes are not well modelled. Step increases in either modelled or measured data not apparent in the other indicate threshold values are inaccurate.

The realization that a degree-day model is inherently an averaging process is required to ensure that over tuning, resulting in the inability to find an optimal set of parameters does not occur.

4.4.2 Lake inflow measurement comparison

Lake inflow data is calculated by NIWA through consideration of lake level, canal inflow and lake outflow records. Daily values are provided. To enable comparison of modelled snowmelt data to be compared to measured lake inflow a water balance approach is taken:

$$Q = P_r + M_s + M_{ice} - E \qquad \textbf{(15)}$$

Where:

Q = lake inflows

P_r = annual precipitation falling as rain

M_s = annual snowmelt

M_{ice} = annual ice melt

E = catchment evapotranspiration

P_r and M_s may be obtained from the SnowSim model. P_r is total catchment precipitation occurring at temperatures greater than the snow/rain threshold. M_s is the cumulative total daily reduction in snow storage. An estimation of annual ice melt may be made by assuming that the catchment is in negative ice balance equal to the long term annual reduction in ice storage, that is, lake inflow is the sum of total precipitation and long term ice melt less evapotranspiration.

$$Q = P + M_{lti} - E \quad \textbf{(16)}$$

Where:

P = annual precipitation

M_{lti} = long term annual ice melt

By combining equations (15) and (16) and rearranging for M_{ice} we get:

$$M_{ice} = P + M_{lti} - \left(P_r + M_s\right) \quad \textbf{(17)}$$

This enables total annual ice melt to be estimated from the modelled precipitation, modelled rainfall, and modelled snowmelt combined with the estimated long term annual ice loss.

The ice melt will vary from day to day in a similar manner to which snowmelt varies but with subtle differences because of the generally lower elevation of the ice, and the different physical properties of ice. SnowSim does not include an ice melt component so the annual ice melt has been simply divided by 365 and allocated to each day of the year as a constant.

SnowSim has no provision for down catchment flow propagation delay complicating comparison of daily measured lake inflows to modelled rain-plus-snowmelt. Delays between snowmelt to river level change of over a day have been measured in the catchment (Neale 1996). While the use of a rainfall-runoff model would provide daily runoff data (as has been done for the verification analysis, see section 4.5), its use in tuning SnowSim was considered inappropriate because of the difficulty in assessing whether differences between measured and modelled data can be attributed to SnowSim, or to the runoff model. As a means of enabling comparison, a 14 day running mean of the daily measured and modelled outputs have been used. This provides a means of assessing the model outputs for seasonal variations without the propagation delay influencing comparisons. The running mean acts as a filter on the daily data reducing the influence of the daily fluctuations on the measured to modelled comparisons.

Evapotranspiration and long term ice loss estimates are annual averages, whereas inflow, precipitation and melt are year specific. Evapotranspiration will vary from year to year depending on available water, solar radiation, vegetation cover air temperature, wind speed

and humidity. Long term ice loss also varies from year to year depending on climatic conditions, moraine conditions, snow conditions, influence of terminal lakes and the quantity of remaining ice available to melt. By not allowing for the annual variation in evapotranspiration and ice melt, an inherent error is introduced into the model. These areas provide opportunities for further development of the SnowSim model.

4.5 Verification criteria

The true test of a model is to apply it to data not used in optimisation. This acts as a check to see whether the model is of value generally or only holds true during its calibration period. By applying the model to new data without further optimisation then comparing outputs to measured values both for the calibration period, and the verification period, an indication of the integrity of the model can be found.

The World Meteorological Organisation compared results from eleven different snowmelt models to provide information for potential operational users (WMO 1982; WMO 1986). Ten years of data from a variety of catchments from around the world were provided including measured output data for the first six years for model testing. The models were calibrated on the first six years of data, and then run on the last four years. Model outputs were compared to measured outputs for the last four years. A range of verification criteria were set out to enable intercomparison of results. Following the intercomparison it was recommended that the verification criteria derived should be used as a basic set for future model comparisons (WMO 1986). The verification involved three graphical and nine numerical criteria. The catchments modelled in the WMO are all in continental locations with significantly lower flows than those measured in the Lake Pukaki catchment, especially those resulting from rainfall events. Table 11 shows the verification criteria results for the Dunajec River (680 km^2) in Poland for the verification years 1975 – 1979 from the WMO model intercomparison exercise. While smaller than the Lake Pukaki catchment, the flow regime is characterised by several peaks throughout the year with a general increase in flow during summer. By way of comparison this catchment was selected as the closest example to the Lake Pukaki catchment. These criteria were used for the SnowSim outputs. This ensures a standard criterion set is used, enabling comparison of the model results to those gained from other models. The criteria are primarily comparing modelled and measured flow data as this is considered the output of primary importance to most operators. As SnowSim does not include a flow propagation component, the 14 day running mean of the modelled catchment free water (melt water plus rainfall) is compared to the 14 day running mean of lake inflow measurements.

Table 11. Verification criteria results for various snowmelt models operating on the Dunajec River in Poland, using data from 1975 to 1979 (Source: WMO 1986).

Name	*CO*	*NTD*	*(1-NTD)VER / (1-NTD)CAL*	*NTM*	*S*	*R*	*A*	*PD*
CEQUEAU	0.89	0.73	0.87	0.65	0.61	-0.02	0.31	0.08
ERM	0.81	0.45	1.90	0.71	0.86	-0.02	0.42	0.06
HBV	1.00	0.74	1.38	0.86	0.6	0.02	0.3	0.09
SSARR	0.94	0.55	1.05	0.73	0.78	0.02	0.34	0.09
Tank	0.87	0.79	1.28	0.88	0.53	0.04	0.27	0.06
UBC	0.88	0.71	1.19	0.86	0.63	-0.08	0.34	0.10

In this way, effectively 2 weeks of model output is compared to measured flow at anyone time. The model was calibrated using 2002 data, and verified using 2000, 2001 and 2003 data. The numerical criteria set of the WMO has been reduced to eight as the ninth criterion requires more than one year of calibration data to be calculated.

4.5.1 Graphical criteria

1. Linear scale plots of modelled catchment free water (fourteen day running mean) and measured lake inflows (fourteen day running mean) plotted separately for the calibration and verification periods. This provides an overview of the accuracy of the model in terms of discharge through time.
2. Flow duration curves of modelled catchment free water (fourteen day running mean) and measured lake inflows (fourteen day running mean), with the vertical scale in runoff/average runoff. The horizontal scale is percent of time that the runoff is equalled or exceeded plotted separately for the calibration and the verification period. This provides an indication of how well the frequency of different flow rates is computed.
3. Scatter diagrams of modelled monthly maximum catchment free water and measured lake inflows, plotted separately for the calibration and the verification period. This provides an indication of how well the peak flow volumes are computed.

4.5.2 Numerical criteria

All these criteria are computed using fourteen day running mean free water and lake inflows in $m^3 s^{-1}$. For ease of notation modeled results are called “computed” and given a “c” subscript, while measured results are called “observed” and given an “o” subscript.

1. Ratio of standard deviations of computed to observed discharges:

$$CO = \sqrt{\frac{\sum \left(y_c - \bar{y}_c\right)^2}{\sum \left(y_o - \bar{y}_o\right)^2}} \quad \textbf{(18)}$$

This provides a measure of how the variation in the computed discharges matches the variation in the observed discharges. An output of 1 would indicate the variability of the computed and observed discharges were the same. A value greater than one indicates the computed discharges have a greater variation, whilst a value less than one indicate the computed discharge has a smaller variation.

2. One minus the ratio of the sum of squares of the daily errors to the centred sum of squares of the daily observed discharges for mean daily discharges:

$$NTD = 1 - \frac{\sum \left(y_c - y_o\right)^2}{\sum \left(y_o - \bar{y}_o\right)^2} \quad \textbf{(19)}$$

This criterion gives an indication of how the daily error of the computed discharge compares to the seasonal variation in observed discharge. This assesses how much better the computed discharge is than the average discharge. A value close to 1 indicates the daily computed discharge error is much less than the seasonal variation in flow. A number close to 0 indicates the daily computed discharge error is as good as the seasonal flow variation while a number less than 0 indicates the daily computed discharge error is a worse indication of observed discharge than the average observed discharge.

3. Ratio of the quantity (1 - *NTD*) for the verification and calibration periods:

$$\frac{\left(1 - NTD\right)_{VER}}{\left(1 - NTD\right)_{CAL}} \quad \textbf{(20)}$$

This criterion provides an indication of how well the model performs on new data. A value greater than 1 would indicate performance on the new data is worse than that achieved on the calibration data. A value of 1 or less would indicate the model performance on new data is equal to or better than that achieved with the calibration data.

4. Ratio of the sum of the squares of the monthly residuals to the centred sum of the squares of the monthly observed discharges for mean monthly discharge:

$$NTM = \frac{\sum (y_o - \bar{y}_o)^2 - \sum (y_c - y_o)^2}{\sum (y_o - \bar{y}_o)^2} \quad \textbf{(21)}$$

This criterion provides an indication of how well the model performs at a monthly timescale. A value of 1 indicates computed and observed monthly variations are identical. A value less than 0 indicate the computed monthly variations are greater than the observed monthly variations. A value greater than 0 indicates the computed monthly variations are less than the observed monthly variations.

5. Ratio of the standard deviation of the errors to the mean observed discharge:

$$S = \frac{\sqrt{\frac{\sum (y_c - y_o)^2}{n}}}{\bar{y}_o} \quad \textbf{(22)}$$

This criterion gives an indication of the relative size of the standard deviation of the discharge error. A value of 0 would indicate no error. A value of 1 would indicate the standard deviation of the discharge error is equal to the average discharge flow.

6. Ratio of the mean error to the mean observed discharge:

$$R = \frac{\sum (y_c - y_o)}{n \cdot \bar{y}_o} \quad \textbf{(23)}$$

This criterion is similar to the previous one except it measures the relative size of the discharge error. A value of 0 indicates no error, a positive value indicates the discharge is on average over estimated, a negative value indicates the discharge is on average underestimated. A value of +/- 1 indicates the average error is equal to the average discharge.

7. Ratio of absolute error to the mean observed discharge:

$$A = \frac{\sum |y_c - y_o|}{n \cdot \bar{y}_o} \quad \textbf{(24)}$$

This criterion is similar to above except that it does not allow for positive and negative errors to cancel each other out. A value of 0 is a perfect model; a value of 1 indicate the absolute error is equal to the average discharge

8. Ratio of the sum of absolute errors to the total observed runoff volume:

$$PD = \frac{\sum_{i=1}^{N} |V_{oi} - V_{ci}|}{\sum_{i=1}^{N} V_{oi}}$$

(25)

This criterion gives a relative measure of the computed discharge volume error. A value of 0 indicates no error in computed discharge volume. A value of 1 indicates the computed discharge volume error is the same as the observed discharge volume.

y_o = observed discharge

$\bar{y}_o$ = mean observed discharge

y_c = computed discharge

$\bar{y}_c$ = mean computed discharge

n = total number of observations

N = number of snowmelt years

$\bar{y}_{od}$ = mean daily observed discharge for each day of the year derived from the calibration period

V_{oi} = observed runoff volume during snowmelt year i

V_{ci} = computed runoff volume during snowmelt year i

This array of graphical and numerical criteria provides a comprehensive analysis of the models effectiveness. The use of this standard set enables simple comparison with other models and provides a mechanism for high lighting the strengths and weaknesses of the model in a robust quantitative manner.

4.6 Summary

Implementation of SnowSim on to a GIS platform is to be carried out in a manner which breaks SnowSim into modular components of temperature estimation, precipitation estimation and snow storage estimation. Through the use of application specific scripts, automation of repeated applications of SnowSim will be possible. This in turn allows for model trials using various parameter combinations enabling identification of optimal parameter sets. Following optimisation, model sensitivity to individual parameters will be carried out, again utilising the model scripts.

Three separate model modifications are to be investigated: use of a measured lapse rate, use of a new precipitation distribution system and inclusion of a radiation component.

Optimisation of the model will occur prior to and following each modification to ensure the best possible results are being compared. Following each modification, model outputs will be

compared to measured data and an assessment of the modifications success carried out. Application of the best performing catchment scale model will be made to new data and standard verification criteria established. This will provide a means of identifying model strengths and allow for comparison for similar models applied in other regions of the world.

5 Model optimisation

5.1 Introduction

This chapter describes the results of the optimisation of the GIS implemented SnowSim and analyses the sensitivity of the model to the various parameters. Snowmelt measurements from the Rose Ridge climate station are first described followed by tuning of the model to these measurements and sensitivity analysis of the model to the various parameters. The lake inflow measurements are then presented with tuning of the model to these measurements, and further sensitivity analysis of the model to its parameters.

5.2 Rose Ridge data

Snow and meteorological data were used from the Rose Ridge climate station situated at 1940 m in the Murchison Valley beneath Rose Peak within the catchment. The location of the climate station with reference to the Aoraki / Mt Cook Village is shown in Figure 22.

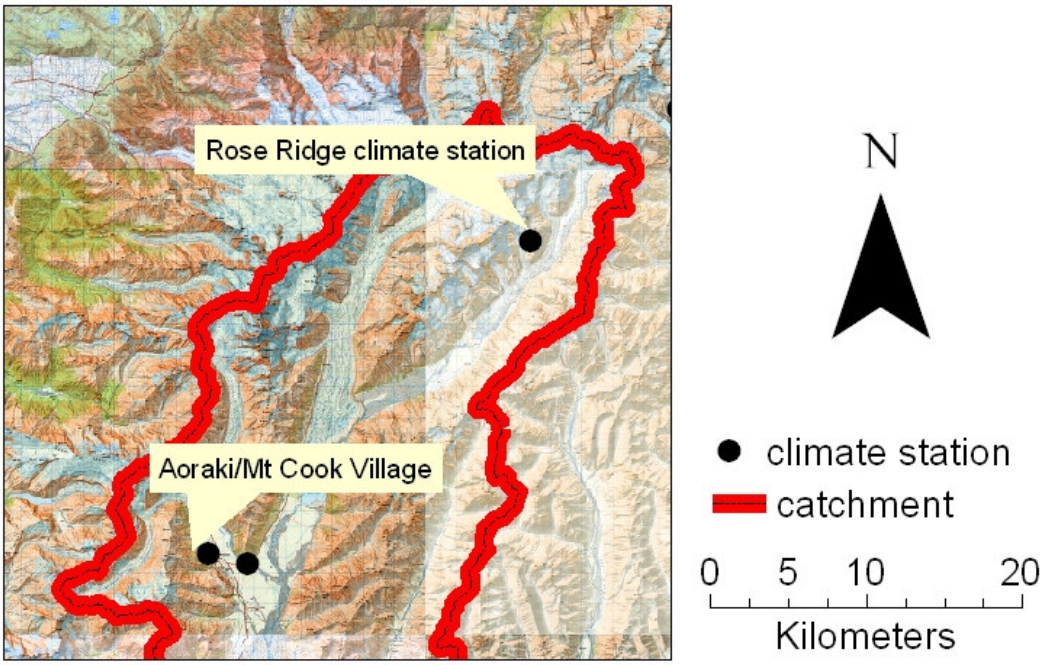

Figure 22. Rose Ridge climate station location.

Data from the station have been managed by NIWA since 2000, and includes hourly rainfall, snow weight, snow depth, snow temperature, air temperature, wind direction, wind speed, and humidity (Halstead et al. 2003). Sensor maintenance has been difficult since installation. In particular the snow pillow, snow stage sensors and weighing bucket rain gauge have been

problematic. This is partly because of the location of the climate station with its accompanying extreme weather but is also a result of limited opportunities for maintenance. The climate station is visited briefly just four times a winter resulting in data gaps during the delay between equipment failure and the next scheduled site visit.

During the site visits snow depth and density measurements are manually taken at five different locations within the vicinity (including one directly beneath the climate station instrument tower) as a means of measuring the average snow water equivalent for the area (see Table 12).

Table 12. Snow course measurements at Rose Ridge for 2002 (Data source: NIWA, Tekapo). Measurements in mm.

	Date							
	5th Jul		***20th Aug***		***4th Oct***		***5th Dec***	
	SWE	***Depth***	***SWE***	***Depth***	***SWE***	***Depth***	***SWE***	***Depth***
Station 1	577	1710	560	1580	813	3510	847	2200
Station 2	707	1890	487	2080	820	3480	960	2190
Station 3	667	2090	603	2390	1073	3740	880	2410
Station 4	770	2510	653	2850	840	3210	853	2050
Climate Station	560	1960	400	1040	823	2510	560	1000
Average	656	2030	541	1990	874	3290	820	1970
Automatically measured	408	2910	536	2820	823	3920	755	2560

The location of the climate station within the seasonal snow zone of the upper catchment makes it ideal for comparison to model outputs. As such the climate station data are not used as model input but are used for calibration of model parameters. The 2002 snow year was chosen for the calibration year as a near complete data set was available for the period, though a data gap does exist between the 17th September and the 4th of October of that year. Snow water equivalent measurements obtained from the climate station are shown in Figure 23. The manual snow course measurements provide a means of relating the automatically derived snow water equivalent measurements to the local area average. Three depth and snow water equivalent measurements are taken at each station. The average measurements for each station for 2002 are shown in Table 12. A correlation coefficient of $R^2 = 0.69$ was found between the snow course and automatic snow water equivalent measurements. A ratio of 0.9:1 describes the relationship between the automatic and local average snow water equivalent measurements.

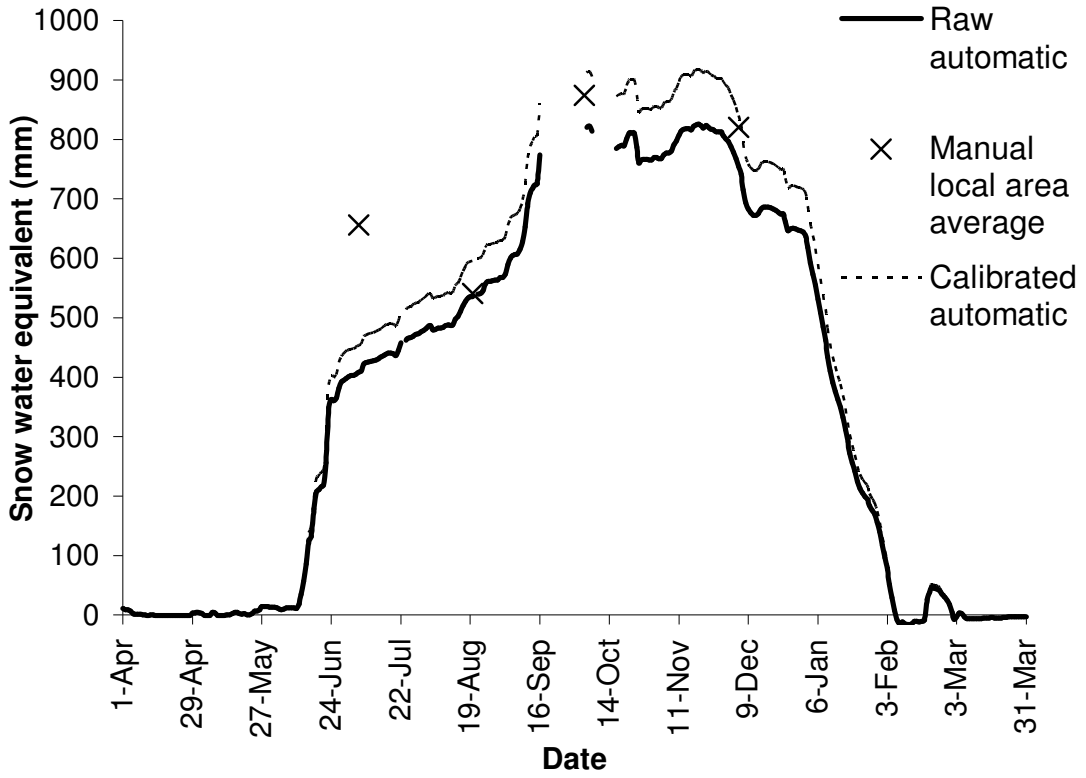

Figure 23. Snow water equivalent measurements at Rose Ridge during 2002-2003 (Data source: NIWA, Tekapo with permission of Meridian Energy Ltd.).

The snow depth record obtained is shown in Figure 24. Depth measurements can be related to snow water equivalent measurements through consideration of snow density. During and immediately after a snowfall the snow density is likely to be low, with the snow settling (and hence reducing the snow pack depth) over time. This is why the snow depth measurements show a high frequency variation not seen in the snow water equivalent measurements obtained from the snow pillow. The snow density is also likely to be less during the early winter when temperatures are lower (Owens et al. 1983). This explains the apparent difference in profile during June and July between the snow depth and snow water equivalent measurements. The snow pillow indicates complete melt at 7th February, while the snow depth sensors record complete melt on the 22nd January. This indicates a deeper snow pack at the snow pillow site than at the snow depth site, demonstrating the variability of snow pack measurements and the difficulty in utilising single site measurements to represent an area. This difference also results in an inability to directly ascertain snow density measurements by combining the snow weight and snow depth measurements together. To further complicate matters, the snow pillow recorded small negative weights after 7th February (not shown on the graph) suggesting the instrument had a temporal drift in its calibration. This would tend to

underestimate snow water equivalent. In the worst case this amounts to 18 mm of snow water equivalent which is less than 0.02% of the range.

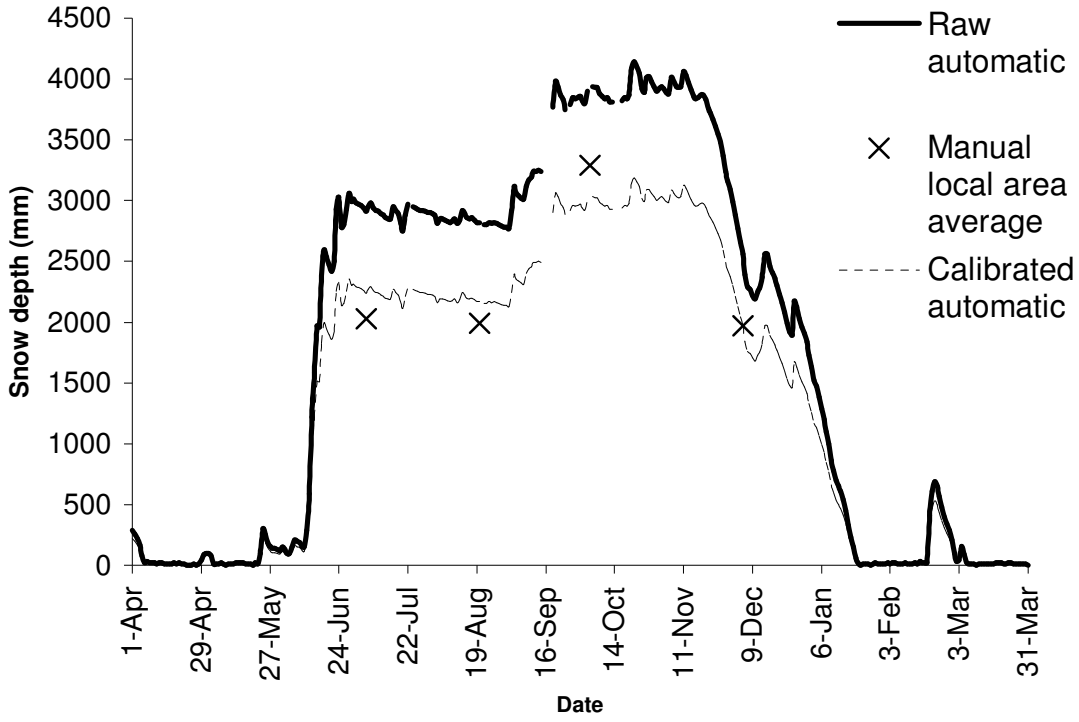

Figure 24. Snow depth measured at Rose Ridge during 2002-2003 (Data source: NIWA, Tekapo with permission of Meridian Energy Ltd.).

A correlation coefficient of $R^2 = 0.95$ was found between the automatic snow depth measurements and the average manual snow course depth measurements. A ratio of 1.3:1 describes the relationship between the automatic snow depth measurements and the manual local average snow depth measurements.

The seasonal variation in snow storage for 2002 shows an initial snowfall at the beginning of the snow year (in April) which completely melts out shortly after. Very little snow fell until late May, when steady snow accumulation culminated in a very large storm from the 11th June until the 18th June (192 mm of snow water equivalent) signifying the first large snowfall of the winter. This was followed shortly after by another large fall (119 mm of snow water equivalent) in just three days on the 22nd - 24th June. Snow continued to accumulate until a peak of 917 mm snow water equivalent on the 19th November, though the depth of snow peaked a month earlier on the 22nd of October following a new snowfall. From this time on the snow steadily melted until early February, by which time it had all gone. Of note is that throughout the winter occasional days of ablation occurred, though the frequency and

magnitude of these events increased from October onwards. The maximum ablation of 28 mm snow water equivalent occurred on the 10th January during an extensive two week period of high ablation averaging 19 mm of snow water equivalent ablation per day.

5.3 Comparison of modelled and measured snow storage at Rose Ridge

The modelled SnowSim snow water equivalent for Rose Ridge using the parameter values set by McAlevey (1998) in the New Zealand wide implementation of SnowSim (see Table 6 in section 4.2.2) is shown in Figure 25.

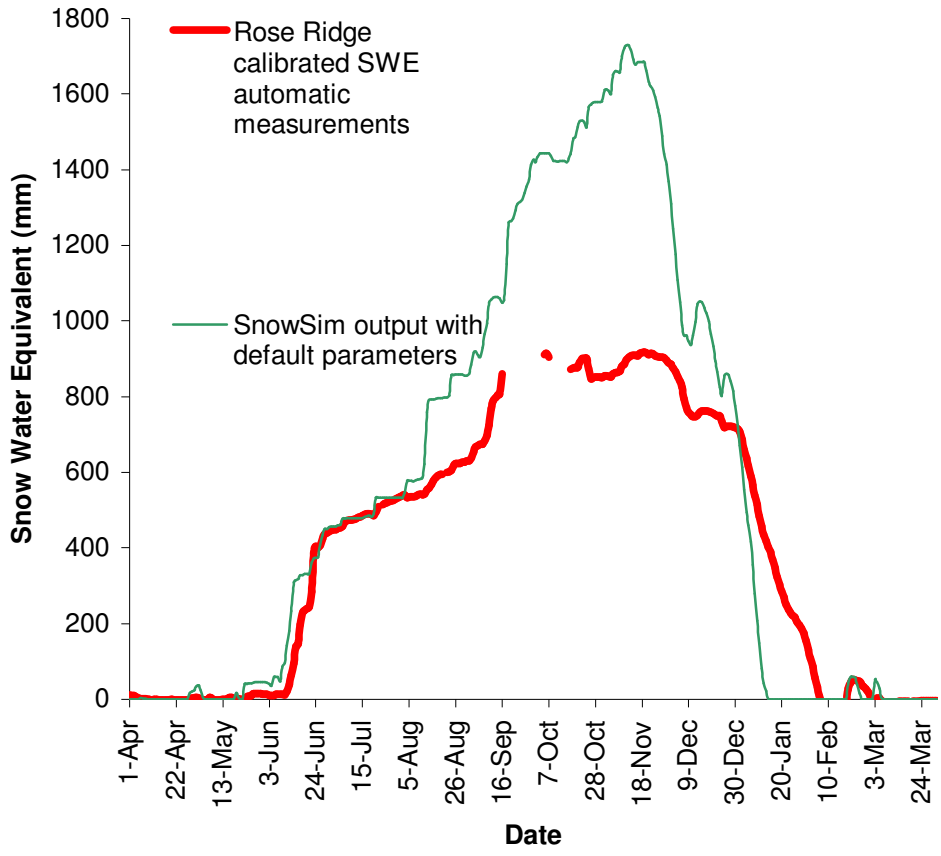

Figure 25. Modelled and measured snow water equivalent for 2002 at Rose Ridge.

The onset of snow accumulation is modelled well in early June. The model shows a much more stepwise increase in snow accumulation than the measured values, though it keeps reasonable track of total volume. Of particular note within this period is a large modelled snowfall in mid August which is not seen in the measured values. From mid September until mid November, the model continues to accumulate snow to a maximum of 1729 mm snow

water equivalent, whereas measurements show snow accumulation reaching a plateau during this period of just 900 mm snow water equivalent. The onset of snow ablation occurs at mid November for both the modelled and measured snow water equivalents. However modelled snow ablation is much more rapid than that which was measured. Overall the model appears to overestimate snow accumulation with an extended snowfall season, and overestimates the rate of ablation. The result of both of these inaccuracies is a close approximation to the length of the snow season. The NTD criterion (see section 4.5, equation (19)) for the modelled SWE output compared to the measured SWE is 0.26.

5.3.1 Lapse rate parameter

Daily lapse rates as measured from the Rose Ridge and Mt Cook climate station temperature data for the year 2002 are shown in Figure 26. The average lapse rate for the year is 0.0055 ^{o}C m^{-1}. If just the time is considered when snow is on the ground at Rose Ridge (from 13th May until 3rd March) then the average is 0.0056 ^{o}C m^{-1}.

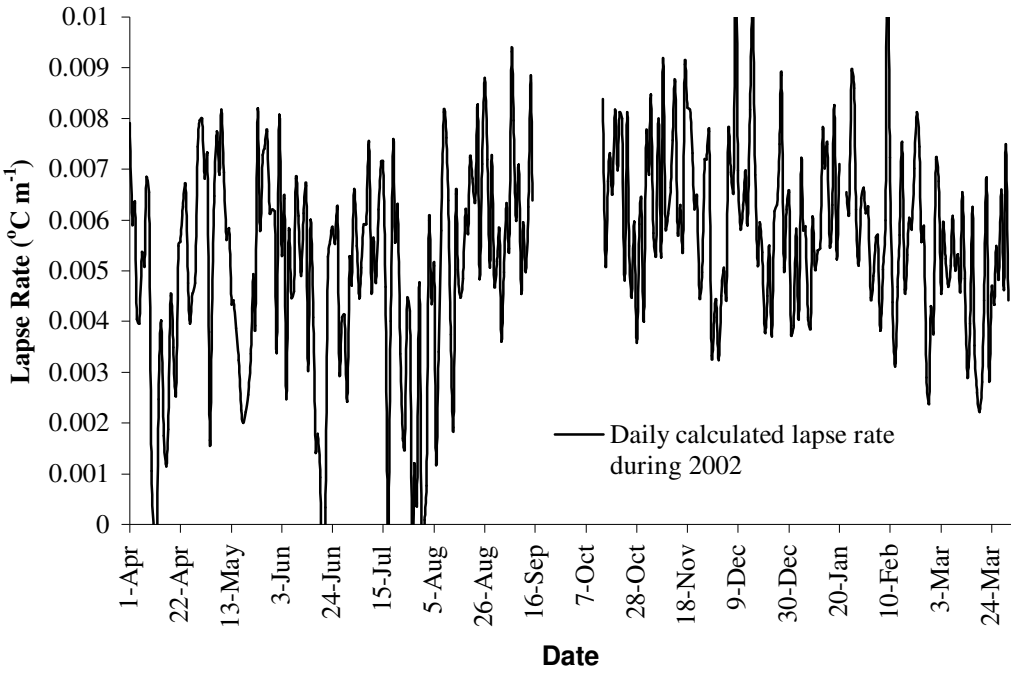

Figure 26. Daily measured temperature lapse rate from Rose Ridge and Mt Cook climate station temperature data.

A temporal variation in lapse rate is apparent at both the daily and seasonal level. A standard deviation of 0.0018 ^{o}C m^{-1} shows how variable the lapse rate is from day to day. Lower lapse rates occur during May until August and higher lapse rates occur during September until December. These measured lapse rates would indicate that a single lapse rate parameter is not

likely to represent the true conditions on any one day. This highlights a deficiency in the model that impacts on the temperature estimation of the model.

Modelled temperatures at Rose Ridge using different lapse rates are compared to measured temperatures for December 2002 in Figure 27. The variation in modelled temperatures for the different lapse rates is small compared to the variation in the temperature from day to day. The modelled temperatures do not estimate the peaks and troughs of the measured temperatures well, though the general trend of the temperature fluctuations is represented. As expected, the higher lapse rates model the lower temperatures well, while the lower lapse rates model the higher temperatures well. The best fit modelled temperature output for Rose Ridge is for a lapse rate of 0.0054 ^{o}C m^{-1} with an NTD criterion value of 0.87 between modelled and measured temperatures.

The effect of varying the lapse rate on modelled snow water equivalent is shown in Figure 28 (note: that the minimum melt factor, initial maximum melt factor, and snow/rain temperature threshold have been held constant at the default values of 3 mm ^{o}C d^{-1}, 8 mm ^{o}C d^{-1}, 2.5 ^{o}C respectively).

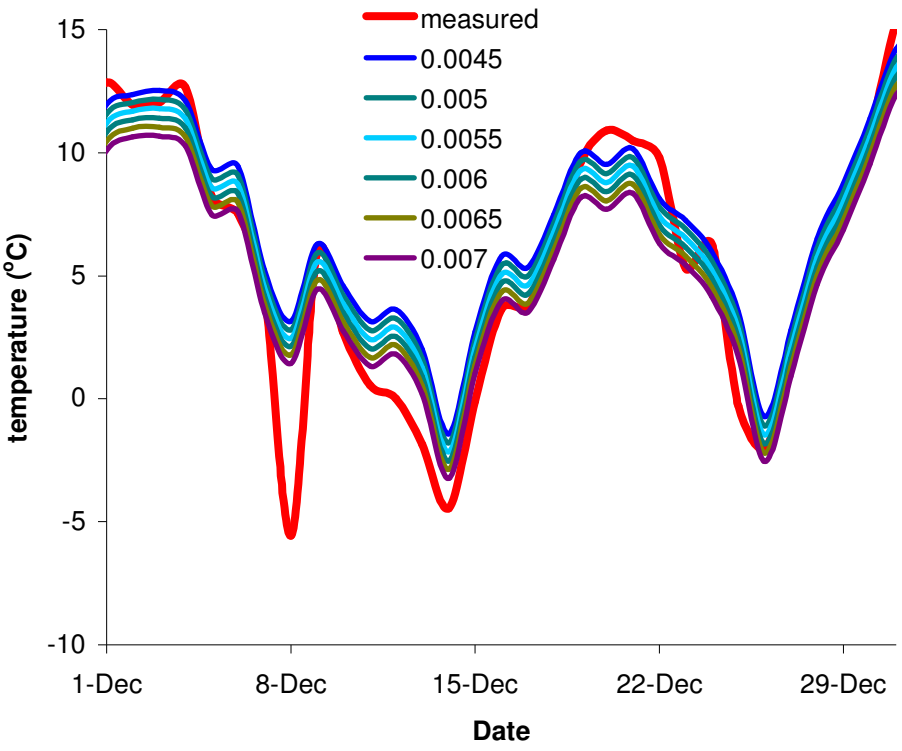

Figure 27. SnowSim temperature outputs for Rose Ridge with varying lapse rates (^{o}C m^{-1}) compared to measured temperatures.

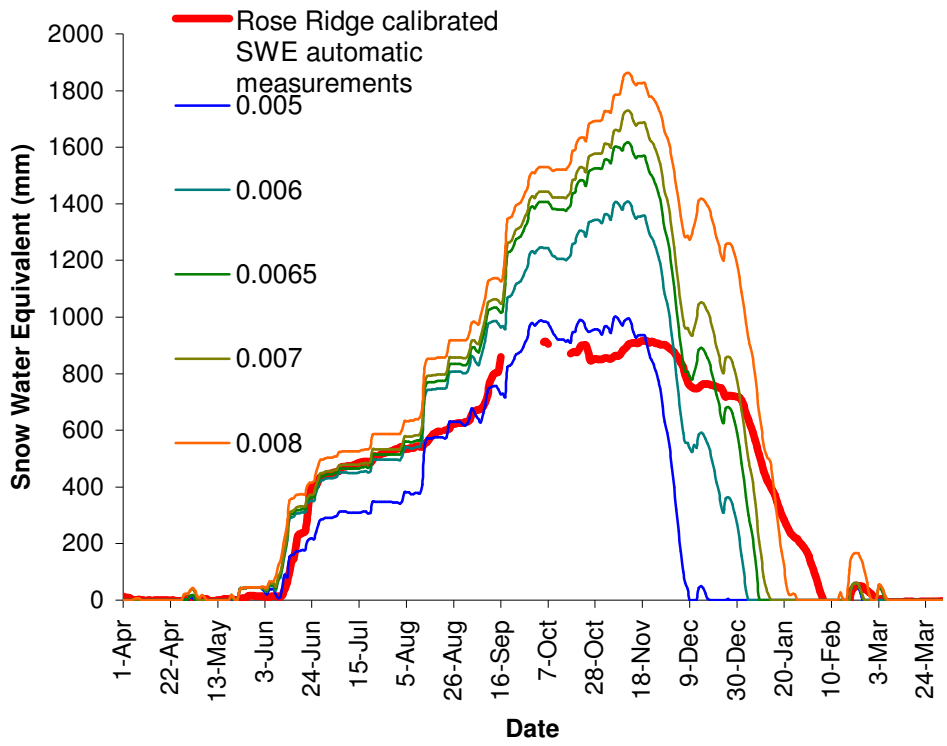

Figure 28. SnowSim snow water equivalent outputs for Rose Ridge point location with different lapse rates ($^{o}C\ m^{-1}$), compared to calibrated measured snow water equivalent.

As the lapse rate is increased (and hence the average modelled temperature decreases) the modeled snow accumulation also increases. This has a varying impact on the results at different times. The initial June snowfall is poorly modelled for the low lapse rate, while snow storage during September and October is modelled much better with the low lapse rate. All lapse rates still modelled the anomalous mid August snowfall indicating that it is not poor temperature modelling that caused that particular model-measurement mismatch. Sensitivity analysis (as shown in Figure 29) for the various lapse rates indicate that lapse rates have a significant impact on the model output, especially as the lapse rate moves away from the optimum.

The spatial variability of lapse rates is demonstrated by the measured lapse rates between climate station pairs as shown in Table 13 and Figure 30. Estimating a single lapse rate that is regionally and temporally representative is problematic. The average of the annual average daily lapse rates measured for the climate station pairs is 0.005 $^{o}C\ m^{-1}$ which is close to the optimized lapse rate of 0.0054 $^{o}C\ m^{-1}$ found for modelling the Rose Ridge air temperatures. These values are considerably lower than the default 0.007 ^{o}C used in the New Zealand version of SnowSim and may explain part of the reason why that model overestimates snow

accumulation at Rose Ridge. Following this analysis, a lapse rate of 0.005 ^{o}C has been selected as a more appropriate value for the operation of SnowSim in the Lake Pukaki catchment.

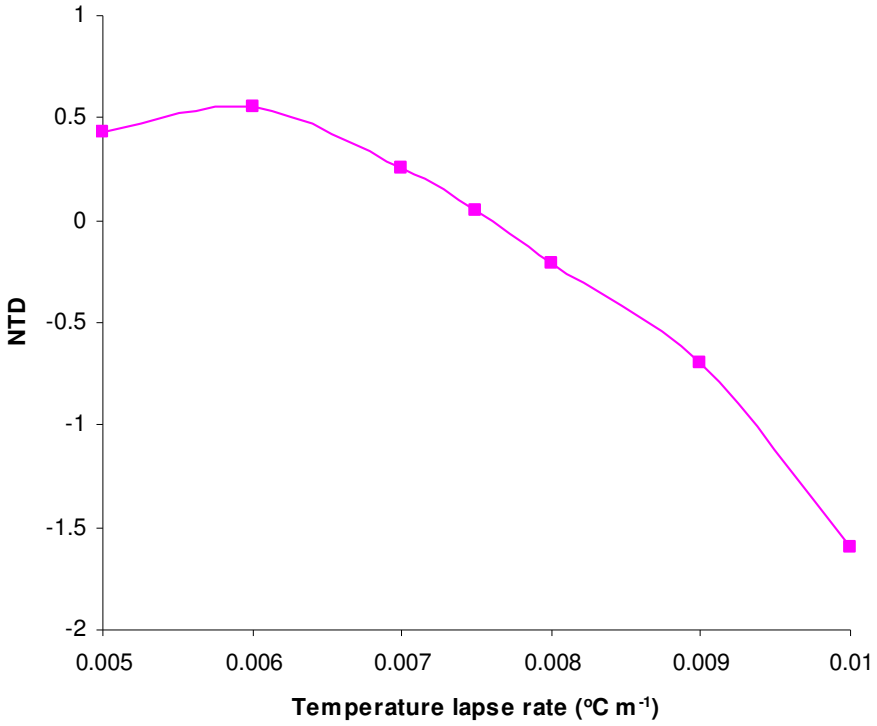

Figure 29. Sensitivity of accuracy of modelled snow water equivalent (as measured by the NTD criterion) to variations in temperature lapse rate.

5.3.2 Daily temperature estimation

Using the average of a day's maximum and minimum temperatures to provide a daily temperature may not be an accurate assessment of the temperatures experienced at a point. The assumption is made that the maximum and minimum temperatures represent equal samples of the daily temperature. This was assessed by comparing max, min averages with 15min daily averages at Rose Ridge. A correlation coefficient of r^2= 0.97 shows the closeness of the relationship; however, the best fit linear relationship equation is:

$$\overline{T}_{\min,\max} = \overline{T}_{15\min} + 0.4 \quad \textbf{(26)}$$

This indicates the average of the maximum and minimum daily temperature is an overestimation by nearly half a degree of the true daily average temperature. This is a similar result to that found by Cazorzi and Dalla Fontana (1986) as discussed in section 3.4.1. This is an important point when considering specific threshold temperatures used within the model.

Table 13. Measured annual average daily lapse rates between climate station pairs for 2002.

Climate Station 1	*Climate Station 2*	*2002 average daily temperature lapse rate ($^oC\ m^{-1}$)*
Mt Cook	Panorama	.0065
Mt Cook	Rose Ridge	.0055
Mt Cook	Franz Josef	.0032
Lake Tekapo	Boanerges	.0055
Mt Cook	Boanerges	.0061
Panorama	Eade Hut	.0068
Boanerges	Elcho Flats	.0034
Rose Ridge	Eade Hut	.0054
Franz Josef	Boanerges	.0048
Franz Josef	Panorama	.0050
Franz Josef	Rose Ridge	.0047
Rose Ridge	Panorama	.0048
Tekapo	Panorama	.0059
Tekapo	Rose Ridge	.0051
	Regional Average	**0.0050**

For instance a snow/rain threshold temperature of 2.5 ^oC would appear high from a physical stand point. However, as it is applied to maximum/minimum average temperatures it actually relates to a true 2 ^oC threshold temperature, which is more realistic. The greatest difference between the maximum and minimum average, and the 15 minute daily average for the 2002 snow year occurred on the 9th February 2003 when the max-min average was greater than the 15 min average by 6 ^oC. This is a significant difference that potentially results in 18 mm of ablation not modelled (assuming a melt factor of 3 mm $^oC^{-1}$ d^{-1}). This is an example of the temporal resolution of climate variables having an impact on the model output.

5.3.3 Parameter optimisation

To determine the optimum values for the remaining parameters (minimum melt factor, initial maximum melt factor, snow/rain threshold) for SnowSim, the model was run with various parameter combinations and the NTD criterion calculated from the model outputs.

The snow/rain threshold was restricted to 1.5 ^oC, 2.0 ^oC and 2.5 ^oC as these were considered the limits of physical reality. To limit the number of parameter combinations, only whole number melt factors were used. The combinations were restricted to physically reasonable values, though an initial maximum melt factor of 0 mm $^oC^{-1}$ d^{-1} was included as a lower limit even though this results in a melt factor of 0 mm $^oC^{-1}$ d^{-1} for two thirds of the year, which is unrealistic. This was done to show the trend in the optimization for initial maximum melt factors below 1 mm $^oC^{-1}$ d^{-1}.

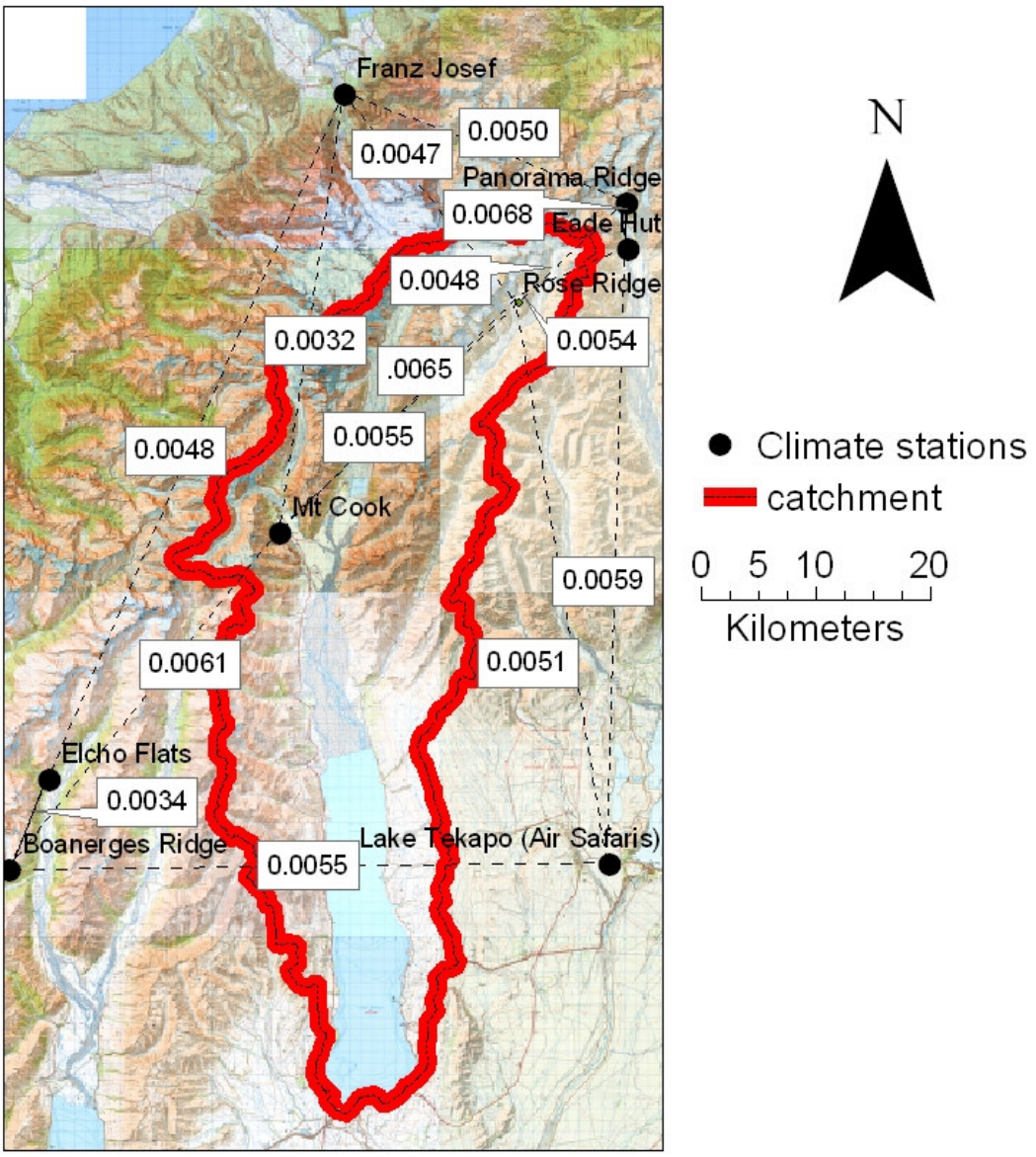

Figure 30. Measured annual average daily lapse rates between climate station pairs for 2002.

The optimisation graph of the NTD criterion for melt factor combinations with the lapse rate set to 0.005 $^{o}C\ m^{-1}$ and snow/rain temperature threshold set to 2.5 ^{o}C 2.0 ^{o}C and 1.5 ^{o}C are shown in Figures 31 to 33 respectively. These graphs show that a much lower initial maximum melt factor than the default improves model performance and that as the snow/rain temperature threshold reduces, the optimum minimum melt factor reduces, while the initial maximum melt factor increases.

The highest NTD criterion value of 0.93 was obtained with a minimum melt factor of 1 mm $^{o}C^{-1}\ d^{-1}$, an initial maximum melt factor of 1 mm $^{0}C^{-1}\ d^{-1}$ and a snow/rain threshold of 1.5 ^{o}C.

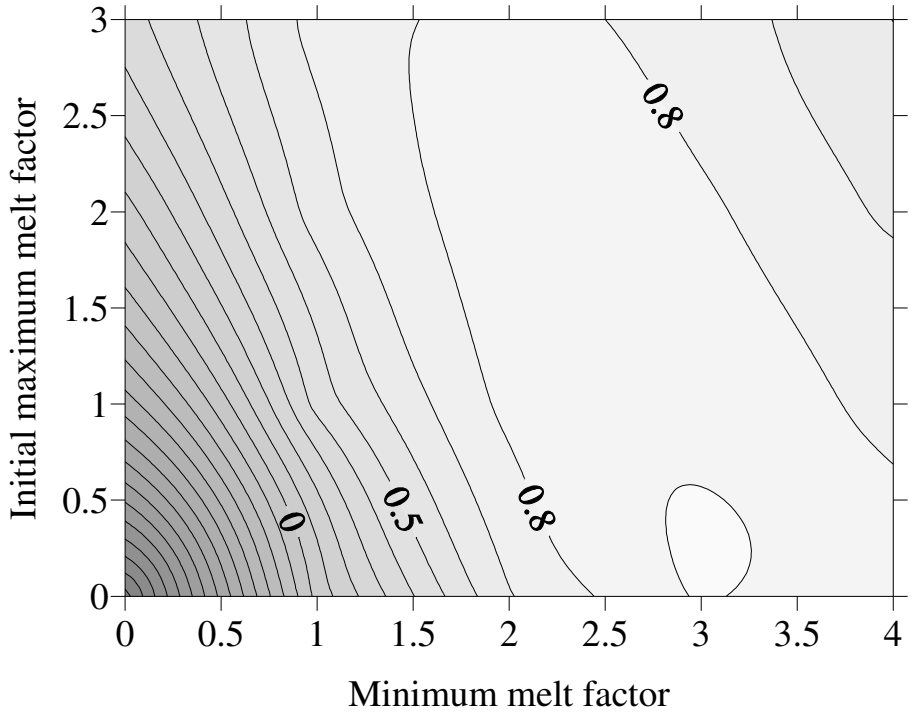

Figure 31. Modelled Rose Ridge snow water equivalent NTD criterion values for various melt factor combinations (units: mm $^{o}C^{-1}$ d^{-1}) with lapse rate set to 0.005 ^{o}C m^{-1} and snow/rain temperature threshold set to 2.5 ^{o}C.

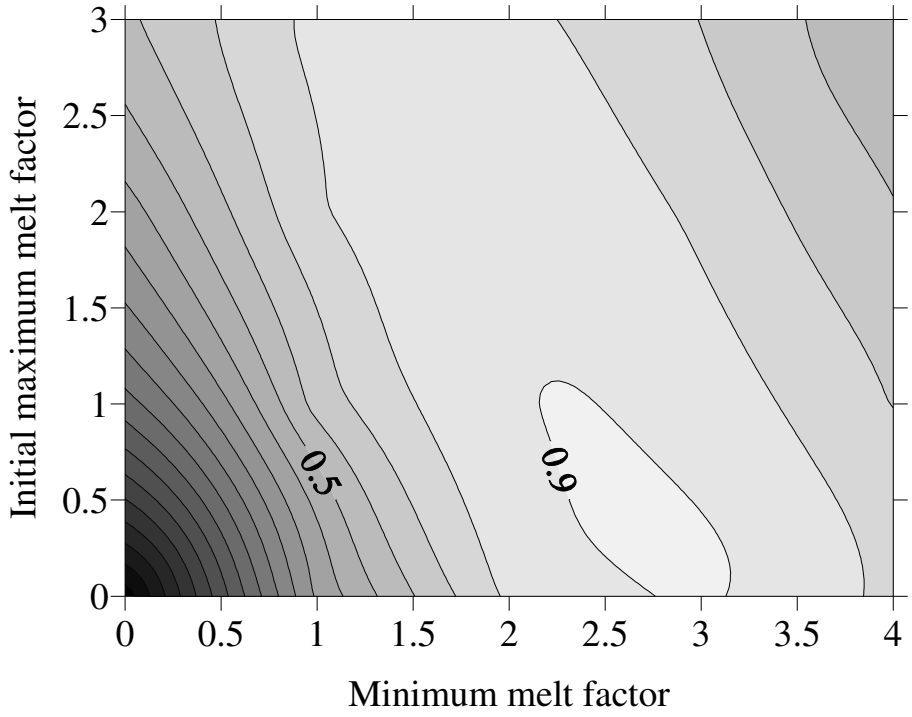

Figure 32. Modelled Rose Ridge snow water equivalent NTD criterion values for various melt factor combinations (units: mm $^{o}C^{-1}$ d^{-1}) with lapse rate set to 0.005 ^{o}C m^{-1} and snow/rain temperature threshold set to 2.0 ^{o}C.

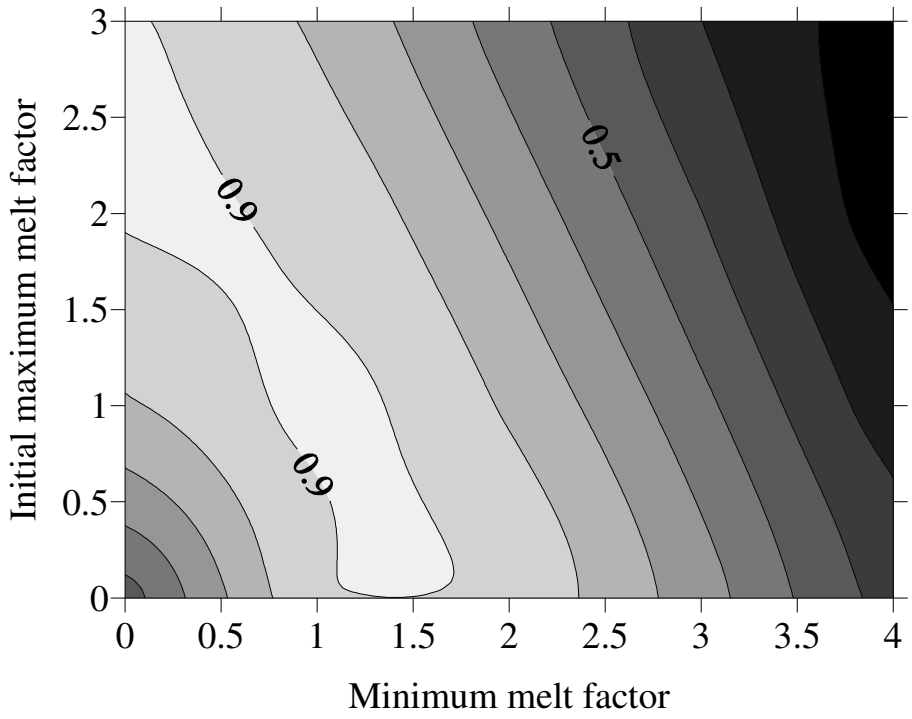

Figure 33. Modelled Rose Ridge snow water equivalent NTD criterion values for various melt factor combinations (units: mm $^{o}C^{-1}$ d^{-1}) with lapse rate set to 0.005 ^{o}C m^{-1} and snow/rain temperature threshold set to 1.5 ^{o}C.

The Rose Ridge SWE output for the optimised SnowSim is shown in Figure 34. The optimized parameters are significantly different to the default values used for New Zealand SnowSim. This demonstrates the regional specificity of the degree-day model. Of interest is the reduction in the melt factor parameters. The optimised values result in a range from 1 to 5 mm $^{o}C^{-1}$ d^{-1} which is more in line with other models as shown in Table 3.

5.3.4 Sensitivity to the minimum melt factor parameter

The result of varying the minimum melt factor (while retaining the other parameters at the optimum values) on modelled output is shown in Figure 35. The effect is most significant from mid September onwards when the modelled outputs become increasingly divergent. This is because the melt factor is of greater importance during ablation periods when the air temperature is greater than 0 ^{o}C. The sensitivity of the model to variations in the minimum melt factor is shown in Figure 36. This shows that the model output is sensitive to the minimum melt factor with the NTD criterion value dropping constantly as the minimum melt factor increases.

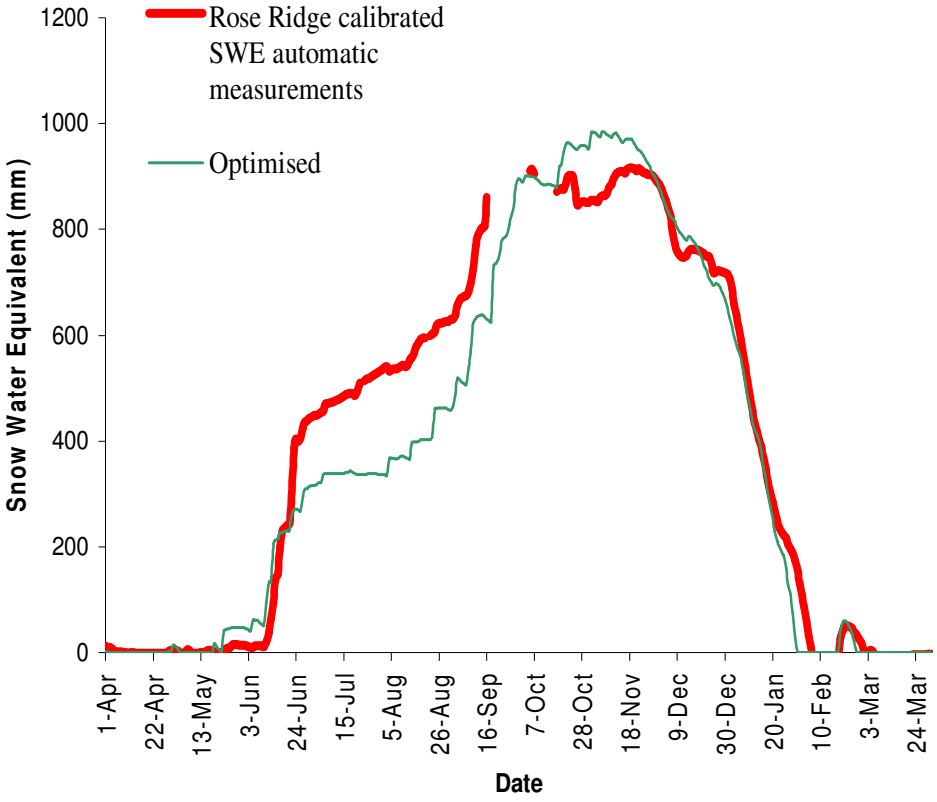

Figure 34. SnowSim snow water equivalent output using optimized parameters for Rose Ridge, compared to calibrated measured snow water equivalent.

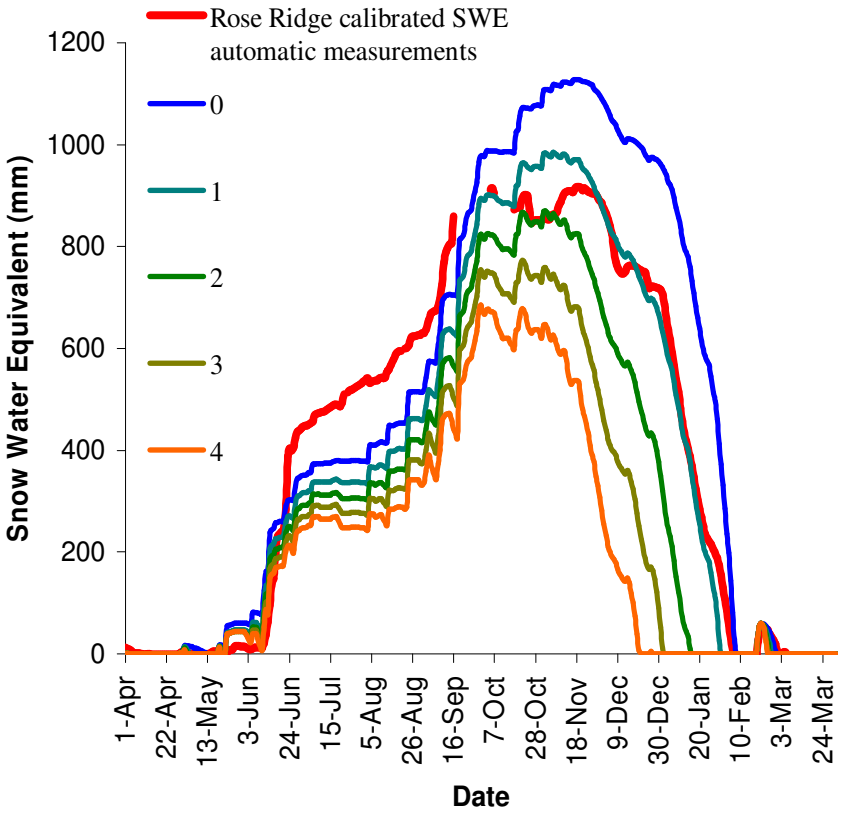

Figure 35. SnowSim snow water equivalent output for Rose Ridge with varying minimum melt factors (mm $^{o}C^{-1}$ d^{-1}), compared to calibrated measured snow water equivalent during 2002-2003.

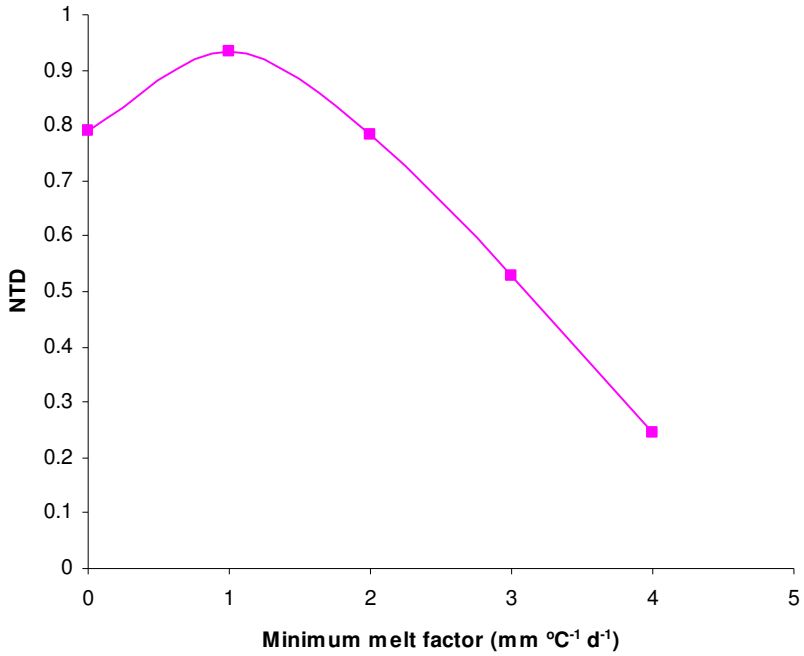

Figure 36. Sensitivity of accuracy of modelled snow water equivalent (as measured by the NTD criterion) to variations in the minimum melt factor.

5.3.5 Sensitivity to the initial maximum melt factor parameter

The effect of varying the initial maximum melt factor on modelled output (while keeping the other parameters at the optimum values) is shown in Figure 37. The variation of the initial maximum melt factor mainly affects the ablation period of the snow storage season with the effect becoming more pronounced as the year progresses. This follows the melt factor equation (equation (5), section 3.4.2) which shows the maximum melt factor to become increasingly significant as the year progresses. This is in contrast to the minimum melt factor, which has an equal effect throughout the year (though still dependent on temperature). Of note is the effect the initial maximum melt factor has on the rate of ablation. The sensitivity of the model to variations in the initial maximum melt factor is shown in Figure 38. This shows that the model is less sensitive to variations in the initial maximum melt factor than to changes to the minimum melt factor which follows when the shorter time period of effect is considered.

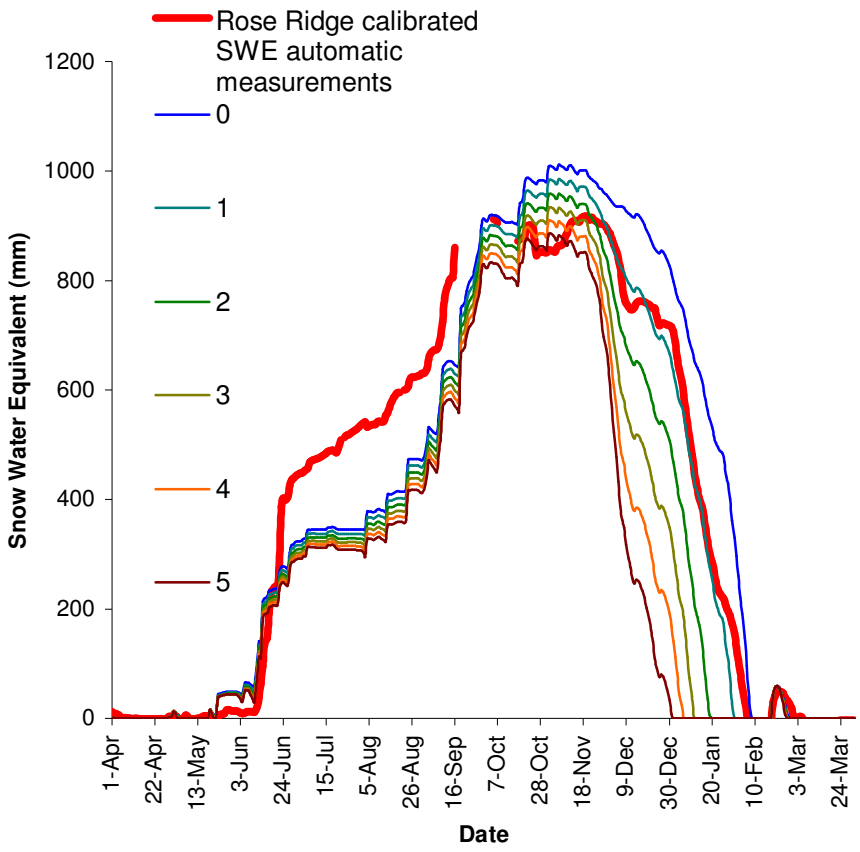

Figure 37. SnowSim snow water equivalent output for Rose Ridge with varying initial maximum melt factors (mm $^{o}C^{-1}$ d^{-1}), compared to calibrated measured snow water equivalent during 2002-2003.

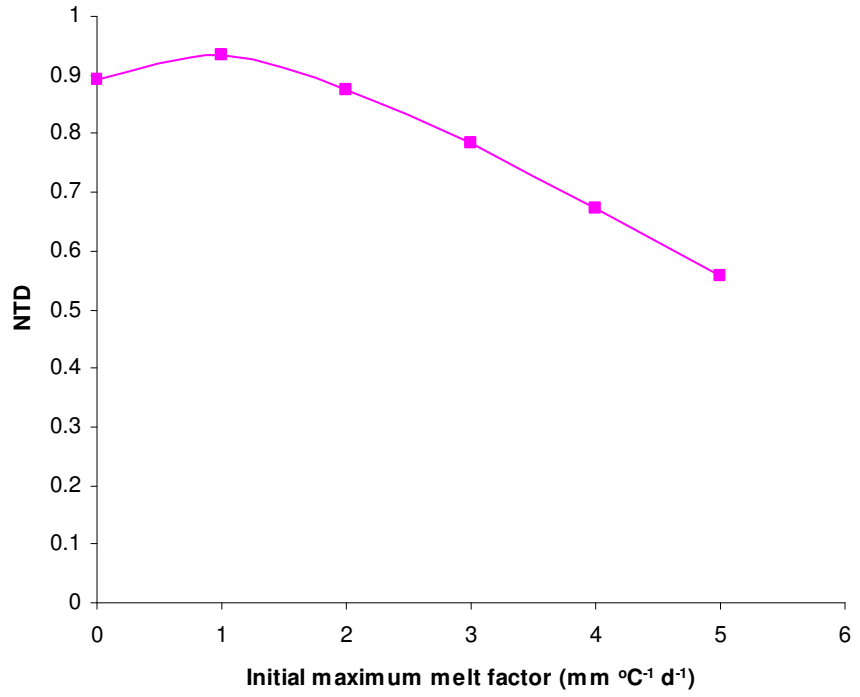

Figure 38. Sensitivity of accuracy of modelled snow water equivalent (as measured by the NTD criterion) to variations in the initial maximum melt factor.

5.3.6 Sensitivity to the snow/rain threshold parameter

The effect of varying the snow/rain threshold on modelled output is shown in Figure 39. This shows that the snow/rain threshold has a large influence on snow storage. The thresholds of 2 °C, 2.5 °C and 3 °C returned similar results for the year while the 1 °C and 1.5 °C thresholds returned much lower snow volumes with a closer approximation to that measured. The two lowest thresholds of 0 °C and 0.5 °C returned still lower snow volumes with less than half of the measured maximum volume modelled.

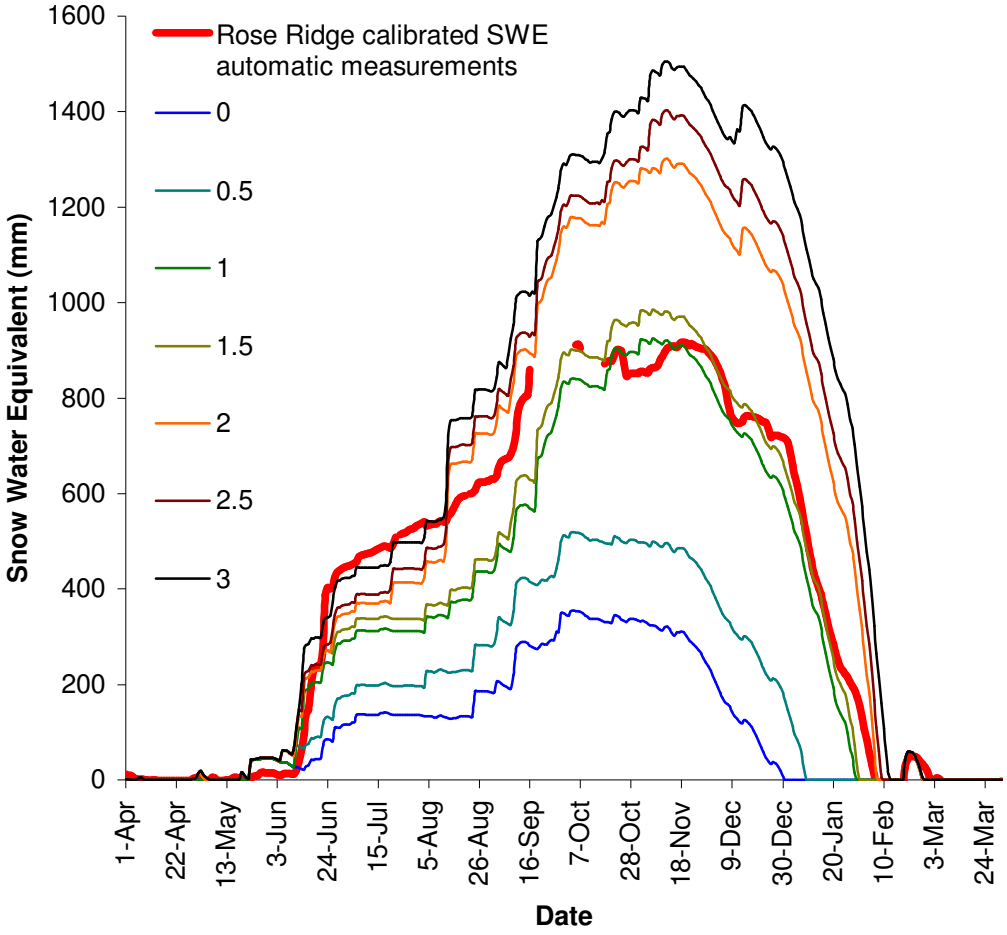

Figure 39. SnowSim snow water equivalent outputs for Rose Ridge with varying snow/rain threshold temperature (°C), compared to calibrated measured snow water equivalent during 2002-2003.

The particular threshold temperature plays a significant part in determining snow accumulation, especially when events occur on days with temperatures close to the temperature threshold. The snow increases of 13th August that are modelled (but not measured) with a snow rain threshold greater than 1.5 °C do not occur for the lower

temperature threshold. This would indicate that 1.5 ^{o}C may be a more appropriate snow/rain temperature threshold. The synoptic charts for the day (Figure 40) show a depression west of the South Island causing a strong northerly flow over the South Island. The warm sector of the depression crossed the island at midday on the 13th providing the large quantities of rain recorded (109 mm at Mt Cook, 158 mm at Franz Josef). By evening the cold front had crossed the island and the temperature dropped as shown by the 15 minute temperature data from Rose Ridge for that day.

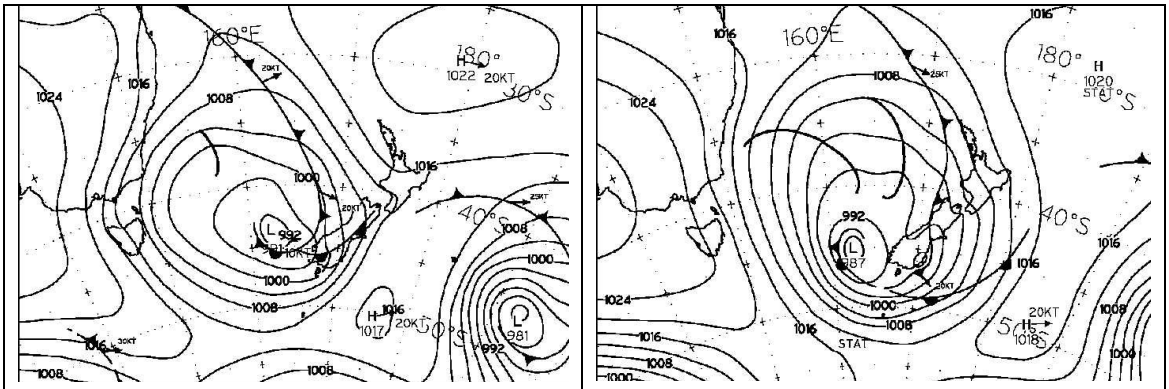

a) 1200 hours | **b) 1800 hours**

Figure 40. Mean sea level barometric pressure analysis on 13th August 2002 (Source: NZ Meteorological service).

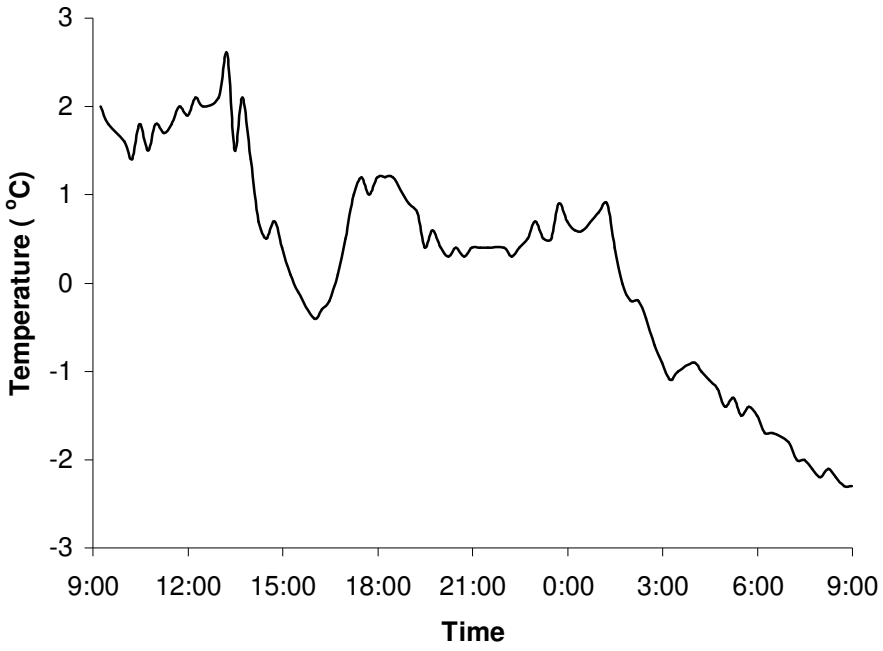

Figure 41. Temperature at Rose Ridge climate station between 0900 on the 13th and 0900 on the 14th of August 2002.

The reason no large snowfall was measured is most likely because of the morning precipitation falling as rain. This would indicate a true snow/rain threshold of less than 1.5 ^{o}C. Accounting for the 0.5 ^{o}C offset introduced through using the average of the daily maximum and minimum temperatures to provide a daily temperature (see section 5.3.2), a physically realistic snow/rain temperature threshold to be used in the model would need to be less than 2 ^{o}C. In this instance, however, because the daily average temperature is low (measured at 0.7 ^{o}C), the rainfall would still be modelled as snow. This demonstrates the temporal limitation of the model, where averaging of climatic conditions to daily values may cause significant inaccuracies. To complicate matters, snow was not modelled using the optimised parameters as the temperature estimated at Rose Ridge on the 13th was 1.7 ^{o}C, a good degree above what was measured. When combined with the snow/rain threshold of 1.5 ^{o}C the result is that the event is modelled correctly as rain. This is a case of two model inaccuracies; daily data averaging and a single constant lapse rate, cancelling each other out to provide a seemingly more accurate result than would normally be expected.

Sensitivity analysis of the snow/rain threshold is shown Figure 42. Thresholds of 1 ^{o}C and 1.5 ^{o}C return the highest NTD criterion values with a notable reduction for thresholds below this, and a gentler but still notable reduction in NTD criterion value for thresholds above this range.

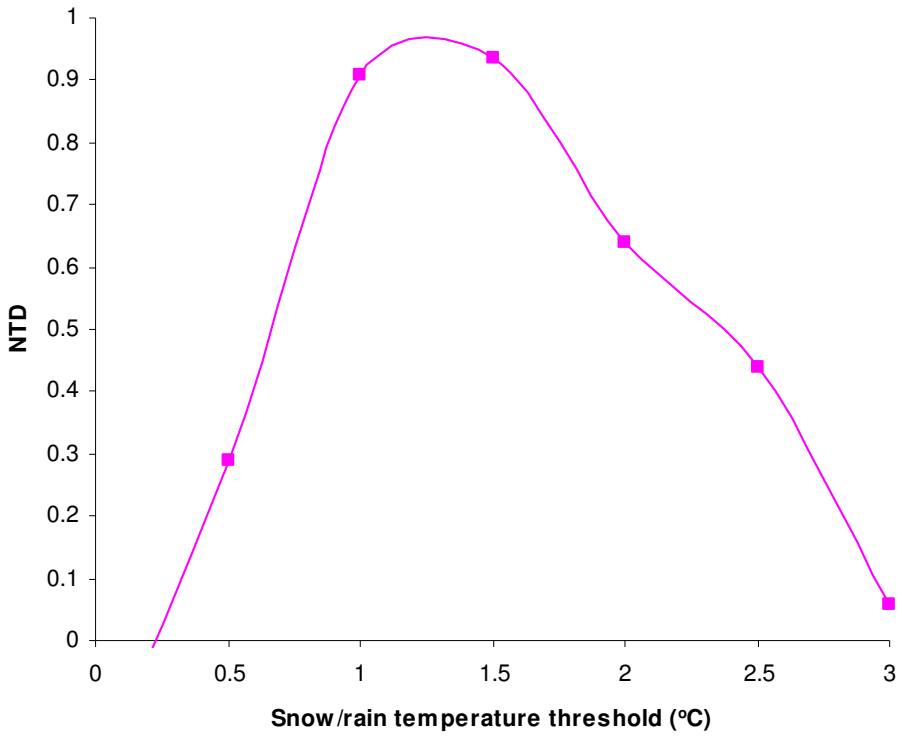

Figure 42. Sensitivity of accuracy of modelled snow water equivalent (as measured by the NTD criterion) to variations in the snow/rain temperature threshold.

5.4 Lake inflow data

Through measurements of lake level and lake outflow, lake inflows may be determined. Among other things, the information is used for electricity market analysis. As lake inflows are an integration of catchment wide processes, they provide a valuable insight into the general validity of the model. This provides a good balance to the site specific analysis carried out for Rose Ridge.

For calibration purposes the snow year of April 1st 2002 until March 31st 2003 has been used, which matches the time period used for the Rose Ridge SWE measurement comparison. The daily lake inflow data for this period is shown in Figure 43.

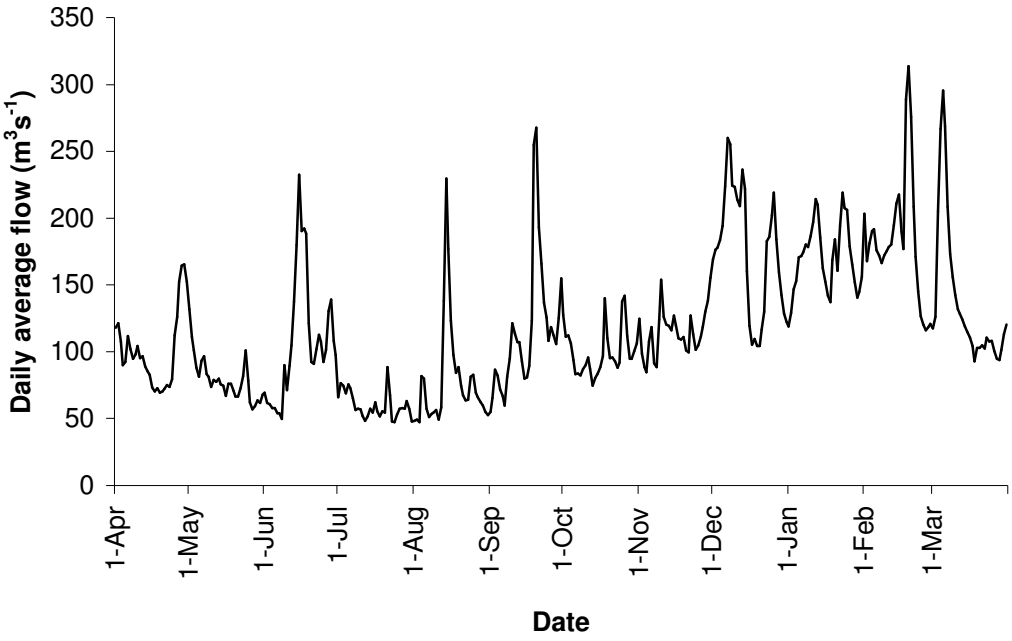

Figure 43. Daily average Lake Pukaki inflows for the 2002 snow year.

The inflow regime is characterised by regular large peaks of flow which usually relate to large rainfall events. The flow peaks generally have a steep rising limb with a less steep descending limb representing recessional flow. The primary flow peak of early December does not show this characteristic shape as it is generated by melt flows with no accompanying rainfall, though its secondary peak is associated with rainfall. The highest peak in February is a result of a combination of high temperatures (causing melt) and rainfall. A general seasonal variation in flow from a July-August minimum base flow of 50 $m^3 s^{-1}$ through to a February maximum base flow of 145 $m^3 s^{-1}$ is evident representing the snow storage cycle. High runoff peaks with amplitudes greater than 50 $m^3 s^{-1}$ occur at any time of the year, though the

frequency of such events is greater through the summer months when a greater proportion of precipitation occurs as rain rather than snow.

The annual inflow total is 3.7 km^3 which, through consideration of estimated evapotranspiration and non-surface glacial melt results in an expected annual rainfall plus melt of 4.42 km^3 (see Table 14).

Table 14. Calculated annual catchment rainfall plus melt based on measured lake inflow for the 2002 snow year.

Measured Inflow (km^3):	3.7
Estimated evapotranspiration (km^3),(see section 4.3.2):	0.75
Estimated iceberg melt (km^3), (see section 4.3.2)	0.03
Calculated annual rainfall and melt (km^3)	4.42

The 14 day running mean of the measured flow is shown in Figure 44. The filter effect of the averaging has removed the high frequency variations as well as the extreme values. The seasonal variation in flow is well displayed with a seasonal minimum in June-July and a clear maximum in January-February. The major flow events are still well represented and more readily identified as six unique events occurring roughly every two months throughout the year.

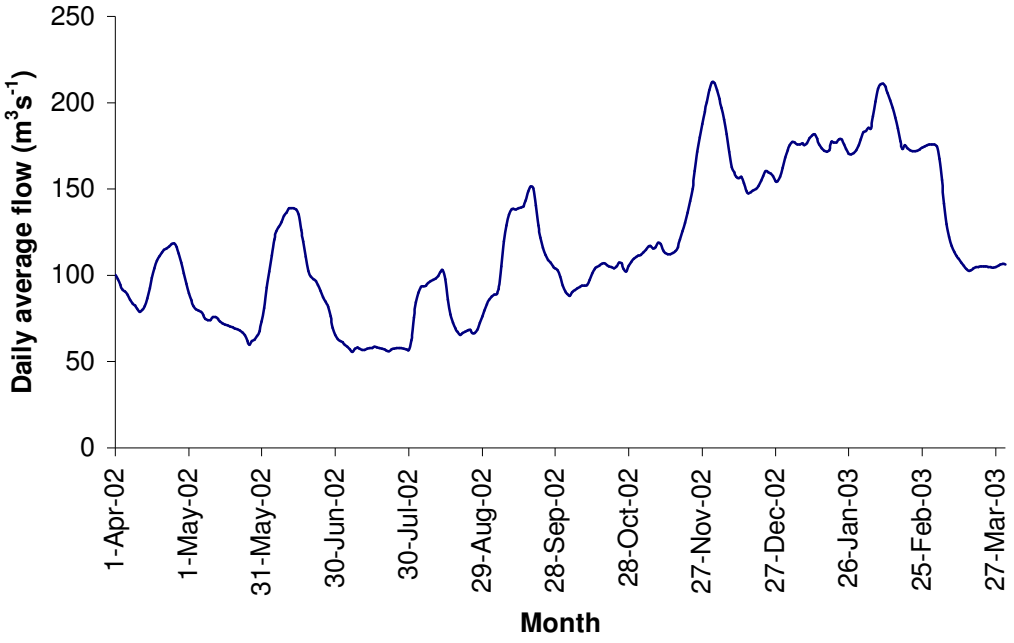

Figure 44. Fourteen day running mean of the daily average Lake Pukaki inflows for the 2002 snow year.

5.5 Comparison between modelled and measured lake inflows

The modelled catchment rainfall plus snowmelt, combined with estimated ice melt and evapotranspiration (free water) using the default New Zealand SnowSim parameters (see Table 6) is shown in Figure 45.

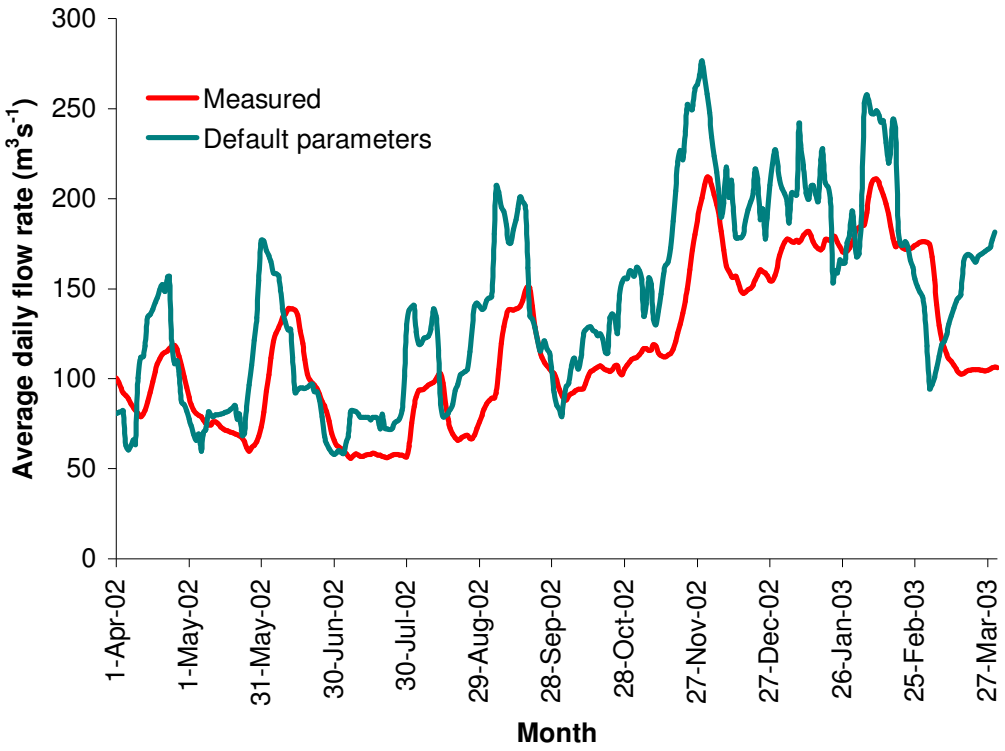

Figure 45. Fourteen day running mean of daily SnowSim modelled catchment free water using the default parameters compared to fourteen day running mean of measured daily lake inflows during 2002-2003.

The modelled result identifies the six major flow peak occurrences and shows the seasonal variation in flow. The NTD criterion for the modelled to measured comparison is 0.16. The model output appears to have a flow offset from the measured data. While the model includes an ice melt adjustment of 68 m^3s^{-1} average daily flow (following equation (17)), by adjusting this value to 43 m^3s^{-1} the NTD criterion increases to 0.54. This confirms the offset error observed in the graphical output. This indicates an excess of 25 m^3s^{-1} average flow per day is modelled. This error could be a result of poor estimation of the evapotranspiration, poor estimation of ice melt, poor precipitation modelling or a combination of these factors. For evapotranspiration to be the cause of the offset error, the evapotranspiration estimate of 23 m^3s^{-1} (see Table 8) would need to be nearly doubled. For the ice melt estimation to be incorrect then either the annual long term ice melt estimate would need to show a positive balance, or the 2002 snow year would have to be a strongly positive balance year leading to a snowpack greater than an average of some 4 m SWE at the end of the snow year on the

permanent snow field regions of the catchment. Neither of these scenarios is likely especially given the increasing terminal lake below the Tasman Glacier which would tend to increase the negative balance. The most likely source of the error appears to be in the precipitation modelling used by SnowSim. As discussed in section 4.3.2 the NZMS precipitation surface used in SnowSim overestimates annual average inflow volume by some 1 km^3. The total volume of precipitation estimated for the year using SnowSim is 4.99 km^3 which is 0.57 km^3 greater than the estimated average annual precipitation volume, determined from the water balance components as discussed in section 4.3.2. This equates to 18 m^3s^{-1} average daily flow. This error would go a long way to explaining the discrepancy between modelled and measured inflows. It is likely that the estimated evapotranspiration and long term ice melt are in error to some degree, and that the 2002 snow year is not an "average" snow year. However it would appear that the primary reason for the excess of modelled water is the precipitation modelling of SnowSim.

With the lapse rate set to 0.005 $^oC\ m^{-1}$ (following section 5.3.1) three sets of models were run for snow/rain thresholds of 2.5 ^oC, 2 ^oC and 1.5 ^oC, each set varying minimum and initial maximum melt factors. The offset was adjusted to ensure an optimum output for each model run. An average offset of 27.9 $m^3\ s^{-1}$ was found with a range of +/- 3 $m^3\ s^{-1}$. As a result, 27.9 $m^3\ s^{-1}$ was set as a constant offset for all model runs. The optimisation graphs for each snow/rain threshold temperature are shown in Figures 46 to 48 respectively.

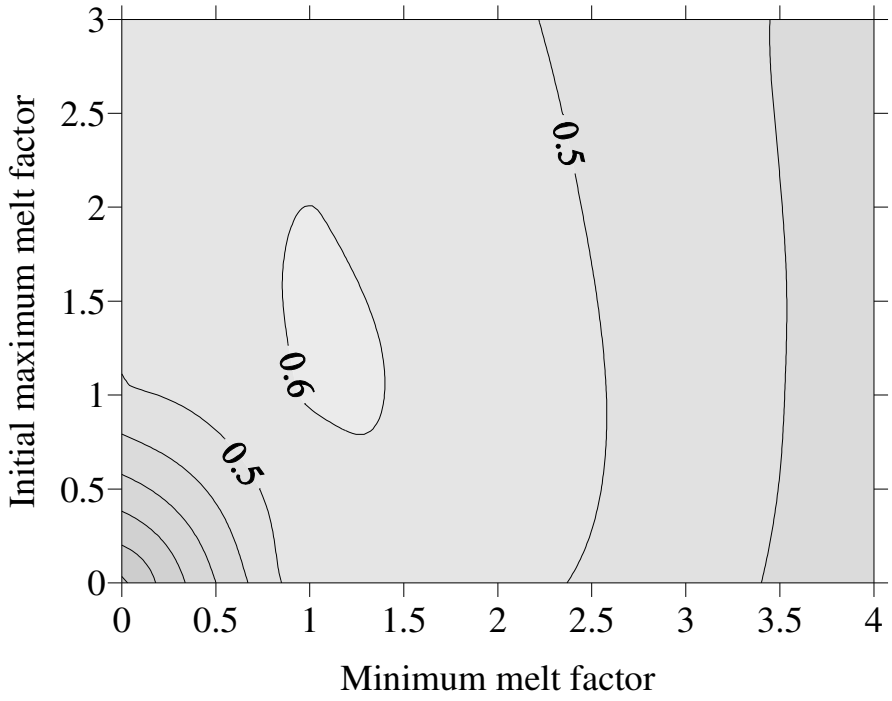

Figure 46. Modelled catchment free water NTD criterion values for various melt factor combinations (units: mm $^oC^{-1}\ d^{-1}$) with lapse rate set to 0.005 $^oC\ m^{-1}$ and snow/rain temperature threshold set to 2.5 ^oC.

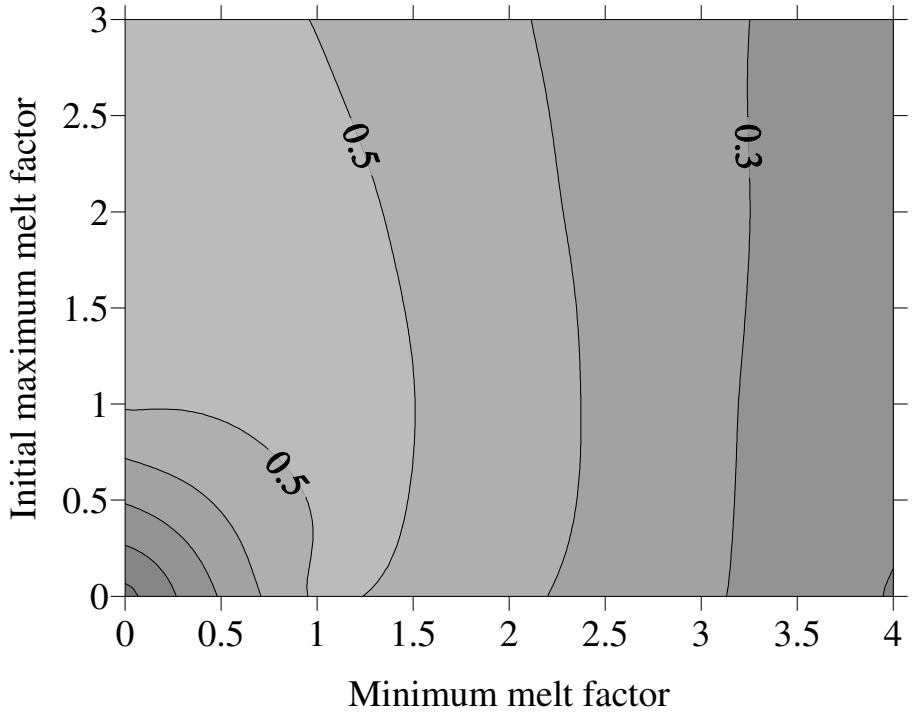

Figure 47. Modelled catchment free water NTD criterion values for various melt factor combinations (units: mm $^{o}C^{-1}$ d^{-1}) with lapse rate set to 0.005 ^{o}C m^{-1} and snow/rain temperature threshold set to 2 ^{o}C.

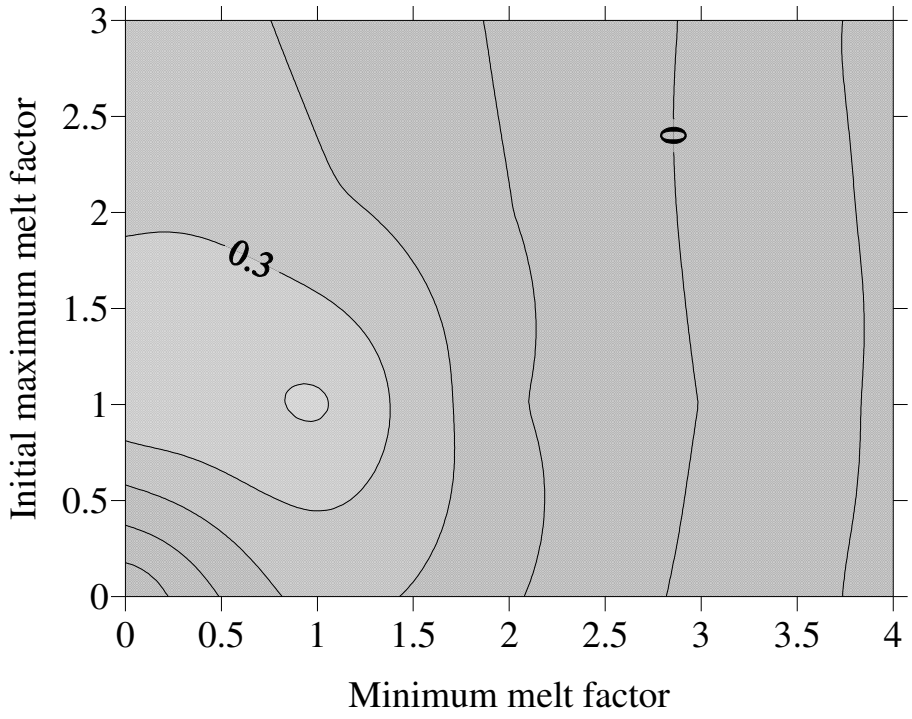

Figure 48. Modelled catchment free water NTD criterion values for various melt factor combinations (units: mm $^{o}C^{-1}$ d^{-1}) with lapse rate set to 0.005 ^{o}C m^{-1} and snow/rain temperature threshold set to 1.5 ^{o}C.

The optimised melt factors are different to the default values used in the New Zealand version of SnowSim but are the same as those found through optimisation using the Rose Ridge SWE data. The snow/rain temperature threshold optimised to 2.5 ^{o}C, a whole degree greater than

that found for the Rose Ridge optimised parameters, and the same as that used in the New Zealand version of SnowSim. The major flow peaks and the seasonal flow cycle are well represented. A temporal offset is apparent, which is to be expected as the measured output is propagated flow, whereas the modelled output is not. Of interest is that the temporal offset is most pronounced in the early winter peaks associated primarily with rainfall while that for the melt peak of November-December the temporal offset is negligible. This may be a result of improved flow through the snow pack and glacier as the drainage network develops with increased summer flow.

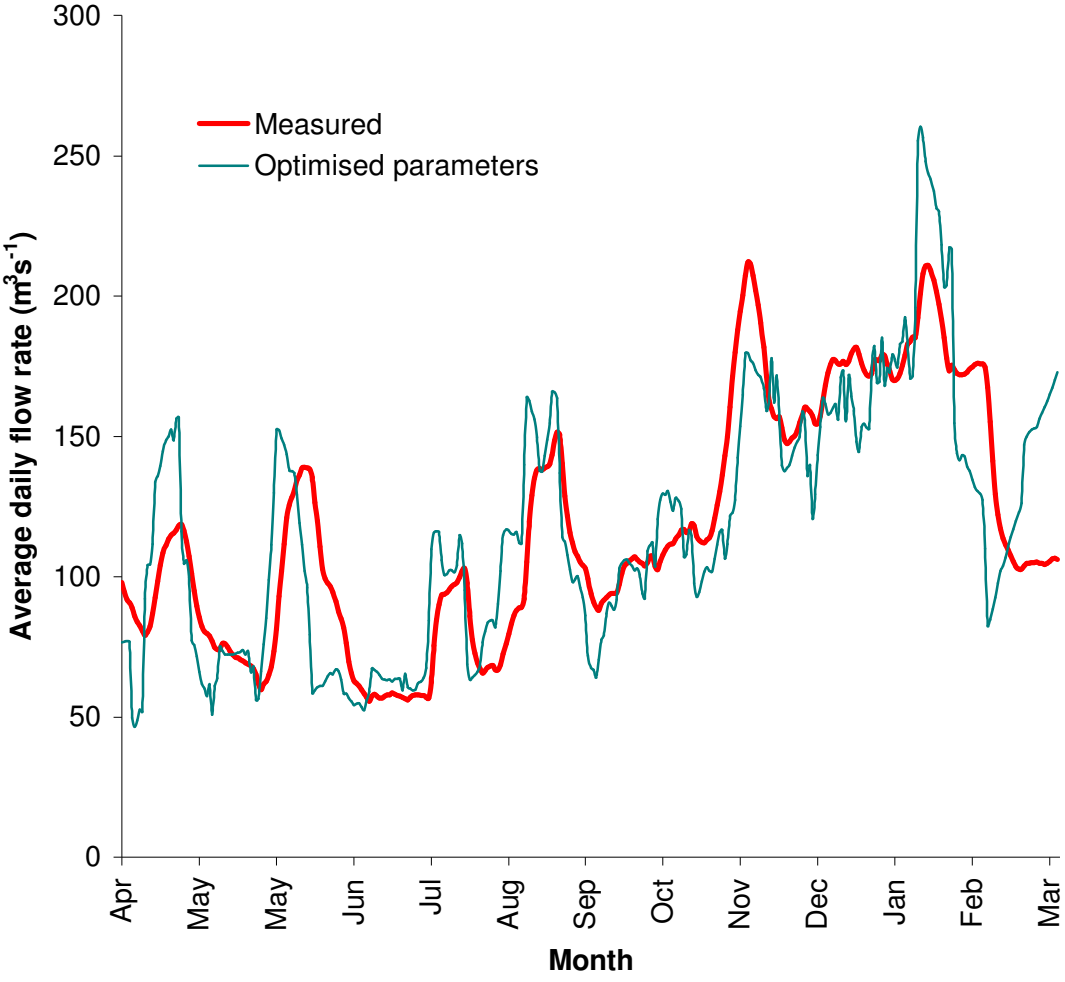

Figure 49. Fourteen day running mean of daily SnowSim modelled catchment free water using optimized parameters and 27.9 m^3s^{-1} daily offset, compared to fourteen day running mean of measured daily lake inflows during 2002-2003.

5.5.1 Sensitivity to the minimum melt factor

The result of varying the minimum melt factor (while retaining the other parameters at the optimum values) on modelled output is shown in Figure 50. The first major flow peak is

similar for all minimum melt factors. This is because the first peak is due primarily to rain prior to any snow accumulation (and hence melt) has occurred. From May through to November the model outputs vary in magnitude with the greatest flow relating to the lowest melt factor, and vice versa. From mid-November onwards the reverse occurs with the largest free water quantities being modelled by the lowest minimum melt factor. This may be related to the availability of snow storage for melt. The higher minimum melt factor models effectively melted the available snow storage prior to summer, resulting in less melt availability late in the season. The sensitivity of the model to variations in the minimum melt factor is shown in Figure 51. This shows that the model output is sensitive to the minimum melt factor with the NTD criterion value dropping constantly as the minimum melt factor increases.

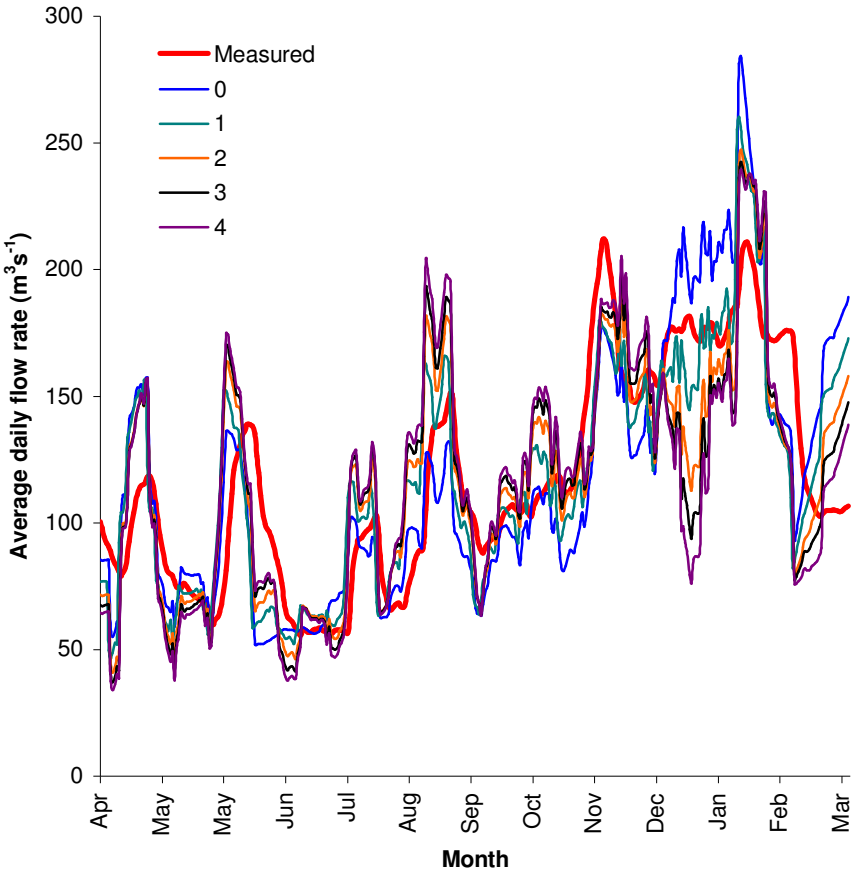

Figure 50. Fourteen day running mean of daily SnowSim free water output with varying minimum melt factors (mm $^{o}C^{-1}$ d^{-1}), compared to fourteen day running mean of daily measured lake inflows during 2002-2003.

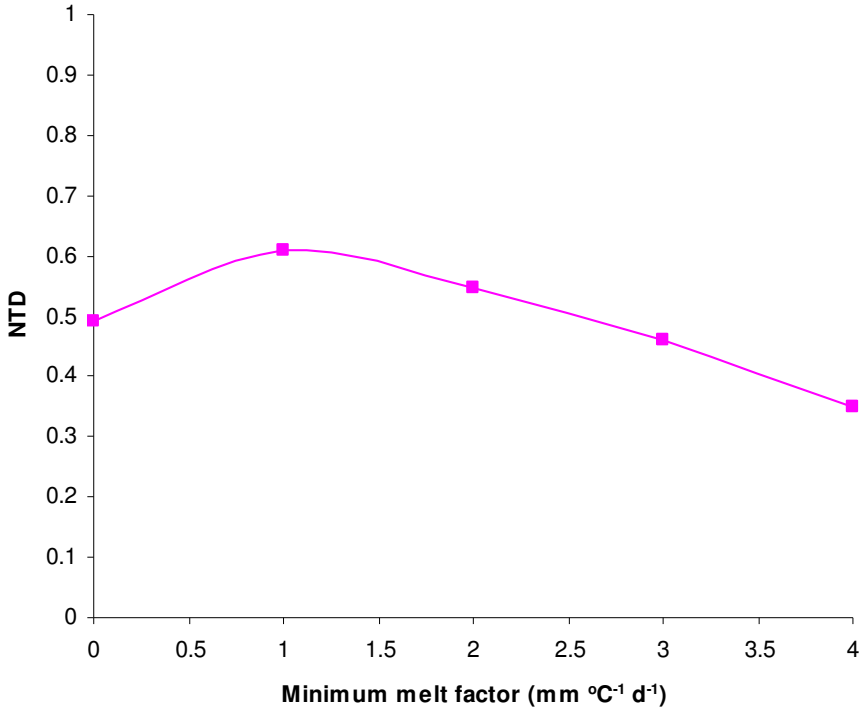

Figure 51. Sensitivity of accuracy of modelled free water (as measured by the NTD criterion) to variations in the minimum melt factor.

5.5.2 Sensitivity to the initial maximum melt factor parameter

The effect of varying the initial maximum melt factor on modelled output (while keeping the other parameters at the optimum values) is shown in Figure 52. The variation of the initial maximum melt factor has little effect on the modelled free water except during the early December peak flow event. During this time the higher initial maximum melt factors resulted in a higher magnitude flow event, whereas the low initial maximum melt factors resulted in a low peak. This result is because the early December peak was largely caused by melt. This is confirmed by rain records that show no rain fell in the region on the 1st and the 2nd of December (the date of the peak). The sensitivity of the model to variations in the initial maximum melt factor is shown in Figure 53. This confirms that the model is not sensitive to variations in the initial maximum melt factor at least in terms of annual flow variations. In terms of particular events though, the early December peak was the second largest for the year and important in terms of summer flow and the fact that no precipitation occurred at the time, precisely the type of flow variation that a snow storage model should be able to detect.

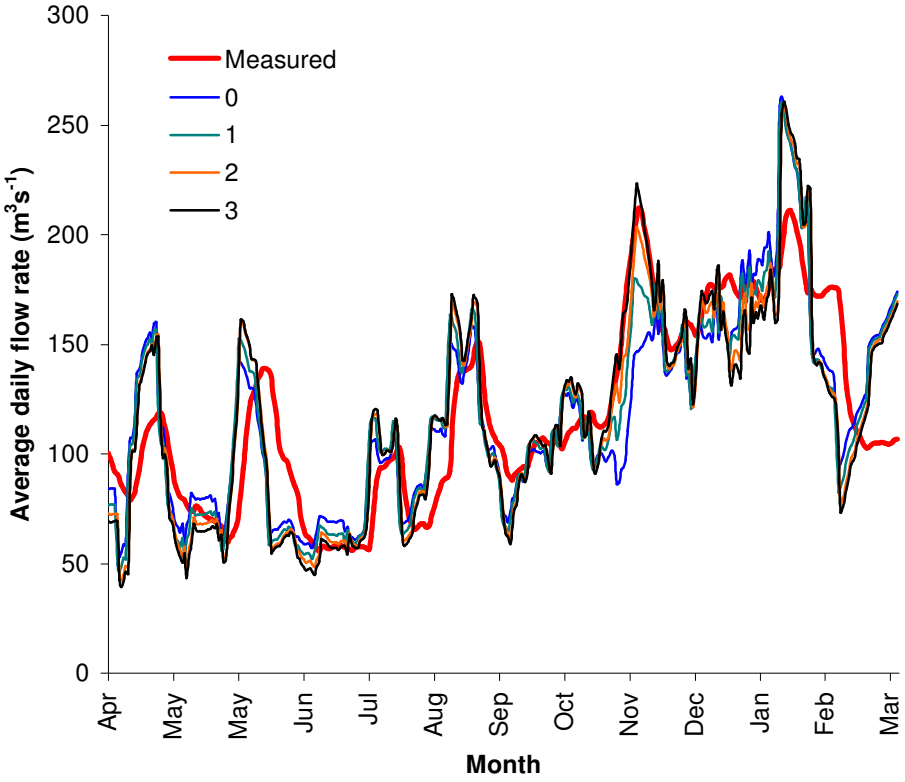

Figure 52. Fourteen day running mean of daily SnowSim free water output with varying initial maximum melt factors (mm $^{o}C^{-1}$ d^{-1}), compared to fourteen day running mean of daily measured lake inflows during 2002-2003.

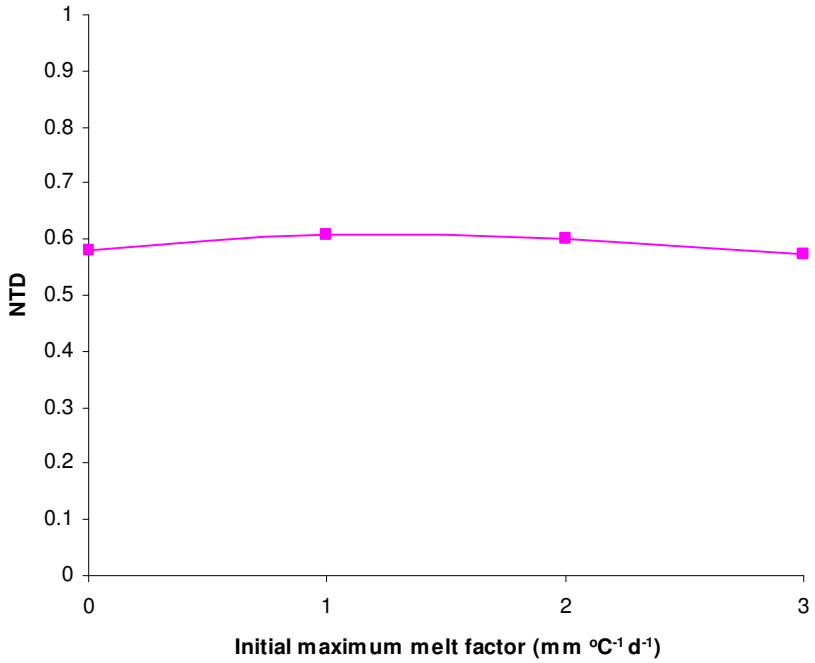

Figure 53. Sensitivity of accuracy of modelled snow water equivalent (as measured by the NTD criterion) to variations in the initial maximum melt factor.

5.5.3 Sensitivity to the snow/rain threshold parameter

The effect of varying the snow/rain threshold on modelled output is shown in Figure 54. This shows that the snow/rain threshold influences the magnitude of the flow in a similar manner to the minimum melt factor. That is from April until November the lower the snow/rain threshold, the greater the flow, and then from November, the greater the threshold the greater the flow. This result is likely to again be because excessive flow early in the season means that snow storage is not available for flow late in the season. Sensitivity analysis of the snow/rain threshold is shown in Figure 55. As the thresholds increase from 0 ^{o}C so does the NTD criterion. 2.5 ^{o}C is considered the limit of physical reality for the snow/rain threshold, though interestingly the higher snow/rain threshold of 3 ^{o}C returns the highest NTD criterion value.

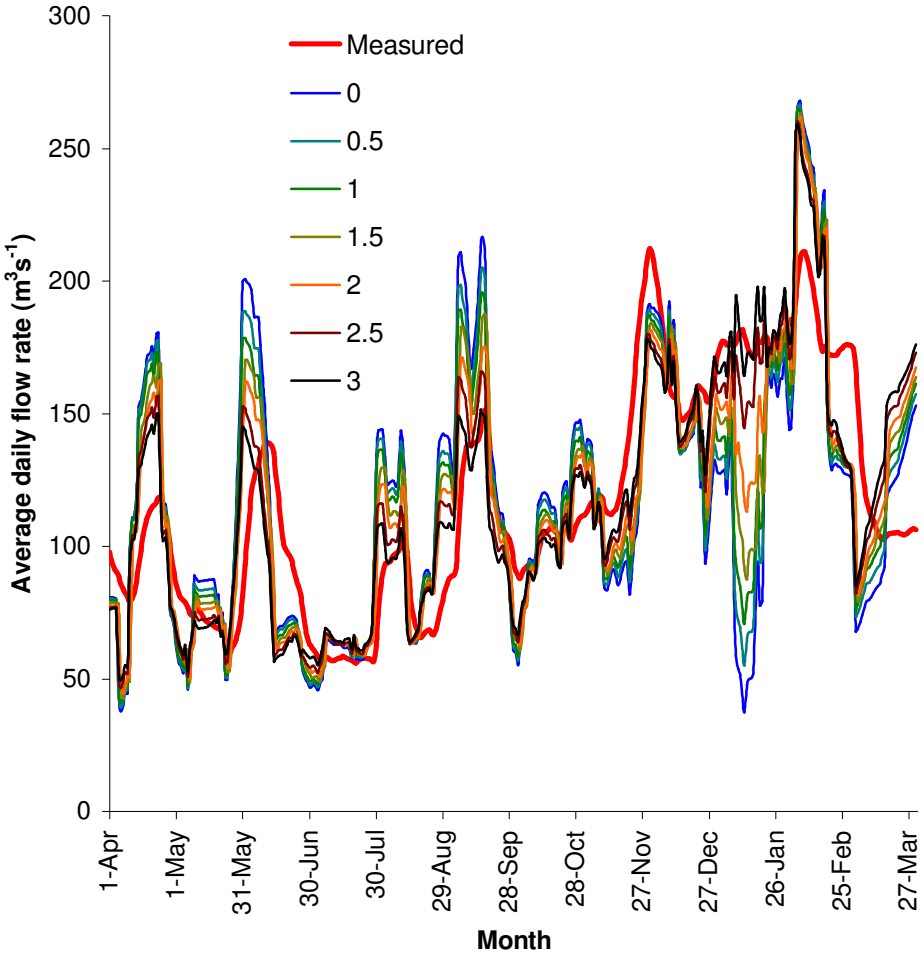

Figure 54. Fourteen day running mean of daily Classic SnowSim free water output with varying snow/rain threshold (^{o}C) compared to fourteen day running mean of daily measured lake inflows during 2002-2003.

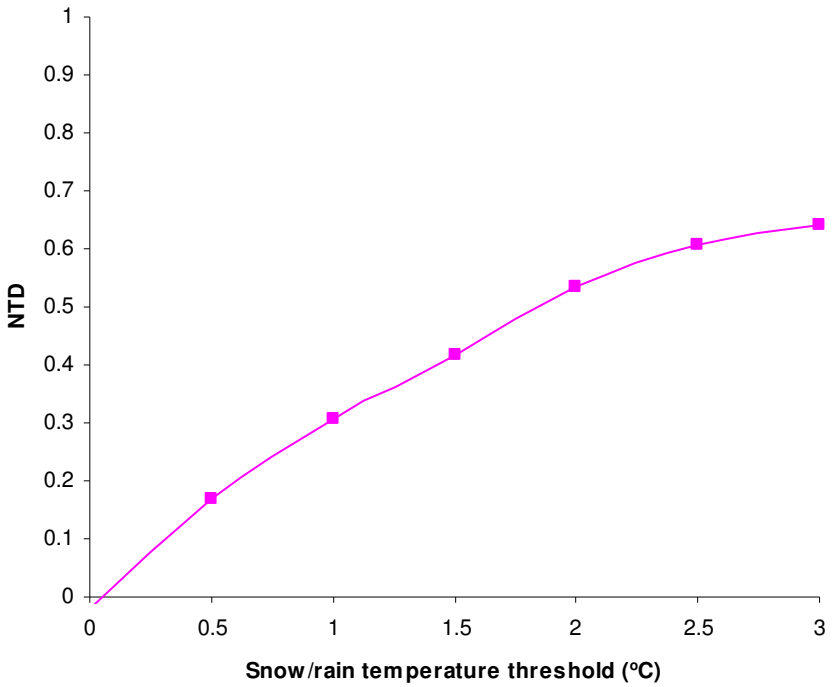

Figure 55. Sensitivity of accuracy of modelled snow water equivalent (as measured by the NTD criterion) to variations in the snow/rain temperature threshold.

5.6 Summary

A single catchment wide constant temperature/elevation lapse rate of 0.005 ^{o}C m^{-1} has been selected as optimal following analysis of climate station data.

Optimisation of SnowSim to a point location provides a large improvement in the quality of model outputs. The model is sensitive to all the model parameters, particularly the snow/rain temperature threshold. This parameter impacts on the estimation of the phase of precipitation which, during intense events, may have a significant effect on snow storage. While the snow/rain temperature threshold primarily affects the accumulation period of the snow season, the effects of varying the melt factor parameters are most significant during the ablation period of the season. The optimised values were: minimum melt factor of 1 mm ^{o}C^{-1} d^{-1}, initial maximum melt factor of 1 mm ^{0}C^{-1} d^{-1} and snow/rain threshold of 1.5 ^{o}C. Optimisation of SnowSim also provides an improvement of model output at the catchment scale. Though not to the level obtained at the point scale, and with a variation in the optimised parameters. While the minimum melt factor and initial maximum melt factor remained at 1 mm ^{0}C^{-1} d^{-1}, the snow/rain temperature threshold increased to 2.5 ^{o}C. The snow/rain temperature threshold is again the most sensitive parameter, with the initial maximum melt factor the least sensitive. A constant offset was required to be added to the catchment level model free water outputs to bring them

into line with the measured lake inflows. This indicates a component of the processes is either being omitted, or incorrectly assessed.

6 Model modification results

6.1 Introduction

This chapter describes the results of amending the SnowSim model firstly by using a daily measured lapse rate, secondly by altering the precipitation distribution system, and lastly by including a radiation component to the model. Each modification is assessed in turn and duly accepted or rejected based on whether an improvement is identified in model output based on comparison to measured data.

6.2 Daily lapse rate estimation

An analysis was made of whether using a daily estimation of lapse rate could improve temperature estimation, and in turn model performance. Following the assessment in section 5.3.1 an annual average temperature lapse rate of 0.0055 ^{o}C m^{-1} has been selected as optimal for determining Rose Ridge temperatures. The annual average lapse rate between Mt Cook and Panorama Ridge is 0.0065 ^{o}C m^{-1} a ratio of 1.18:1 to the Rose Ridge optimised lapse rate. A correlation coefficient of $r^2 = 0.92$ exists between the temperature record of Panorama, and the temperature record of Rose Ridge for 2002. SnowSim was trialled using a scaled daily Panorama – Mt Cook measured lapse rate to see if improved temperature estimation could be achieved. The NTD criterion (see section 4.5) was used to assess the performance of the model outputs against the measured temperature at Rose Ridge.

The modelled temperatures at Rose Ridge using the measured lapse rate compared to those modelled utilising a 0.0055 ^{o}C m^{-1} lapse rate and to the measured temperatures and are shown for December 2002 in Figure 56. The use of the measured lapse rate results in a more variable temperature than that achieved using a fixed lapse rate. Visual comparison indicates that no general improvement in modelled temperatures is achieved. An NTD criterion value of 0.82 was returned when comparing measured to modelled temperatures using a measured lapse rate. This compares to an NTD value of 0.86 when the single constant lapse rate is used. These results show that no improvement in temperature estimation is achieved through the use of a daily measured lapse rate. This result is most likely a result of lapse rates being variable spatially as well as temporally. Lapse rate measurements from one pair of climate stations do not provide an indication of general lapse rate variation in a region. Following this analysis the use of a single measured lapse rate was considered to not improve the model output of SnowSim.

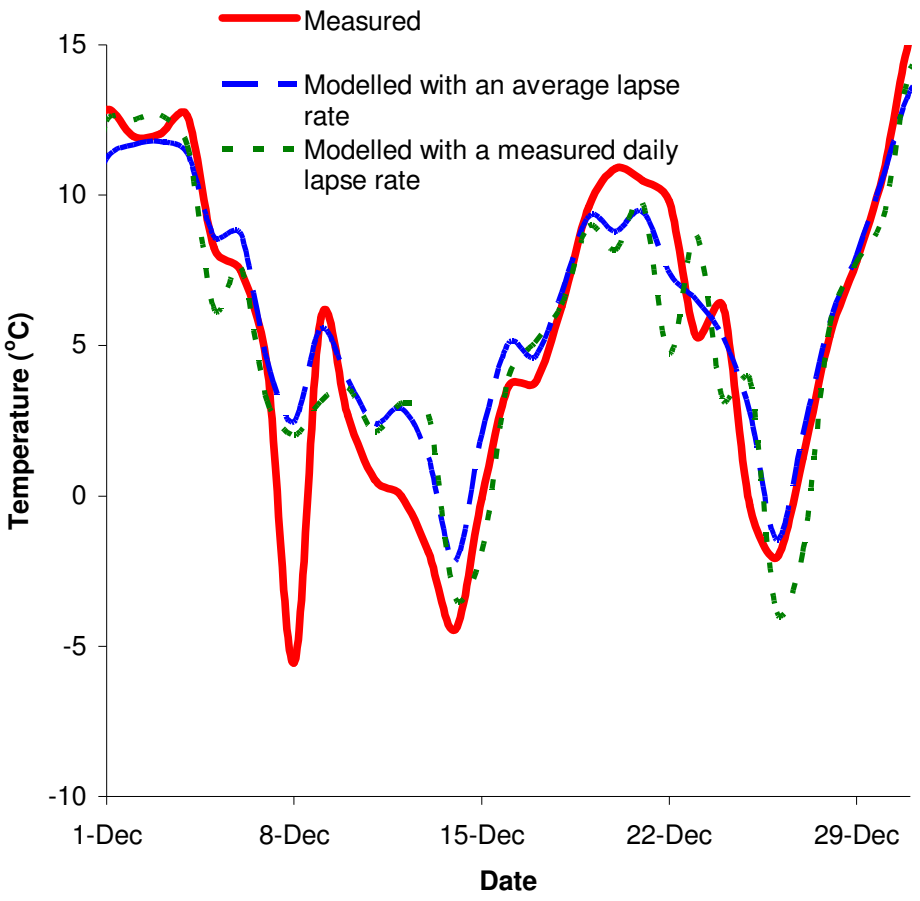

Figure 56. Classic SnowSim temperature outputs for Rose Ridge with a measured lapse rate compared to measured temperatures and modelled temperatures using a fixed 0.0055 $^{o}C\ m^{-1}$ lapse rate during December 2002.

6.3 New precipitation surface

Utilising the new precipitation surface and estimation system as outlined in section 4.3.2 the Rose Ridge SWE NTD criterion values were determined for melt factor parameter combinations with the snow/rain temperature threshold set to 2.5 ^{o}C, 2.0 ^{o}C and 1.5 ^{o}C. The results are shown in Figures 57 to 59 respectively.

The highest NTD criterion value of 0.91was found with a snow/rain threshold = 1.5 ^{o}C, a minimum melt factor = 2 mm $^{o}C^{-1}\ d^{-1}$, and an initial maximum melt factor = 1 mm $^{o}C^{-1}\ d^{-1}$. This is a reduction in NTD criterion of 0.02 from that returned using the precipitation distribution system of New Zealand SnowSim. The parameter values are also different from those found when optimizing New Zealand SnowSim in that the minimum melt factor has increased from 1 mm $^{o}C^{-1}\ d^{-1}$ to 2 mm $^{o}C^{-1}\ d^{-1}$. The Rose Ridge SWE output for the model

versions using the original precipitation distribution and the new precipitation distribution is shown in Figure 60.

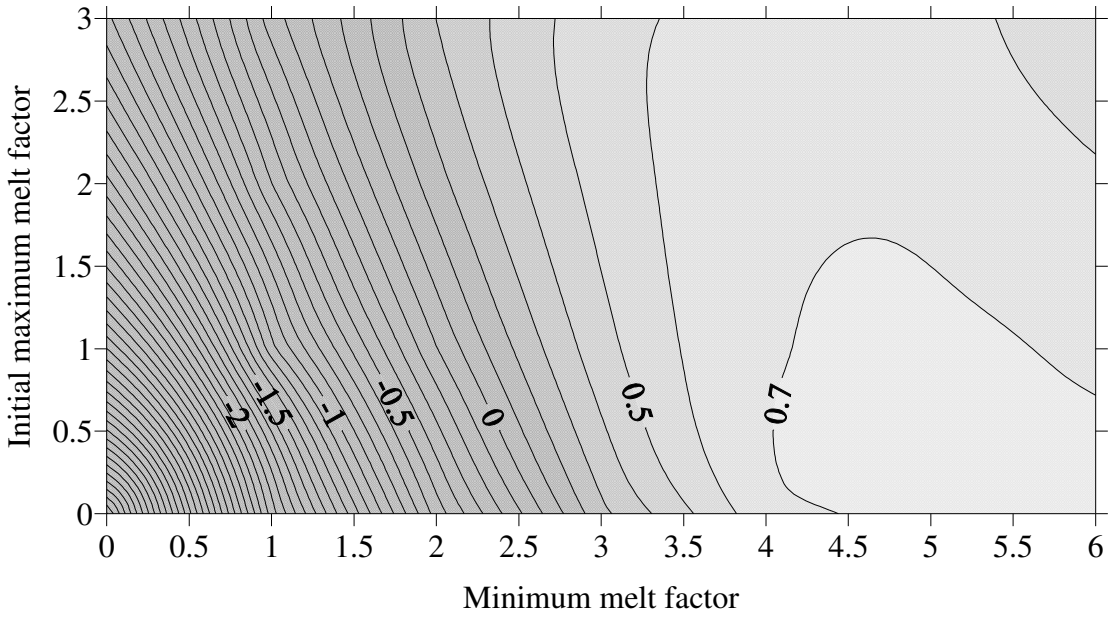

Figure 57. Modelled Rose Ridge snow water equivalent NTD criterion values for various melt factor combinations (units: mm $^{o}C^{-1}$ d^{-1}) with lapse rate set to 0.005 ^{o}C m^{-1} and snow/rain temperature threshold set to 2.5 ^{o}C.

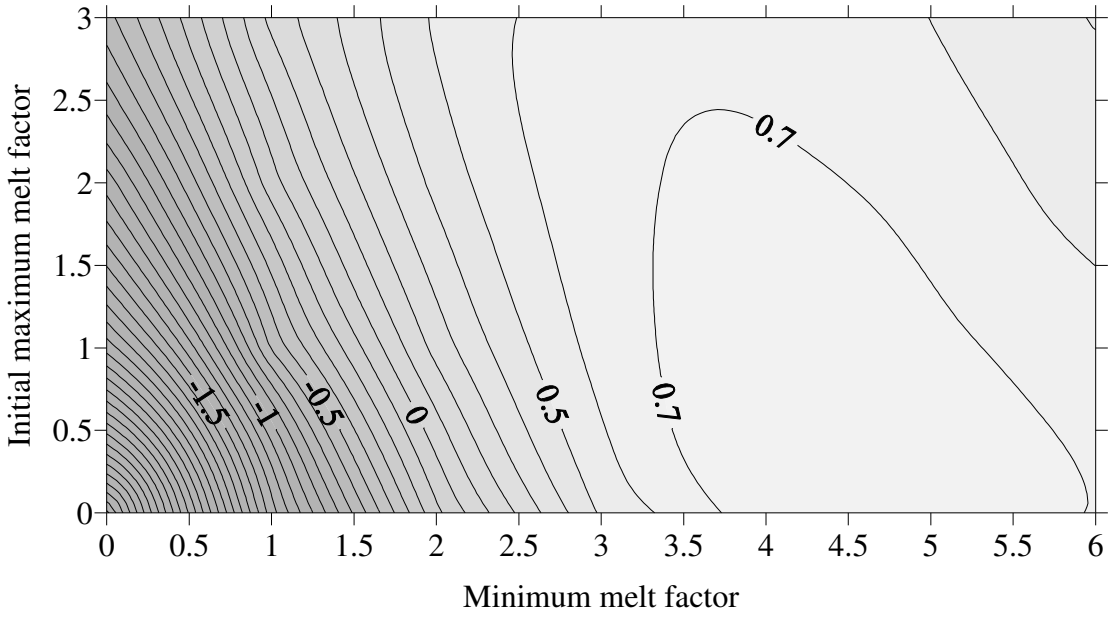

Figure 58. Modelled Rose Ridge snow water equivalent NTD criterion values for various melt factor combinations (units: mm $^{o}C^{-1}$ d^{-1}) with lapse rate set to 0.005 ^{o}C m^{-1} and snow/rain temperature threshold set to 2.0 ^{o}C.

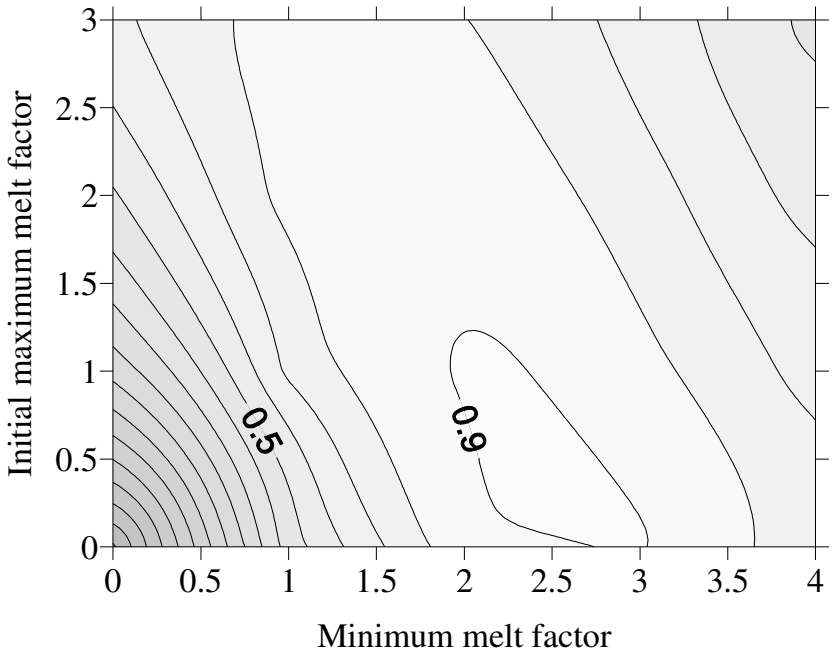

Figure 59. Modelled Rose Ridge snow water equivalent NTD criterion values for various melt factor combinations (units: mm $^{o}C^{-1}$ d^{-1}) with lapse rate set to 0.005 ^{o}C m^{-1} and snow/rain temperature threshold set to 1.5 ^{o}C.

The new precipitation distribution has increased accumulation, even with the greater minimum melt factor. This leads to a closer representation of accumulation at the beginning of the snow season but an over estimation in mid season. In September a maximum snowpack of 1155 mm is modelled, 238 mm greater than that measured, and 170 mm greater than that found with the New Zealand SnowSim precipitation distribution system.

The catchment free water NTD criterion values as determined for melt factor parameter combinations with the snow/rain temperature threshold set to 2.5 ^{o}C, 2.0 ^{o}C and 1.5 ^{o}C are shown in Figures 61 to 63 respectively. The highest NTD criterion value of 0.71 was returned with a snow/rain threshold = 2.5 ^{o}C, a minimum melt factor = 1 mm $^{o}C^{-1}$ d^{-1}, and an initial maximum melt factor = 2 mm $^{o}C^{-1}$ d^{-1}. This is an improvement of 0.1 from the optimized New Zealand SnowSim with the original precipitation distribution system. The parameter values are also different from those found when optimizing New Zealand SnowSim in that the initial maximum melt factor has increased from 1 mm $^{o}C^{-1}$ d^{-1} to 2 mm $^{o}C^{-1}$ d^{-1}.

The free water output for the model versions compared to measured lake inflows are shown in Figure 64.

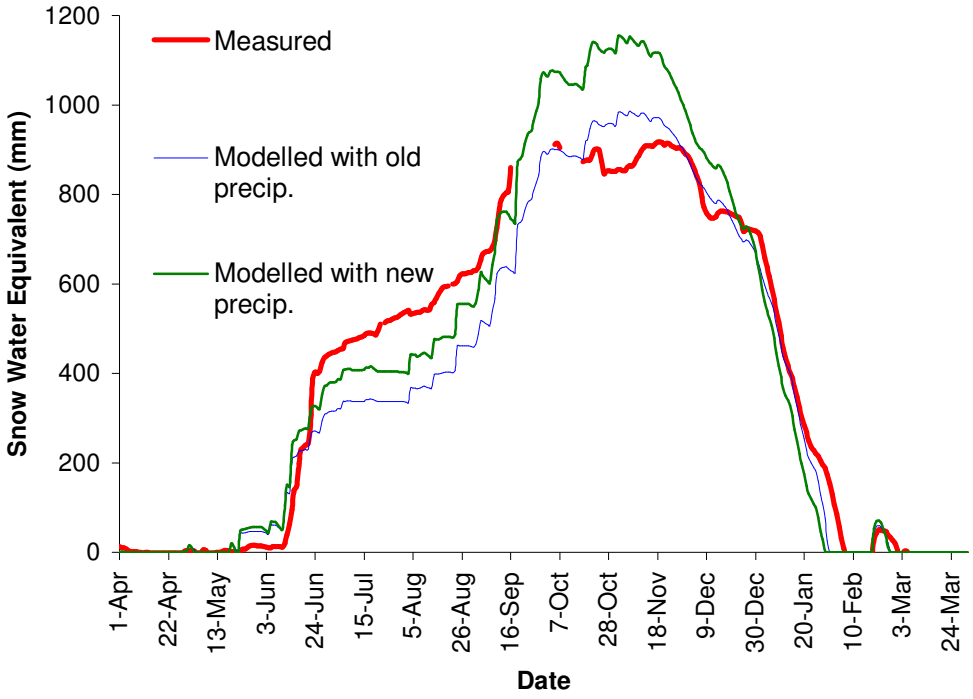

Figure 60. Classic SnowSim output for Rose Ridge SWE with the original precipitation distribution and the new precipitation distribution, compared to measured SWE during 2002-2003.

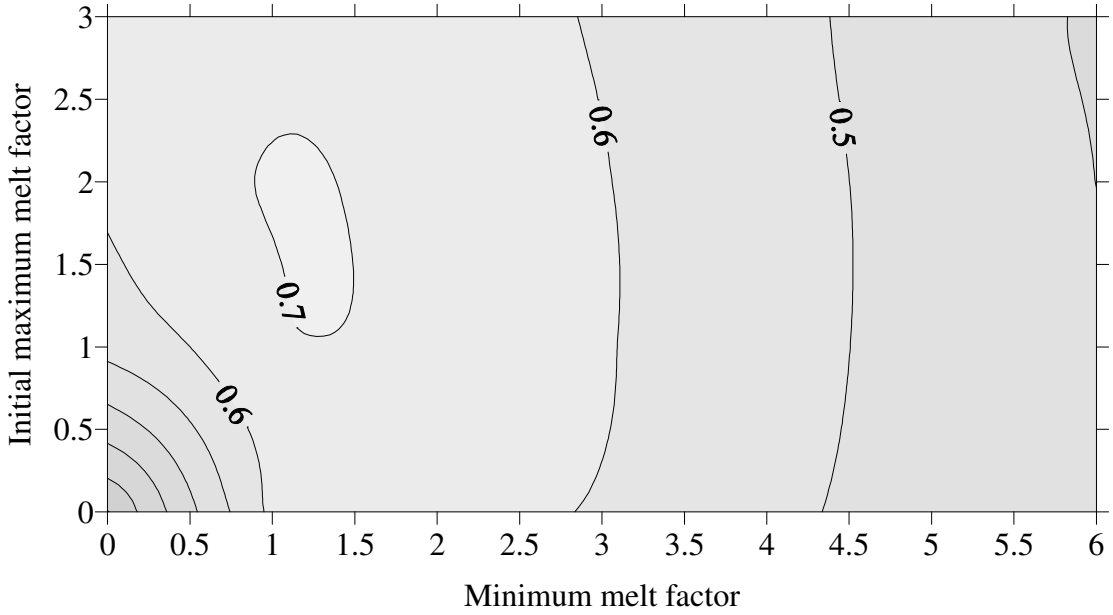

Figure 61. Modelled catchment free water NTD criterion values for various melt factor combinations (units: mm $^{o}C^{-1}$ d^{-1}) with lapse rate set to 0.005 ^{o}C m^{-1} and snow/rain temperature threshold set to 2.5 ^{o}C.

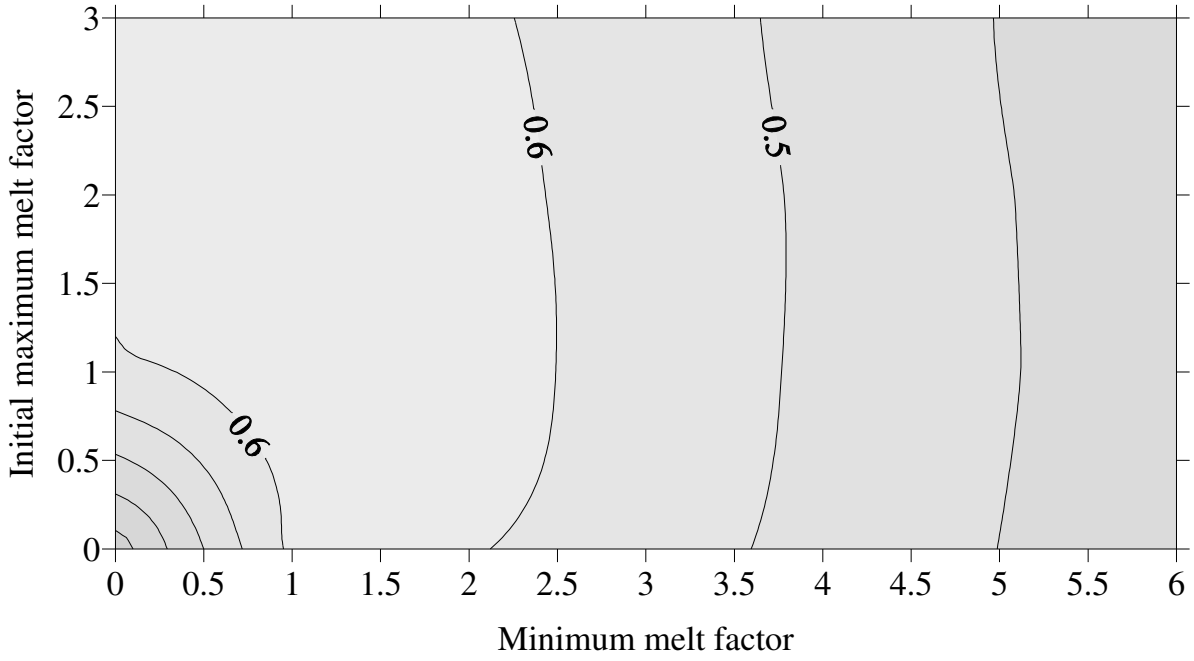

Figure 62. Modelled catchment free water NTD criterion values for various melt factor combinations (units: mm $^{o}C^{-1}$ d^{-1}) with lapse rate set to 0.005 ^{o}C m^{-1} and snow/rain temperature threshold set to 2.0 ^{o}C.

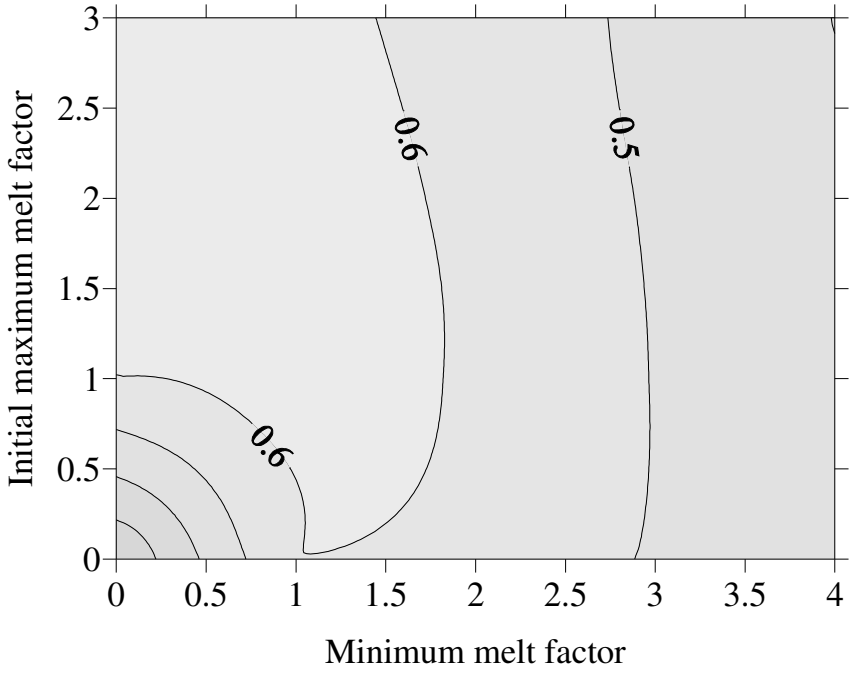

Figure 63. Modelled catchment free water NTD criterion values for various melt factor combinations (units: mm $^{o}C^{-1}$ d^{-1}) with lapse rate set to 0.005 ^{o}C m^{-1} and snow/rain temperature threshold set to 1.5 ^{o}C.

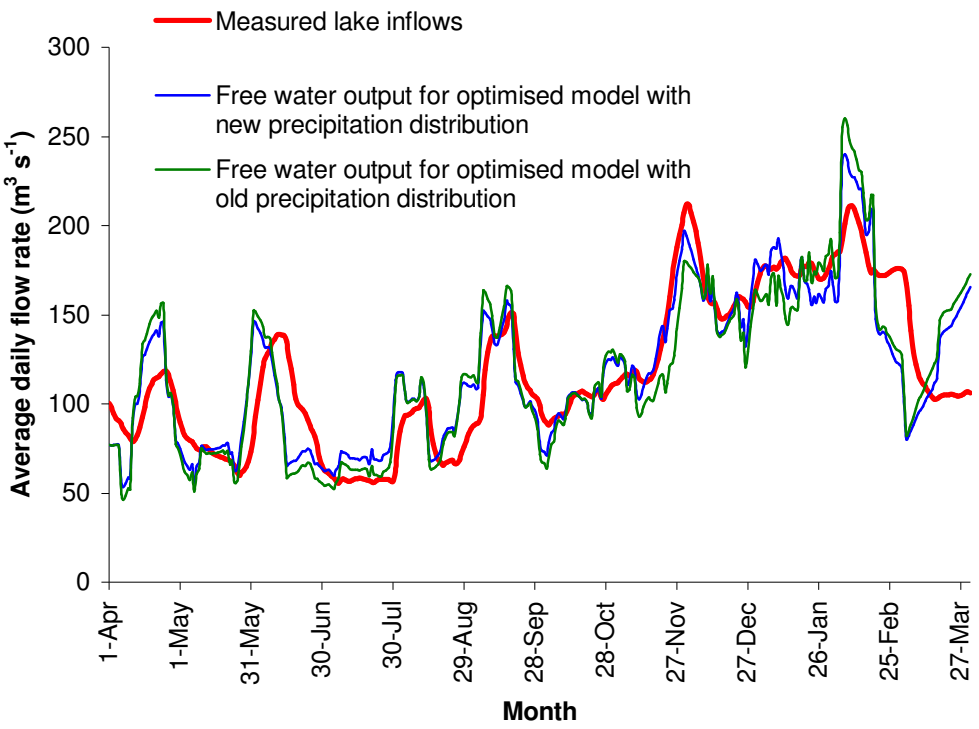

Figure 64. Fourteen day running mean of the SnowSim output for catchment free water with the original precipitation distribution and the new precipitation distribution, compared to fourteen day running mean of the measured lake inflows during 2002-2003.

The new precipitation distribution system has two distinct effects on the free water model output. Firstly, the early season peaks are lower. This is most likely a result of the generally lower catchment-wide precipitation that the new system estimates. The early season peaks are primarily caused by rainfall with little melt, so their magnitudes are directly related to precipitation magnitude. The second effect is the increased melt occurring during the early December peak. This peak is primarily from snowmelt. The optimized initial maximum melt factor is higher for SnowSim when the new precipitation system is used. This in turn causes increased late season melt, bringing the free water values during the snowmelt season more in line with the measured lake inflow quantities. Of particular interest is that the offset between modelled and measured flow has gone from being a daily excess of 27.9 m^3s^{-1}, to a daily deficit of 27.9 m^3s^{-1}. This may be explained to some extent by the increased influence that the terminal lake has on glacial melt which is not accounted for in the glacial melt estimates used. However, the amount of offset is much greater than can be wholly explained by this, suggesting that another error exists in either the model or the way the model output is related to the measured lake inputs.

The model results using the new precipitation estimation system shows an improvement in catchment flow modelling but a reduction in the quality of point site SWE modelling. This indicates that while the new distribution describes the general precipitation regime better, at any single point this may not be the case. This is not surprising in such a topographically variable landscape as local effects (e.g. wind flow, proximity to small scale precipitation barriers) are likely to have a strong influence on precipitation at any one location. As a catchment wide model, the new precipitation estimation system is considered an improvement to SnowSim.

6.4 Radiation component for snow storage at Rose Ridge

The optimized model output for Rose Ridge SWE following modification of SnowSim to include a radiation component as set out in section 4.3.3 is shown in Figure 65.

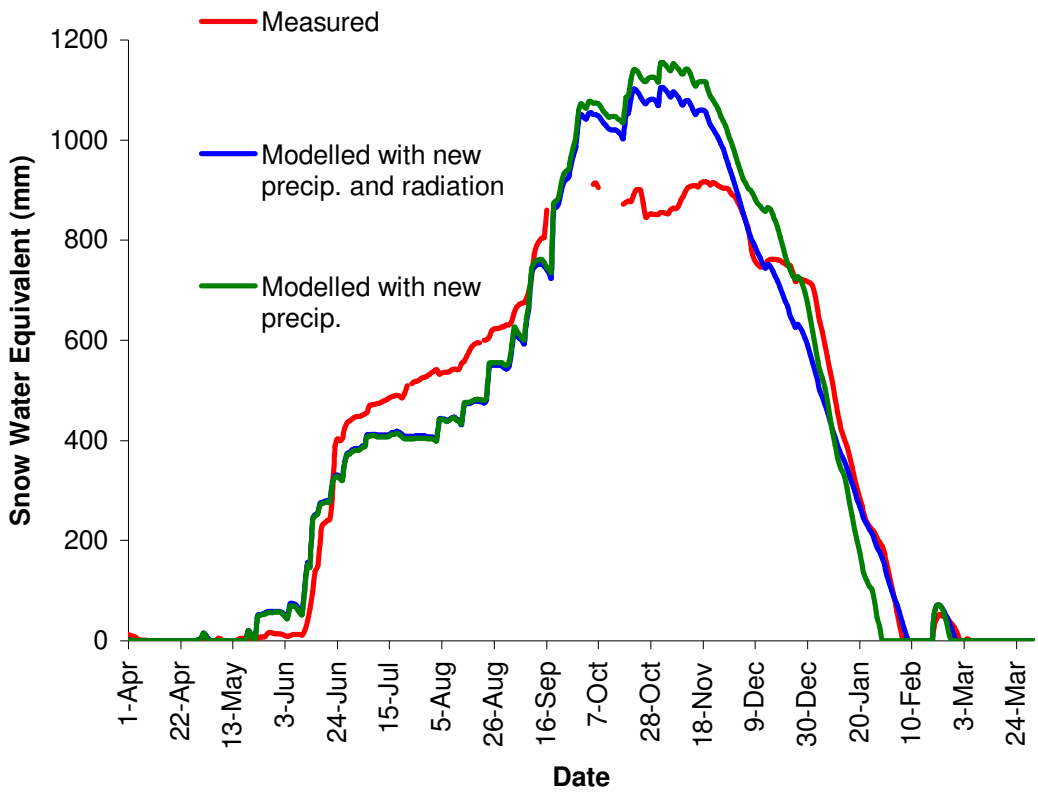

Figure 65. New Zealand SnowSim and Radiation SnowSim output for Rose Ridge SWE, both with the new precipitation distribution compared to measured SWE during 2002-2003.

The radiation component results in very little change to the modelled Rose Ridge SWE output when compared to New Zealand SnowSim. A lower peak snow storage quantity occurs because of the slightly increased ablation through spring, which is compensated for by

decreased ablation in late summer. By decomposing the daily ablation quantities into that modelled by the radiation component, and that modelled by the temperature component, the seasonal variation in relative contributions to melt may be identified as shown in Figure 66. The influence of new snow on radiation melt can be seen by the drop in radiation melt immediately following a break in ablation (when new snow falls) then a steady increase in radiation melt as time progresses and no snow falls. Peaks in radiation melt occur on wet days when the albedo parameter is increased in significance (see equation (14) in section 4.3.3). In reality less radiation melt is likely to occur on rainy days as there is less direct radiation, but because of the use of a constant clear sky component in the model, the influence of the rain on the modelled albedo is carried through to the heightened radiation melt values.

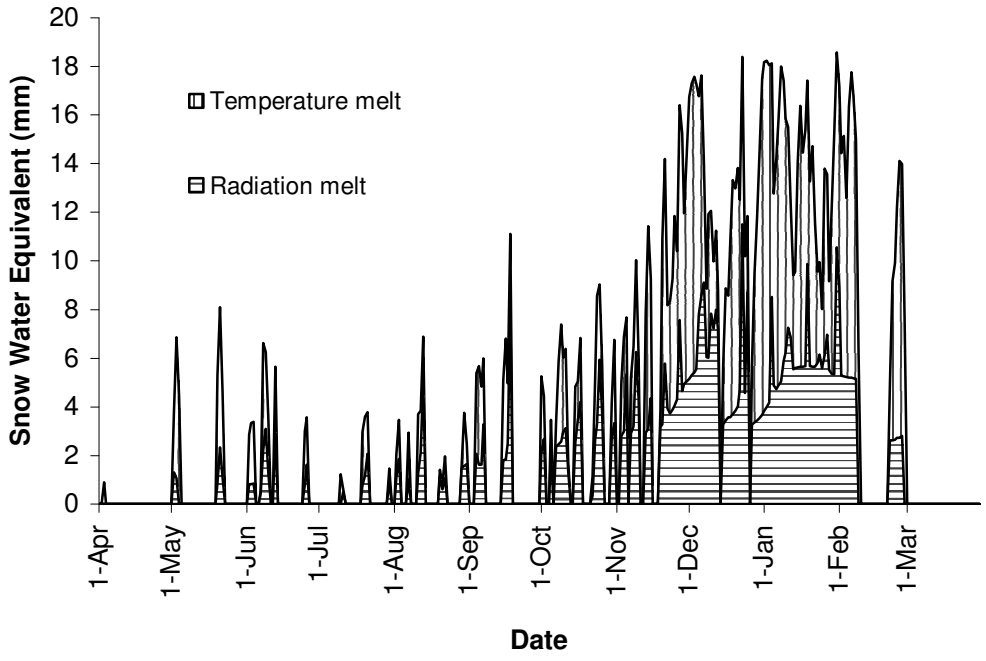

Figure 66. Components of modelled ablation at Rose Ridge according to Radiation SnowSim.

The highest NTD criterion value of 0.94 was returned for Radiation SnowSim with a minimum melt factor of 1 mm ^{o}C d^{-1}, a new snow albedo of 0.9, an old snow albedo of 0.8, a clear sky coefficient of 0.3, and a snow/rain temperature threshold of 1.5 ^{o}C. The high albedo factors and low clear sky coefficient indicate that just 0.045 of the maximum daily solar radiation is on average used in melt at Rose Ridge.

The NTD criterion value of 0.94 is 0.01 higher than that returned using New Zealand SnowSim and 0.03 higher than that returned using SnowSim with the new precipitation distribution system.

6.4.1 Sensitivity to the new snow albedo parameter

The result of varying the new snow albedo (while retaining the other parameters at the optimum values) on modelled output is shown in Figure 67. The effect is primarily from late September onwards when temperatures are more frequently above zero. The greater the new snow albedo the greater the maximum SWE, and the later the end of the snow storage season. The difference is most notable directly after a snowfall as this is when the new snow albedo is the primary component of the albedo parameter. The sensitivity of the model to variations in the new snow albedo is shown in Figure 68. This shows that the model output is not greatly sensitive to high new snow albedo values especially for values greater than 0.8 which can be considered to be physically realistic for new snow (Paterson 1994). Indeed in the Franz Josef névé, adjacent to the Lake Pukaki catchment, new snow albedo measurements of between 0.67 and 0.93 have been made (Kelliher et al. 1996).

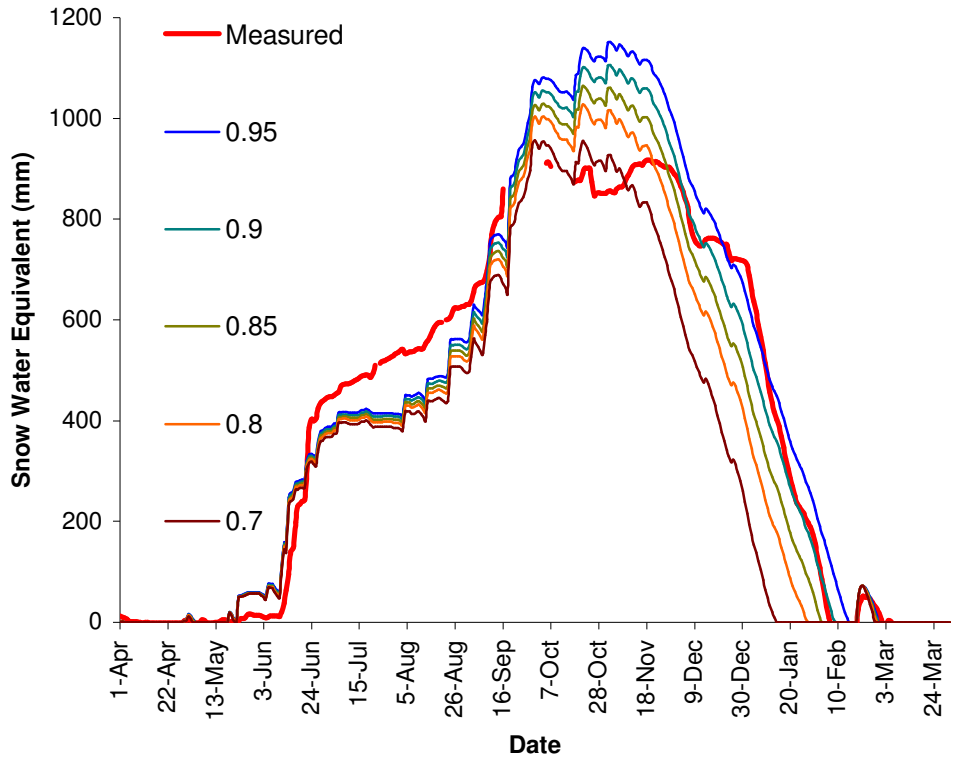

Figure 67. Radiation SnowSim snow water equivalent output for Rose Ridge with various new snow albedo parameters compared to calibrated measured snow water equivalent during 2002-2003.

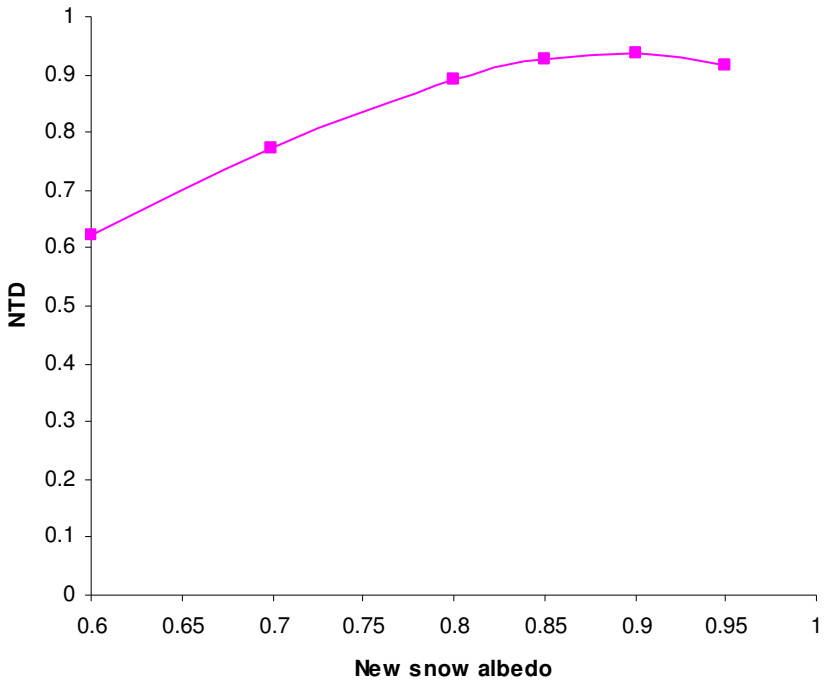

Figure 68. Sensitivity of accuracy of modelled snow water equivalent (as measured by the NTD criterion) to variations in the new snow albedo.

6.4.2 Sensitivity to the old snow albedo parameter

The effect of varying the old snow albedo on modelled output (while keeping the other parameters at the optimum values) is shown in Figure 69. The variation of the old snow albedo mainly affects the rate of ablation at the end of the snow season. This is when enough time has elapsed since a snowfall for the old snow albedo to become the dominant component of the albedo parameterisation. While the optimal model has an old snow albedo of 0.8, the value that results in a late season ablation rate (i.e. slope of the SWE curve) most similar to that measured is 0.5. This indicates that the high ablation rate with a high old snow albedo is compensating for the over estimation of SWE earlier in the season. The sensitivity of the model to variations in the old snow albedo is shown in Figure 70. This shows that the model has little sensitivity to the old snow albedo parameter setting. The maximum NTD value was returned for an old snow albedo of 0.8. This is higher than is likely to occur (Paterson 1994) indicating either the albedo parameterisation is not ideal, or (more likely) the radiation component is merely an index of a variety of melt processes, and not solely representing melt resulting from short wave radiation.

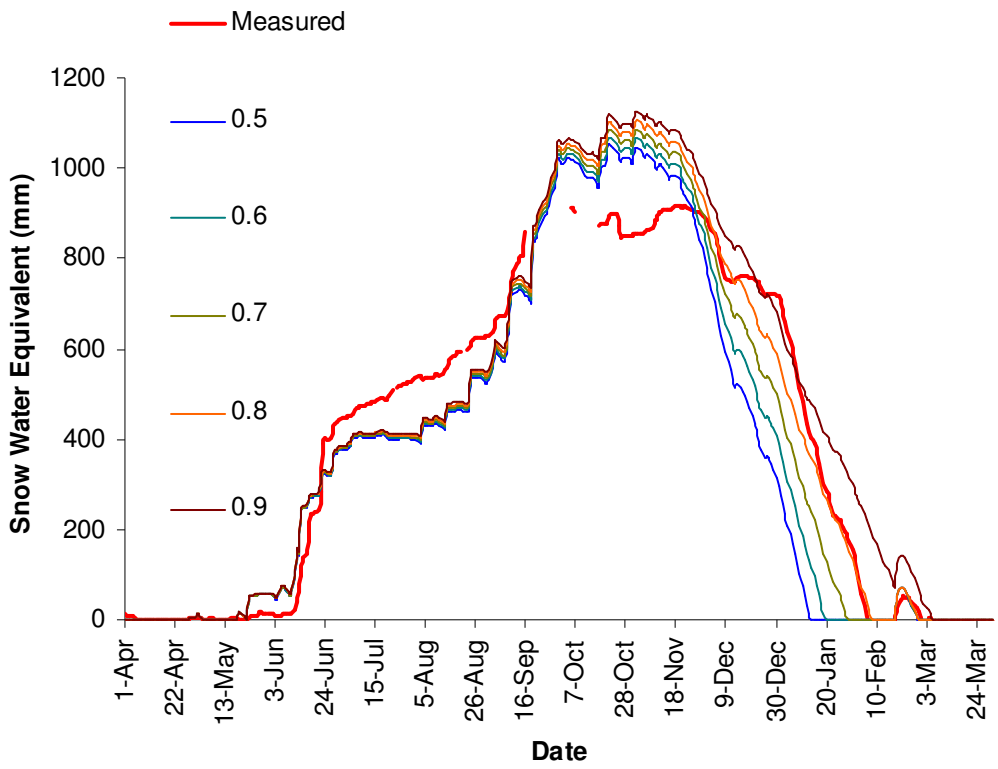

Figure 69. Radiation SnowSim snow water equivalent output for Rose Ridge with various old snow albedo parameters, compared to calibrated measured snow water equivalent during 2002-2003.

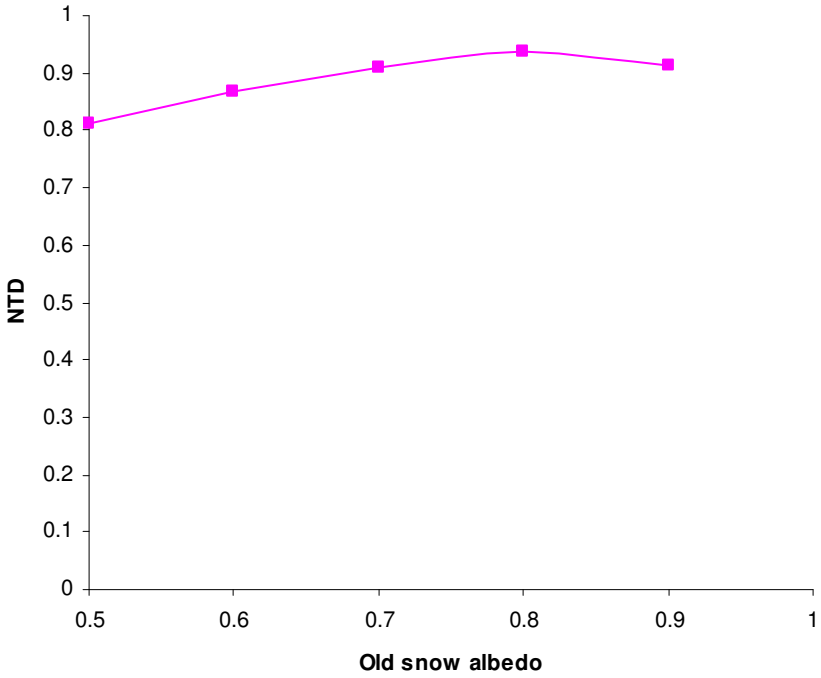

Figure 70. Sensitivity of accuracy of modelled snow water equivalent (as measured by the NTD criterion) to variations in the old snow albedo parameter.

6.4.3 Sensitivity to the clear sky coefficient parameter

The effect of varying the clear sky coefficient on modelled output is shown in Figure 71. This shows that the clear sky coefficient effectively scales the ablation once temperatures reach above zero. Sensitivity analysis of the clear sky coefficient is shown Figure 72. A coefficient of 0.3 returns the highest NTD criterion values but the variation in coefficient has little effect on the quality of the model output.

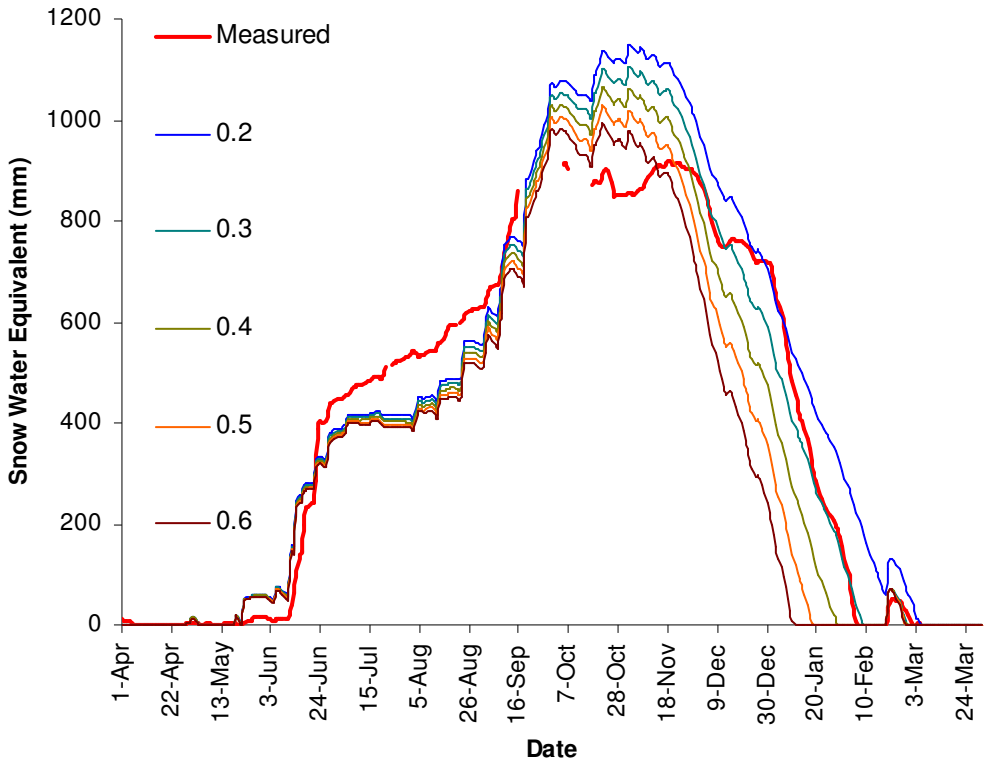

Figure 71. Radiation SnowSim snow water equivalent outputs for Rose Ridge with various clear sky coefficients compared to calibrated measured snow water equivalent during 2002-2003.

These results indicate that the albedo parameterization as used in Radiation SnowSim is not a crucial part of the model. Using average values from the literature for the new snow and old snow albedo would have provided a very similar result to that gained from optimization. The clear sky coefficient is more likely to require tuning to a particular location and provides an indication of how large a contributor to melt short wave radiation is. With the optimized melt factor of 1mm ^{o}C d^{-1}, the proportion of modelled short wave radiation melt through the season at Rose Ridge may be analysed. On the 23rd of December a maximum radiation melt of 12mm was achieved contributing 64% of the days melt as the temperature was modelled as being just 6.5 ^{o}C on that day.

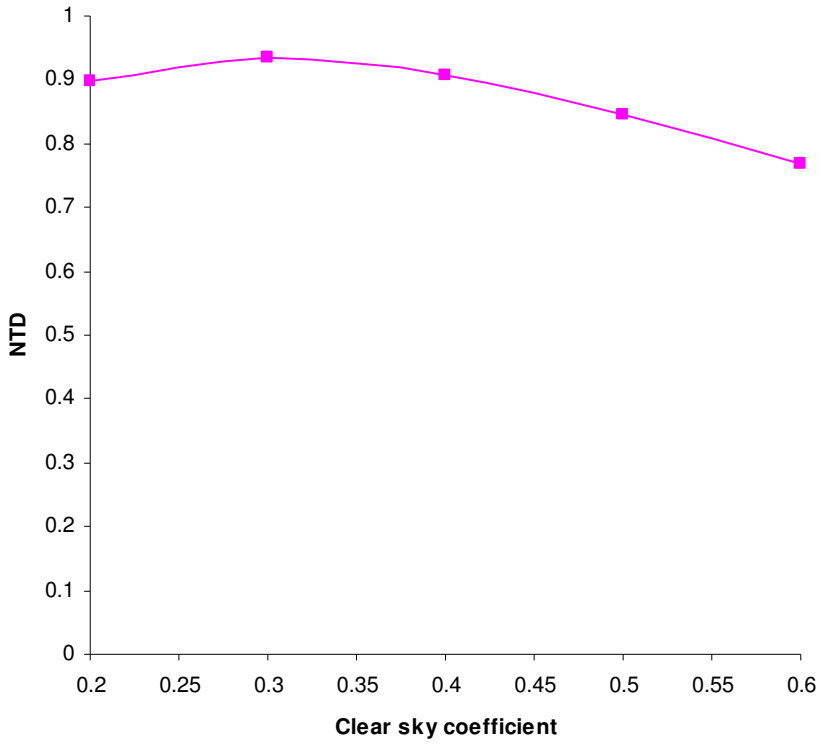

Figure 72. Sensitivity of accuracy of modelled snow water equivalent (as measured by the NTD criterion) to variations in the clear sky coefficient.

On the 27th of February, just 3mm of radiation melt was modelled, 22% of melt for the day, with an 11 ^{o}C day ensuring that most melt was modelled because of the high temperature. Overall approximately 50% of ablation was modelled as being from radiation melt. This compares to 63% measured from October 16th to November 25th in 1995 by Neale (1996) at Mueller Hut and 33% measured from 19th January to 22nd Feb in 2002 by Cutler (2002) on the Tasman névé, both high elevation sites within the catchment.

6.5 Radiation component for catchment free water

The Radiation SnowSim output for catchment free water is shown in Figure 73.

The radiation model has improved modelling of the early December and January flow peaks over the other versions of the model. However overall, inclusion of the radiation component in the model does not improve the catchment free water output when compared to lake inflows.

The highest NTD criterion value of 0.65 was returned for Radiation SnowSim with a minimum melt factor of 0 mm $^{o}C^{-1}$ d^{-1}, a new snow albedo of 0.95, an old snow albedo of 0.6, a clear sky coefficient of 0.5, and a snow/rain temperature threshold of 2.5 ^{o}C. The old snow albedo and clear sky coefficients are higher for the catchment wide optimisation than that

obtained for the Rose Ridge SWE output indicating short wave radiation is a greater contributor to melt processes on a catchment scale than is experienced at Rose Ridge.

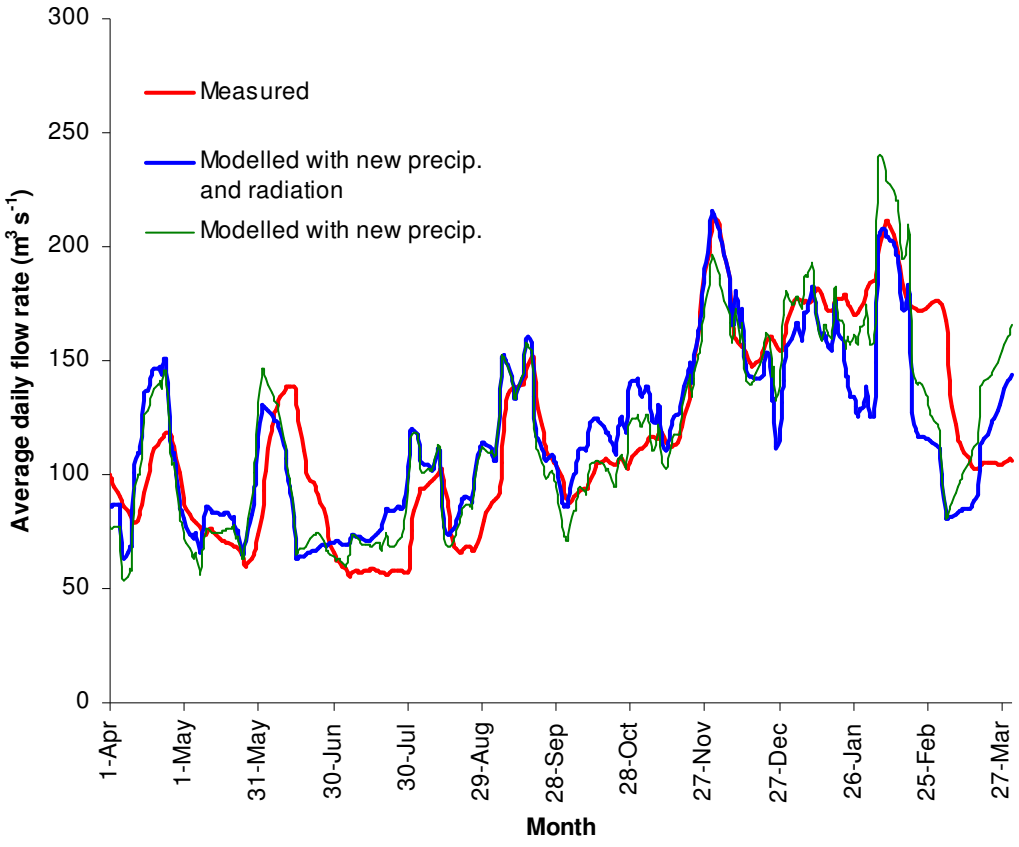

Figure 73. New Zealand SnowSim and Radiation SnowSim fourteen day running mean free water outputs , both with the new precipitation distribution, compared to measured fourteen day running mean daily lake inflows during 2002-2003.

The NTD criterion of 0.65 is 0.06 less than that returned using New Zealand SnowSim with the new precipitation distribution system and 0.04 higher than that returned using New Zealand SnowSim with the old precipitation distribution system. This indicates the inclusion of the radiation component provides no improvement to catchment scale modelling of snow storage.

6.5.1 Sensitivity to the new snow albedo parameter

The result of varying the new snow albedo (while retaining the other parameters at the optimum values) on modelled output is shown in

Figure 74. The new snow albedo has little effect at the beginning of the snow season as would be expected as there are few days of melt at that time. As the season progresses and melt quantities increase, the lower the new snow albedo the greater the melt. From November and December the effect changes with greater flows occurring with the higher new snow albedo values. This may be a result of less snow being available to melt as it has already melted earlier in the season. The November and February peaks are interesting in that new snow albedo has little impact on the output. Through these periods there was little snowfall so the modelled albedo across the catchment would be influenced more by the old snow albedo parameter. The sensitivity of the model to variations in the new snow albedo is shown in Figure 75. This shows that the model output is not greatly sensitive to new snow albedo values especially around the physically likely values of 0.8 and 0.9. This is a similar result to that obtained for the Rose Ridge SWE optimised model outputs. The model does perform better with the highest possible new snow albedo of 1.0 indicating that the melt modelled immediately after a snowfall is not measured. This may be a result of re-freezing of melt water within the snow pack, a process not included in the model.

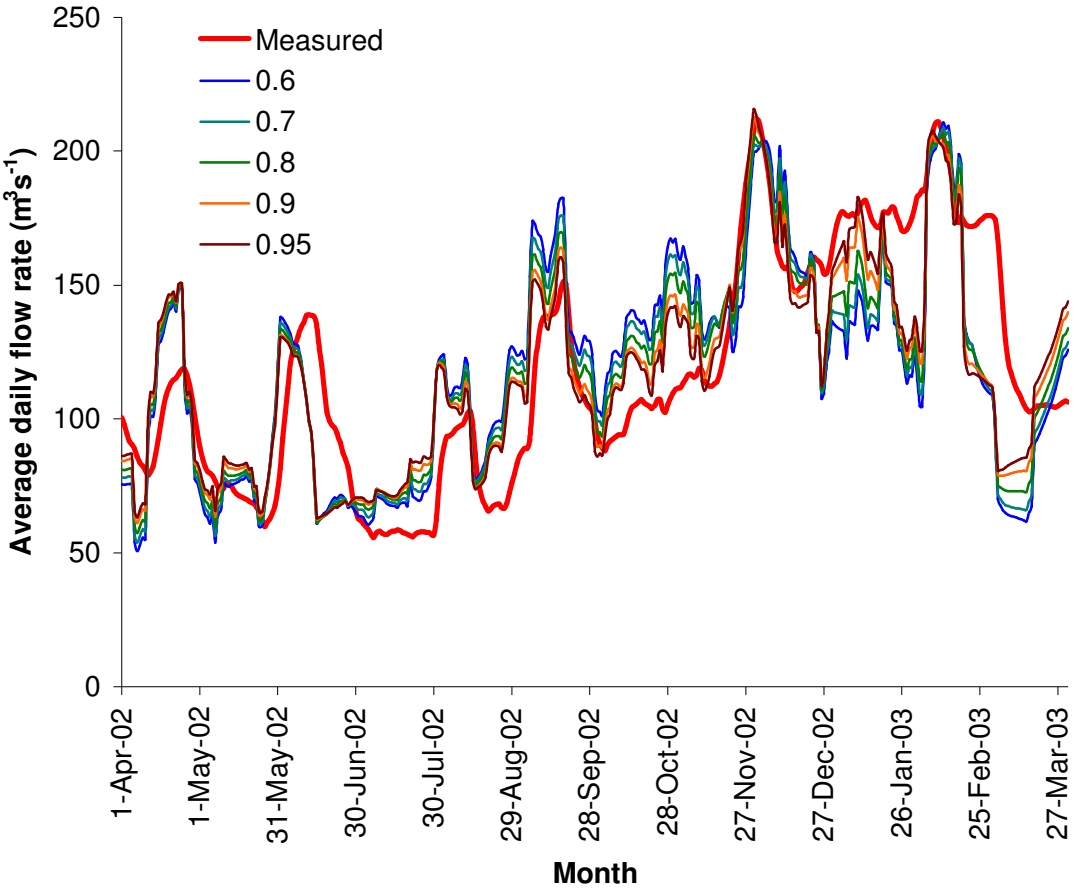

Figure 74. Radiation SnowSim fourteen day running mean catchment free water output with various new snow albedo parameters compared to fourteen day running mean daily lake inflows during 2002-2003.

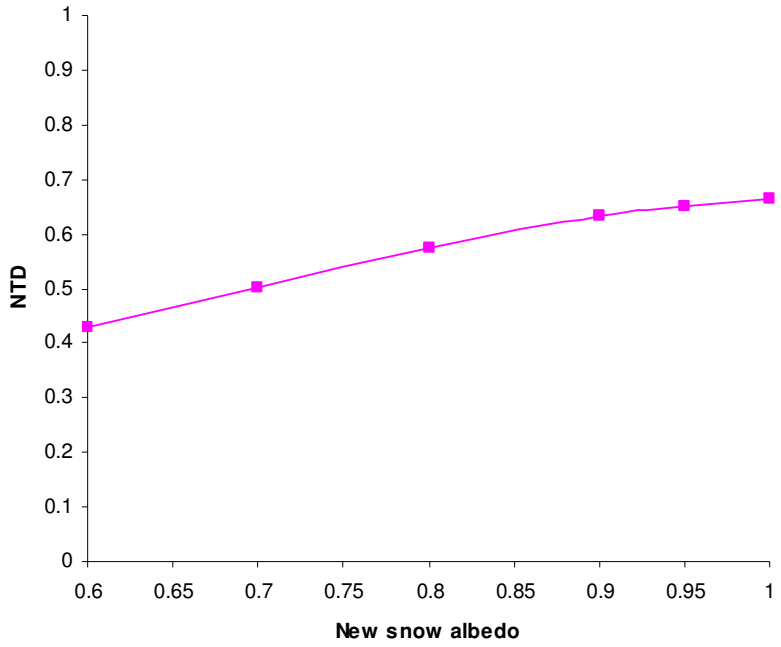

Figure 75. Sensitivity of accuracy of modelled catchment free water (as measured by the NTD criterion) to variations in the new snow albedo.

6.5.2 Sensitivity to the old snow albedo parameter

The effect of varying the old snow albedo on modelled output (while keeping the other parameters at the optimum values) is shown in Figure 76. The variation of the old snow albedo has little effect during the early season flow peaks. These peaks were associated with precipitation, so any associated snowmelt would have had a modelled albedo near the new snow albedo value, rather than the old snow albedo value. It is not until the long fine period associated with the early December peak that the influence of the old snow albedo becomes evident. The high old snow albedo values result in a lower December peak, while the low values result in a high peak as would be expected. The same occurs through to the February peak. Over the entire year the old snow albedo shows little effect on the free water in the catchment. This could be attributed to the regularity of precipitation ensuring that new snow albedo is of greater consequence to albedo values. The sensitivity of the model to variations in the old snow albedo is shown in Figure 77. This shows that the model has little sensitivity to the old snow albedo setting. The maximum NTD value was returned for an old snow albedo of 0.6. This is a more physically likely value for old snow than that returned for the Rose Ridge SWE optimisation. Old snow albedo is highly variable spatially as well as temporally (Brock et al. 2000a) which may explain the difference between the catchment wide old snow albedo value and that returned for the Rose Ridge site.

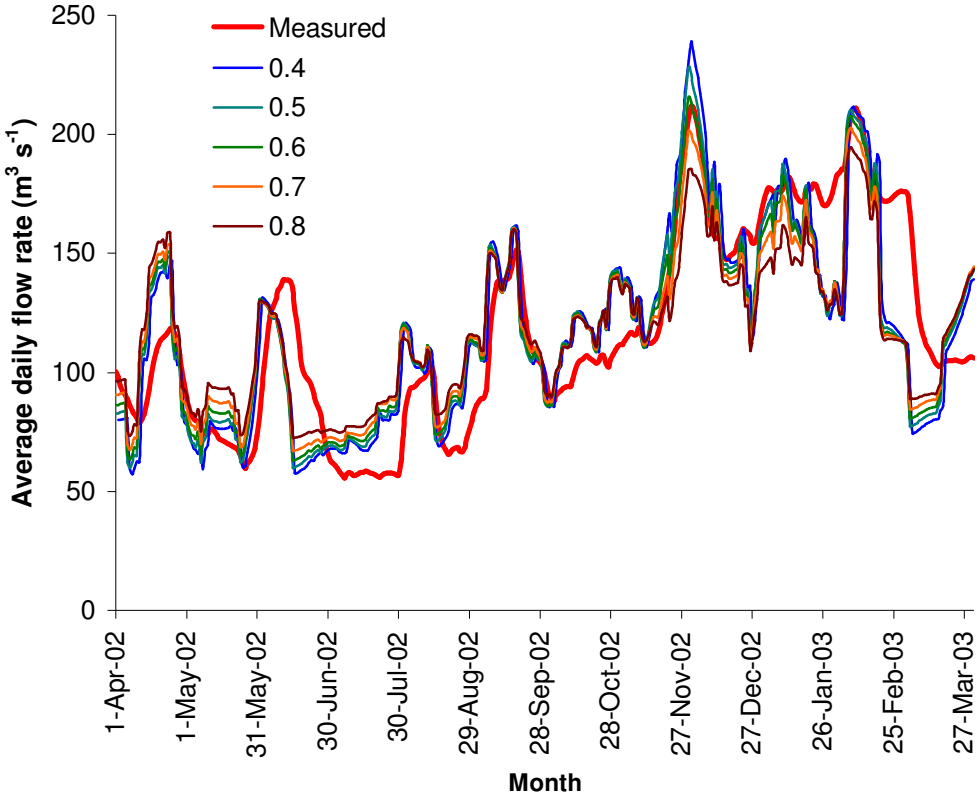

Figure 76. Radiation SnowSim fourteen day running mean catchment free water output with various old snow albedo parameters, compared to fourteen day running mean measured lake inflows during 2002-2003.

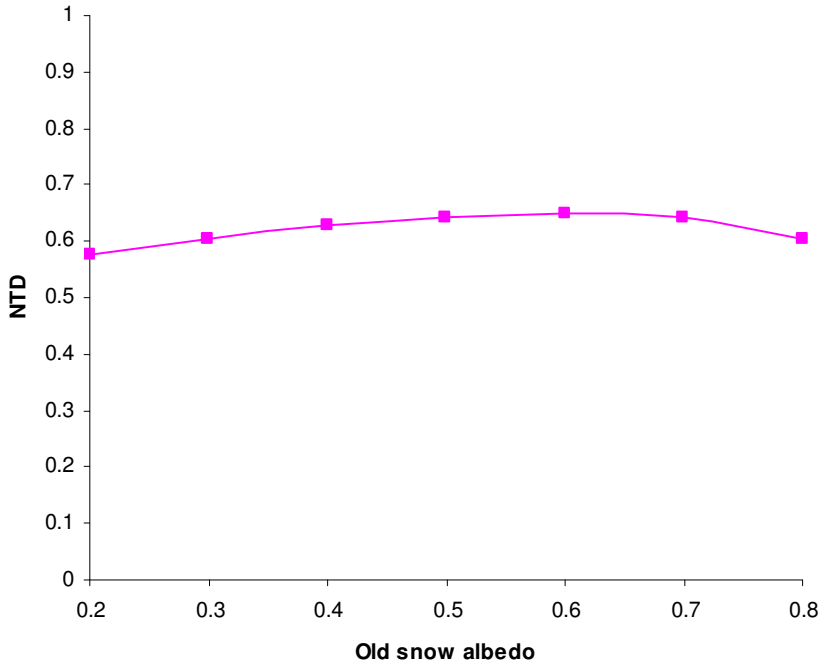

Figure 77. Sensitivity of accuracy of modelled catchment free water (as measured by the NTD criterion) to variations in the old snow albedo parameter.

6.5.3 Sensitivity to the clear sky coefficient parameter

The effect of varying the clear sky coefficient on modelled output is shown in Figure 78. The effect of varying the clear sky coefficient closely mirrors that found through varying the old snow albedo except that in this case, higher clear sky coefficient values result in higher free water flows. Once again it is the December peak when the greatest variation is observed, with little effect occurring during high rainfall periods. Sensitivity analysis of the clear sky coefficient is shown Figure 79. A coefficient of 0.5 returns the highest NTD criterion values but the variation in coefficient has little effect on the quality of the model output. This value is slightly higher than that returned for the Rose Ridge SWE analysis. With the minimum melt factor optimised to 0mm $^{o}C^{-1}$ d^{-1} all melt must be accounted for by the radiation component. Physically this is unrealistic and indicates the radiation component of the model is being used as an index for all melt processes.

The inclusion of the radiation component in SnowSim provides a small improvement in snow storage modelling at Rose Ridge and a deterioration of model output at the catchment scale.

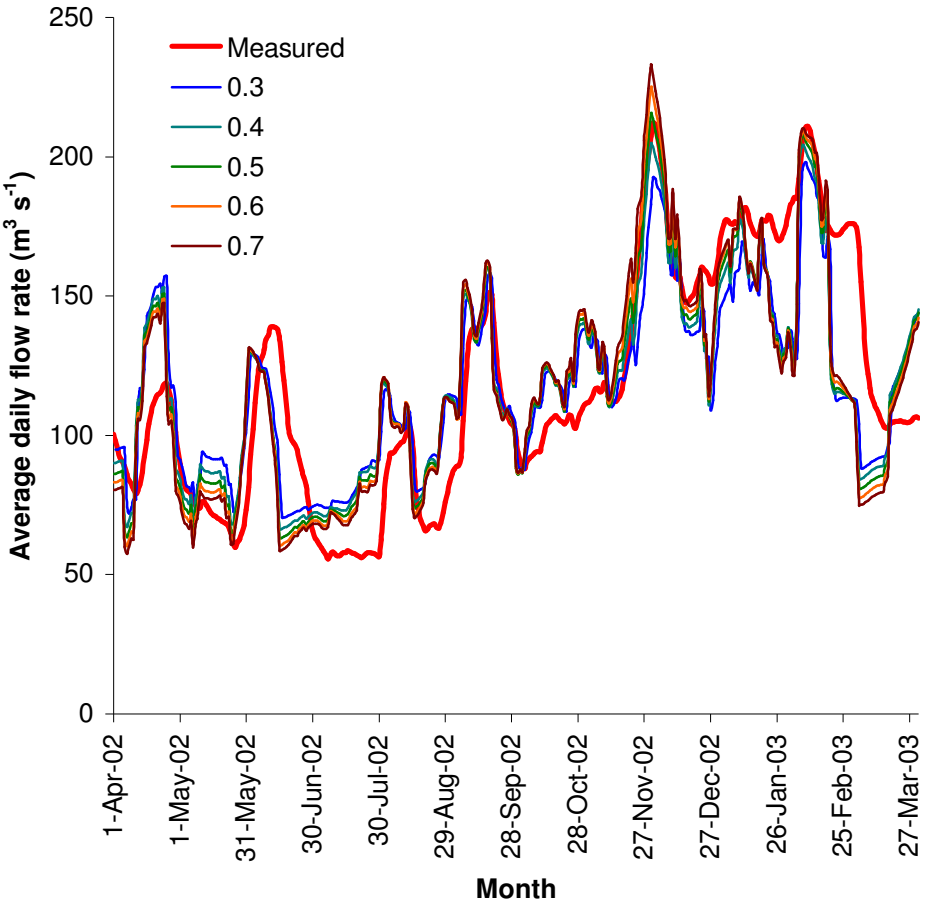

Figure 78. Radiation SnowSim fourteen day running mean catchment free water outputs with various clear sky coefficients compared to fourteen day running mean lake inflows during 2002-2003.

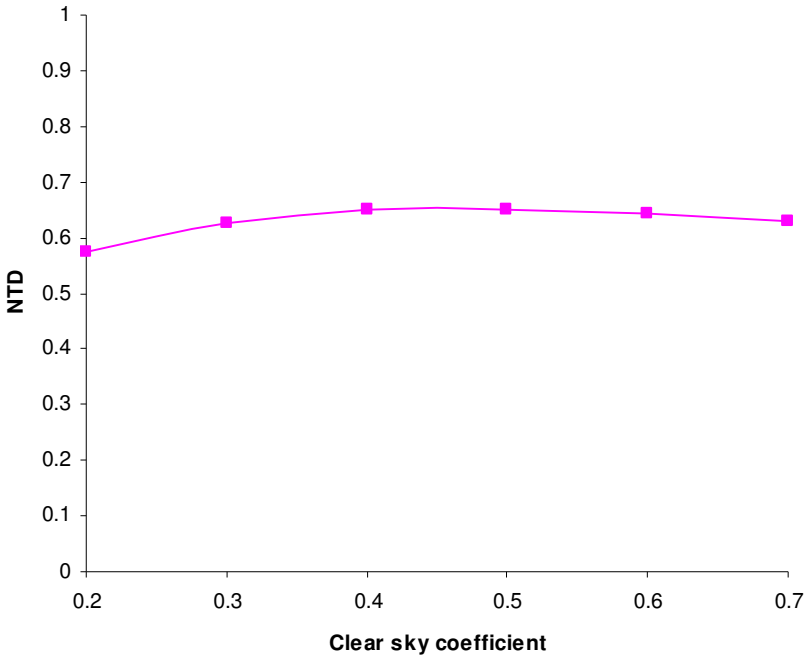

Figure 79. Sensitivity of accuracy of modelled catchment free water (as measured by the NTD criterion) to variations in the clear sky coefficient.

For clear sky calm conditions as experienced during early December, the radiation model appears to provide a very high quality of output. However the occurrences of such situations are too infrequent for a general improvement in model output. One period during which the radiation melt output consistently performed poorly was late January until early February when a reduction in melt was modelled, but measured values indicate a relatively constant flow. During this period small amounts of precipitation fell every few days with reasonably low temperatures so that snowfall was modelled in the mountain regions. This effectively "reset" the albedo values back to the new snow albedo level with the resulting reduction in melt. The model assumes that snow albedo reduces in a constant manner and does not account for step changes associated with specific layers of snow. This highlights an area of the model that could be improved. The generally poor result of the radiation model indicates that the relationship between melt magnitude and the day of the year (the basis of the melt factor parameterization used in New Zealand SnowSim) is stronger than that between melt magnitude and available shortwave radiation. Factors that affect melt with time include decreased albedo from accumulated dust and change in crystal shape, improved drainage channels in the snow pack, reducing the time for melt water to percolate through the snow pack, warming of the snow pack to its full depth reducing re-freezing of melt water, snow patch formation allowing air masses to reheat between patches increasing available melt

energy, and increased humidity (associated with warmer air and sea surface temperatures) enabling greater turbulent flux energy exchanges. The relative success of Radiation SnowSim with regard the Rose Ridge SWE output may be accounted for by the shorter season of snowmelt. The early and late periods of the season when Radiation SnowSim performed poorly at a catchment scale are ignored at the Rose Ridge site as there is no snow there at those times.

6.6 Summary

Substitution of the constant lapse rate with a measured lapse rate provides no improvement of temperature estimation. Modification of the precipitation distribution system, including a new annual average precipitation surface for the region, improves catchment scale model output significantly. Use of a radiation component within the model provides slightly improved model output at Rose Ridge, but a generally poorer model output at the catchment scale.

7 Model performance and verification

7.1 Introduction

The results of optimising and modifying SnowSim highlight the strengths and weaknesses of the model and the techniques used for its assessment. This chapter reviews and discusses the model performance, firstly at the point scale, then secondly at the catchment scale. This is done by identifying occasions when model and measurement results differ and analysing the cause of that difference. Following this, results of verifying the best performing catchment scale model by applying it to several years of new data are presented and discussed.

7.2 Model output performance for Rose Ridge SWE

The optimisation of New Zealand SnowSim to the Rose Ridge climate station location provided the greatest improvement in model output accuracy. This optimisation lifted the *NTD* criterion from 0.26 to 0.93. Compared to this improvement, the model enhancements varied the *NTD* criterion by just 0.02, with the new precipitation system returning a slightly poorer output and Radiation SnowSim returning a slightly improved output. This is shown in Table 15. The most notable change in the optimised parameters is the reduction in the magnitude of the melt factor with the upper limit reduced from 12 mm $^{o}C^{-1}$ d^{-1} for New Zealand SnowSim to 5 mm $^{o}C^{-1}$ d^{-1} for the optimised versions. This is more in line with values used by various other models applied in New Zealand and around the world as shown in Table 2.

Table 15. Parameter and accuracy criterion for different model versions optimised to the Rose Ridge location.

	Melt factor range (mm $^{o}C^{-1}$ d^{-1})	***Snow/rain temperature threshold (^{o}C)***	***Lapse Rate (^{o}C m^{-1})***	***NTD***
New Zealand SnowSim	3 - 12	2.5	0.007	0.26
Optimised New Zealand SnowSim	1 - 5	1.5	0.005	0.93
Optimised NZ SnowSim with new precipitation system	2- 5	1.5	0.005	0.91
Optimised radiation SnowSim	1	1.5	0.005	0.94

Analysis of the model results with consideration of particular snow storage events enables an understanding of the strengths and weaknesses of the model. The onset of snow storage at Rose Ridge during the 2002-2003 snow season was associated with the passing of an intense depression to the south of New Zealand in early June. This brought south westerly followed by southerly conditions to the South Island with a complex series of fronts and cyclonic conditions ensuring a large quantity of snow fell. The snowfall from the 12th to 14th of June was modelled but not that which occurred on the 17th and 18th while the snowfall of the 22nd and 23rd was underestimated. From the synoptic charts shown in Figure 80 it can be seen that the 12th-14th were characterised by westerly conditions, the 17th and 18th by cyclonic conditions and the 22nd-23rd by south westerly conditions.

The response of the model to these different conditions as shown in Figure 81, demonstrates that the closer the experienced precipitation conditions are to the annual average, the better the modelling. Hence the westerly conditions were modelled well, the south westerly less well, and the cyclonic poorly. To further complicate matters it is likely that the widespread cold weather experienced during the cyclonic conditions resulted in under-gauging at many rain measurement sites. Tipping bucket rain gauges require liquid water for operation so that during a snowfall inaccurate readings may be returned. It is possible that this exacerbated the poor modelling of snowfall during the 17th and 18th at Rose Ridge. This highlights the reliance SnowSim has upon the integrity of the input data

Another time of significant discrepancy between the modelled and measured snow storage quantities is from the 12th December until the 1st of January. The measured values show two distinct periods when there is no snowmelt, while the modelled snow storage shows continual snow depletion at the same time (see Figure 82). The temperature records show cooler sub-zero temperatures from the 11th to the 15th and the 25th to 26th December at Rose Ridge on these days. The modelled temperatures, however, only show sub-zero temperatures on the 14th and 26th, with temperatures above 1.5 ^{o}C on the other days around this time.

This results in the precipitation for this period being modelled as rain rather than snow as actually occurred. The only parameter options that show an indication of these halts in ablation are those with the higher lapse rates, (see Figure 28) and higher snow/rain temperature thresholds (see Figure 39). This indicates that accurate temperature modelling is critical in capturing such events. In general the assessment of SnowSim against point measurements indicates the primary limitation is in estimating precipitation and temperature. The sensitivity of the model to the threshold temperatures (see Figure 42) and the lapse rate (see Figure 29) indicates temperature estimation in particular is critical for accurate results.

With tuned melt factor parameters, the rate of ablation shows a close match between modelled and measured results. This indicates the melt to temperature relationship is well founded. Perhaps the most important outcome of this analysis is the confirmation of the quality of SnowSim as a point location SWE model.

The tuned parameters for the Rose Ridge site are of interest when compared to values obtained elsewhere. The tuned melt factor parameters lead to a range of possible melt factors from 1 mm $^{o}C^{-1}$ d^{-1} to 5 mm $^{o}C^{-1}$. At Mueller Hut, within the catchment, Neale (1996) found an optimum melt factor of 2.3 mm $^{o}C^{-1}$ d^{-1} during measurements between October 16th and November 25th. With the Rose Ridge optimised SnowSim (with the new precipitation system) parameters, the melt factor would be set to 2 mm $^{o}C^{-1}$ d^{-1} during this period though this is the maximum possible requiring no snow to fall. Using the catchment wide optimised SnowSim just 1 mm $^{o}C^{-1}$ d^{-1} would be estimated. In the Tasman névé, Cutler (2002) found an average melt factor of 4.9 mm $^{o}C^{-1}$ d^{-1} was optimal during a period from 19th January until 22nd February. With the Rose Ridge optimised SnowSim (with new precipitation system) parameters, the melt factor would be set to 4.8 mm $^{o}C^{-1}$ d^{-1} during this period, though again this is a maximum. With the catchment wide optimised SnowSim 5.5 mm $^{o}C^{-1}$ d^{-1} would be estimated. These figures demonstrate the variability of ablation within the catchment but also indicate that the optimised SnowSim parameters are not unreasonable according to what measurements exist.

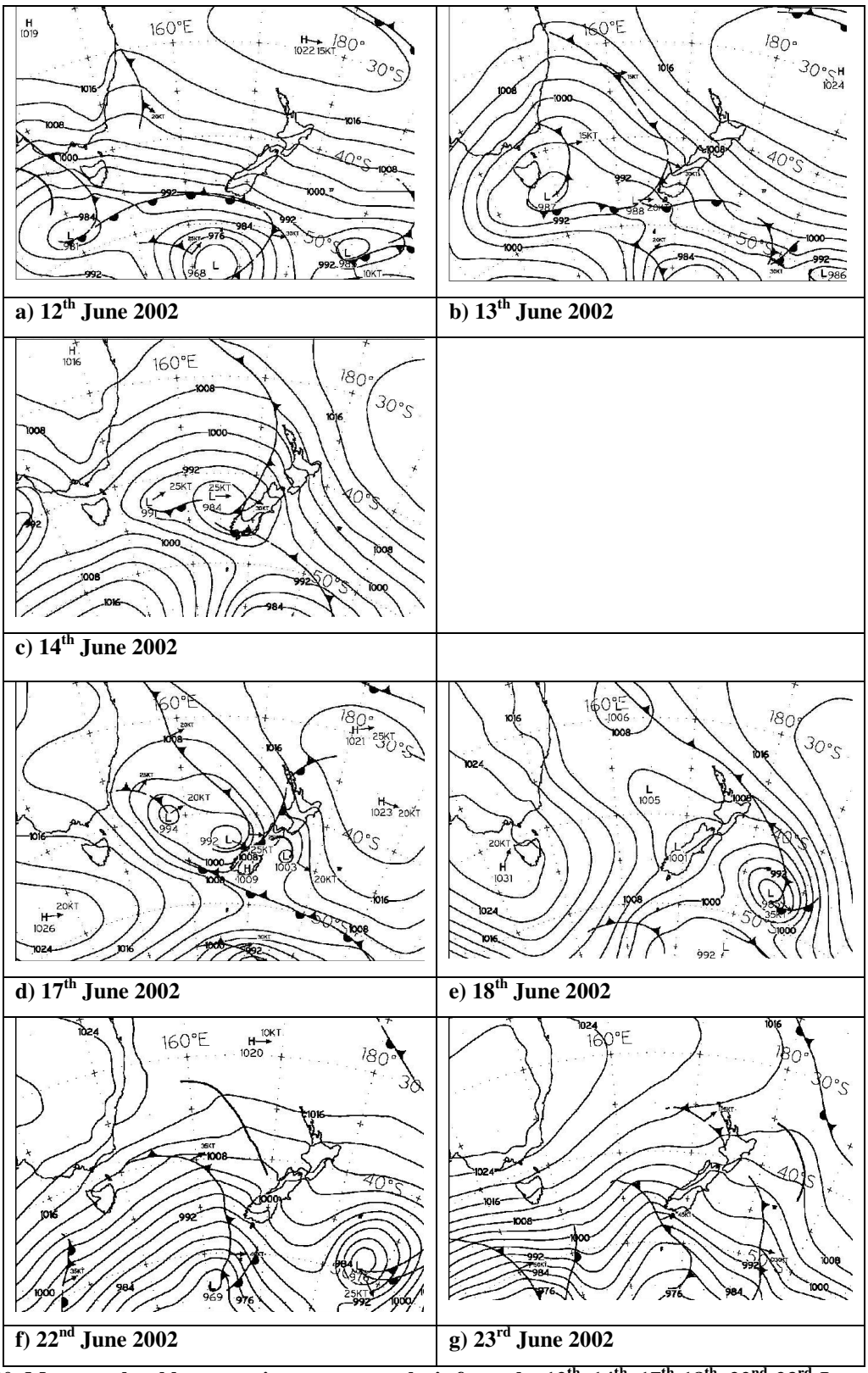

Figure 80. Mean sea level barometric pressure analysis from the 12th–14th, 17th-18th, 22nd-23rd June 2002 (Source: NZ Meteorological service).

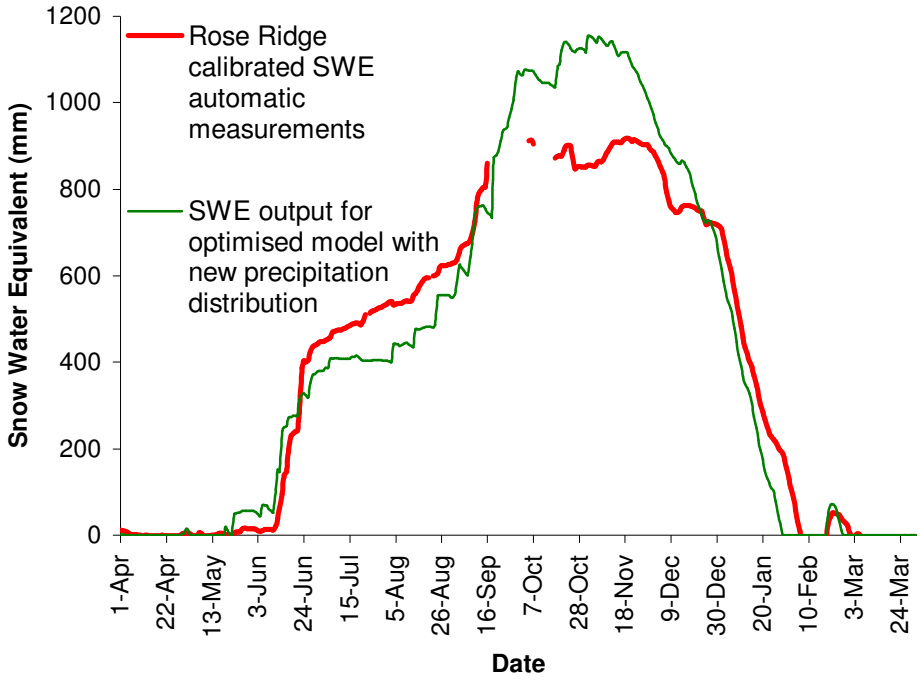

Figure 81. Optimized SnowSim snow water equivalent output for Rose Ridge compared to calibrated measured snow water equivalent during 2002-2003.

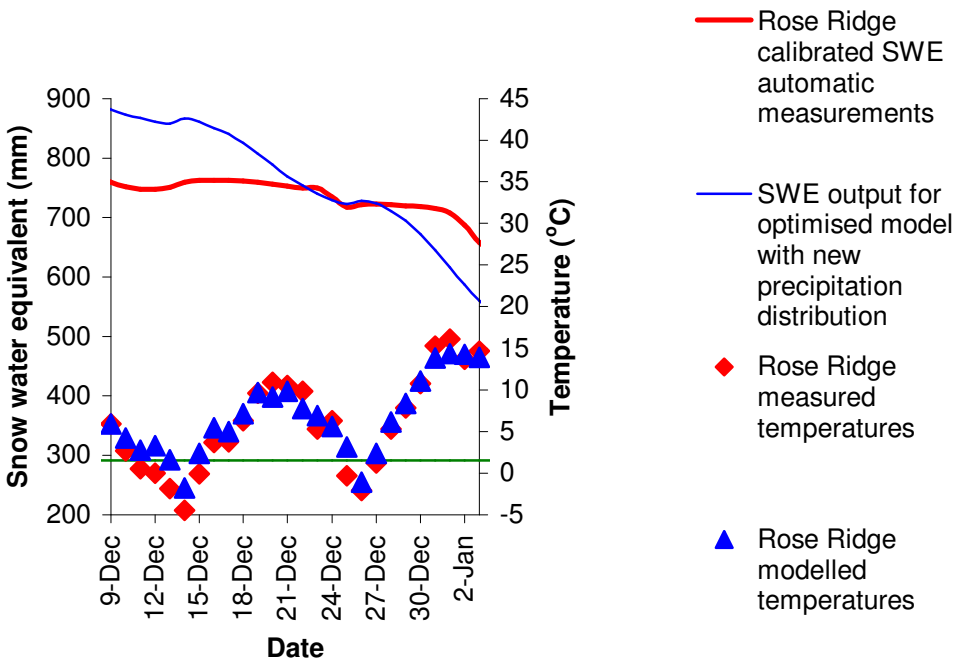

Figure 82. Optimised SnowSim snow water equivalent and temperature output for Rose Ridge compared to calibrated measured snow water equivalent and temperature from the 9th December 2002 until the 3rd January 2003.

7.3 Model output performance for catchment free water

The default New Zealand SnowSim model outputs compared well to the measured lake inflows. With optimisation this was improved, though not nearly as much as that which occurred at the Rose Ridge site. The optimisation required a similar reduction in the melt factors as found when optimising the model for the Rose Ridge site. Inclusion of the new precipitation system resulted in another jump in accuracy to 0.71 from 0.61. The inclusion of the radiation component, however, caused a significant drop in accuracy. The optimal parameters found for each model version are shown in Table 16. The optimised SnowSim with the new precipitation system was selected as the preferred snow storage model for the Lake Pukaki catchment. The lower *NTD* criterion values for the catchment scale output, compared to the Rose Ridge output, is a reflection of the method of output comparison. At Rose Ridge, the measured to modelled comparison occurred for just a portion of the year (that which had snow on the ground) and considered snow water equivalent quantities only. At the catchment scale, the entire year of free water is modelled, an entirely more complex system. The optimised New Zealand SnowSim (with new precipitation system) free water output and measured lake inflows are again shown in Figure 83. Discrepancies between the modelled free water and the measured lake inflows provide insight into the situations in which the model works well and when the model works not so well. This in turn provides an indication of the accuracy of the results, limitations of the model and potential applications of the model and direction to where future work could most likely provide benefit.

The offset in flow magnitude is possibly the greatest shortcoming of the model. A consistent daily average of 27.9 m^3s^{-1} is needed to raise the free water estimates into line with those measured. As discussed in Section 6.3 the source of this error is unknown. The application of SnowSim to more snow seasons provides an indication of whether the offset is constant or variable and is discussed in section 7.4.1 below. This offset error means the model output is most accurate as an indicator of variation in catchment flow, rather than absolute flow magnitude.

The variable temporal offset between modelled and measured flow peaks is an interesting phenomenon that provides insight into the hydrological processes in the catchment. At the beginning of the snow season the modelled peaks anticipate the measured peaks by several days (11 days for the June peak), while the December and February peaks are well matched (1 day for the December peak). An offset may be explained by the fact that no propagation delay is incorporated in the modelled results. The reduction in this delay as the season progresses may be a reflection of the change in: flow volumes, drainage channels and various storage

volumes. Drainage channels in snow and ice are become more efficient with increased flow volumes, so less delay occurs between melt and inflow as the melt season advances. Ground water, sub glacial reservoirs, terminal lakes and even snow pack each contribute to the catchment reservoirs which will fill and deplete at varying rates. Each type of storage has unique processes affecting it, for instance ground water storage is influenced by growth vigour of plants (Kelliher and Jackson 2001) and glacial storage is influenced by drainage channel dynamics and changing glacier morphology. In general though, at times of average low flow (winter) these reservoirs will be depleted ensuring a delay to flow as they fill up, while during average high flow conditions (summer), these reservoirs will be full, so that any extra water will propagate down stream without first "topping up" the various storage components.

Table 16. Parameter and accuracy criterion for different model versions optimised to the catchment.

	Melt factor range ***(mm $^{o}C^{-1}$ d^{-1})***	***Snow/rain temperature threshold (^{o}C)***	***Lapse Rate*** ***(^{o}C m^{-1})***	***NTD***
New Zealand SnowSim	3 - 12	2.5	0.007	0.54
Optimised New Zealand SnowSim	1 - 5	2.5	0.005	0.61
Optimised NZ SnowSim with new precipitation system	1 - 6	2.5	0.005	0.71
Optimised radiation SnowSim	0	2.5	0.005	0.65

The flow peak of the third of December demonstrates a special case in that no rainfall occurred at this time. The synoptic charts for this period are shown in Figure 84. Temperatures were very high, with 12 ^{o}C modelled and measured at the Rose Ridge climate station and the entire catchment being above 0 ^{o}C. Interestingly the best model for this peak was achieved by Radiation SnowSim with a very close relationship between measured and modelled output (see Figure 73). The satellite images for the period show clear skies in the catchment for each day as shown in Figure 84. The calm clear conditions ensure that radiation melt is likely to be the most important component of the melt fluxes during this period and with no rain, the most important contributor to catchment free water.

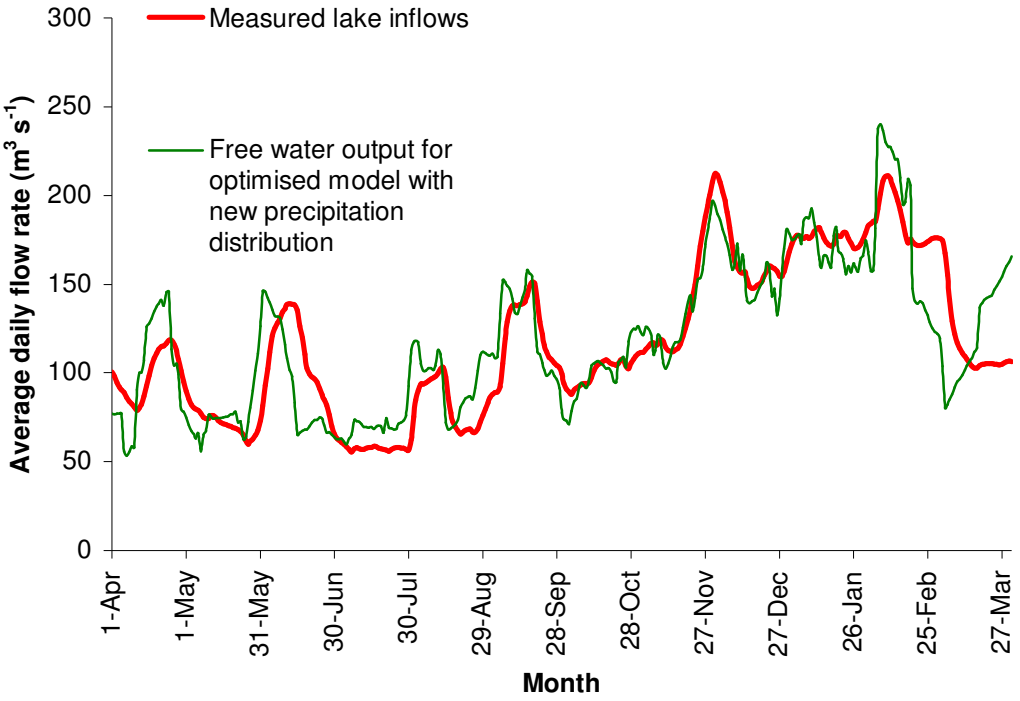

Figure 83. 14 day running mean of the SnowSim output for catchment free water with the new precipitation distribution, compared to 14 day running mean of the measured lake inflows during 2002-2003.

This explains why Radiation SnowSim performed so well during this period. Without consideration of the snowmelt processes this peak would not be anticipated by water users in the catchment. At a time of year when water for irrigation is important for summer plant growth, knowledge that such a peak is likely under these conditions, may enable improved planning of irrigation schedules. In a similar manner hydro-electric lake management could utilize the knowledge of the arrival of the peak to step up generation. For recreation users and tourism operators the snow pack will become very wet during such conditions creating hazardous conditions for travel associated with increased likelihood of wet snow avalanches. The modelled fall in free water on the 18th and 19th of February which was not measured, at first appears to be a model deficiency. On these days the temperature in the catchment reduced considerably. Just 3 ^{o}C was measured at Mt Cook on the 18th indicating that much of the catchment was below zero. This means that what precipitation did fall was modelled as snow. Hence no rain or melt was modelled. The flows into Lake Pukaki, however, would not have stopped because of recessional flow from the various catchment reservoirs. This discrepancy therefore is a result of the method of model-to-measured comparisons, not because of a failure in the model itself. The majority of issues highlighted in the results are related to the use of lake inflows as a comparison to free water estimations. Combining

SnowSim with a proven flow propagation model would identify the accuracy of the delay and recession assumptions described above as well as provide a valuable product in itself. The greatest error in SnowSim alone is the flow magnitude offset. This anomaly restricts the application of SnowSim to identification of variability in snow storage rather than to absolute flow magnitudes. What SnowSim does well is identify the major melt events both in terms of timing and relative size and the importance of these events as part of the seasonal cycle of flow. This information is crucial for understanding the hydrology of the catchment and provides a valuable tool for those affected by it. The accuracy of the free water modelling by SnowSim is of a similar magnitude to that found by Kustas and Rango (1994) for the Dischma Basin in Switzerland. However in the Swiss case, the addition of a radiation component greatly increased the quality of the output. Likewise Hock (1999) found that for the Storglaciären in Sweden a radiation enhanced temperature-index model performed better than the basic temperature-index model, although the difference was not as marked as that found by Kustas. Hock considered the ability to model at sub daily time intervals, and the improved accuracy at the grid square level was where the true worth of the radiation enhanced model was found. Cazorzi and Dalla-Fontana (1996) also found a radiation enhanced temperature-index model provided a high quality of output, though in this case no comparison to a standard temperature-index model is made. Unfortunately the use of differing model accuracy criteria prevents comparison between the various models. A broad review of modelling techniques by Hock (2004) found that in general, the addition of a radiation component improved temperature-index models with the exception of the application of such a model to two outlet glaciers in Greenland. The results from the Lake Pukaki catchment indicate either another exception has been found, or the method of implementation could be improved. The nature of the snowmelt processes may provide an indication of why the radiation component provided little improvement. A review of energy balance contributions to melt by Willis et al. (2002) reveals that on average 77% of melt is from radiation in continental locations. In maritime locations, on average just 49% of melt is attributable to radiation. Admittedly, Storglaciären is considered maritime though radiation melt of ice during summer has been measured to contribute 66% of the melt there. Measurements from Mueller Hut indicate 63% of melt is derived from radiation (Neale 1996), with just 33% from radiation in the Tasman névé (Cutler 2002). Approximately 130 km north east of the Lake Pukaki catchment just 30% of melt was attributed to radiation in the Craigeburn mountains (Prowse and Owens 1982) and a mere 16% at Temple Basin (Moore and Owens 1984a), a small catchment lying immediately east of the divide.

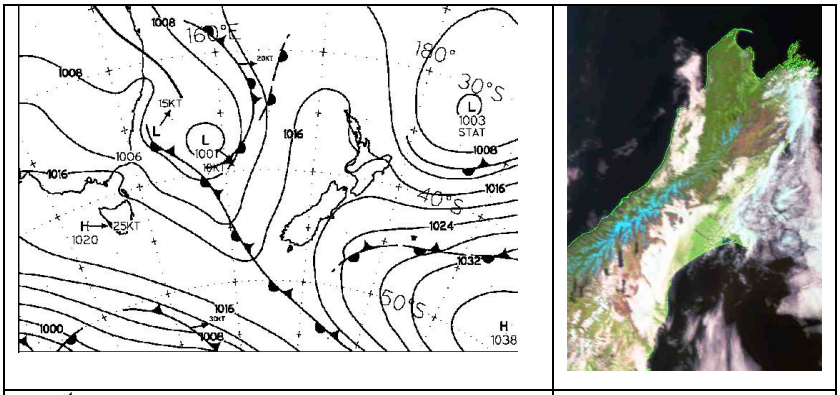

a) 1st December 2002

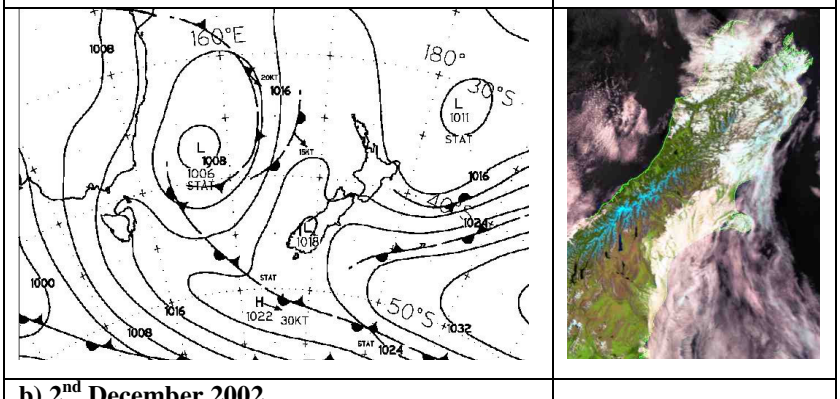

b) 2nd December 2002

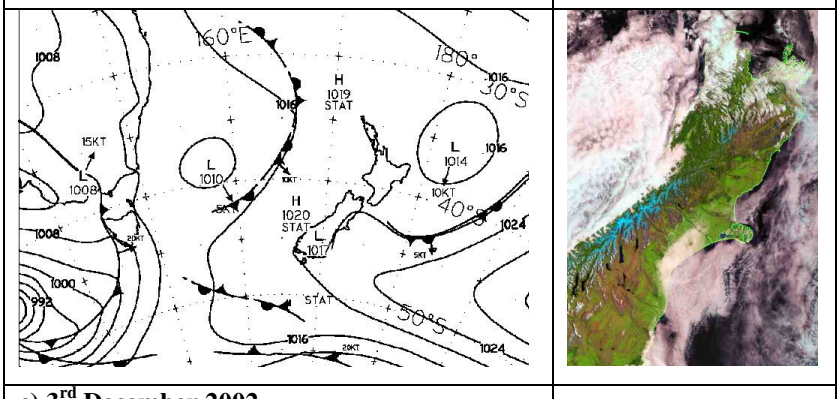

c) 3rd December 2002

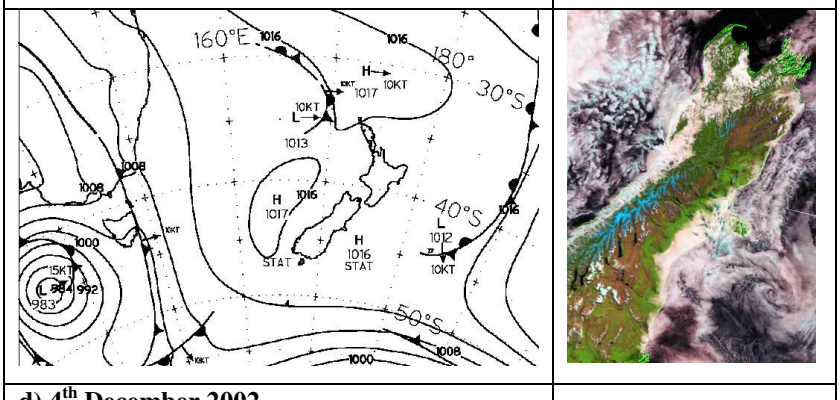

d) 4th December 2002

Figure 84. Mean sea level barometric pressure analysis from the 1st to 4th of December 2002 (Source: NZ Meteorological service) and NOAA satellite imagery of the South Island for the same dates (Source: Landcare).

These measurements point to radiation melt having a smaller influence on melt energies in the Lake Pukaki catchment than at locations where radiation enhanced temperature-index models have provided improved snowmelt modelling. This provides an explanation of why the radiation component provided no improvement in melt modelling in the Pukaki catchment.

7.4 Verification results

The results of applying the optimised model to the snow years from April 1st 2000 until March 31st 2004 are described in this section. Criteria set out by the World Meteorological Organisation as outlined in section 4.5 are used. Note that because the model does not incorporate a flow propagation component, 14 day running means of free water and lake inflows have been used in place of daily discharge. Each year a different offset was applied to optimise the model output for that year. The array of graphical and numerical criteria results gives insight into the accuracy of SnowSim, provides an indication of where the strengths and weaknesses of SnowSim lie and enables comparison to other models on other catchments.

7.4.1 Graphical criteria

The free water to lake inflow comparison for snow years 2000-2001, 2001-2002, 2002-2003 and 2003-2004 are shown in Figures 85 to 88 respectively.

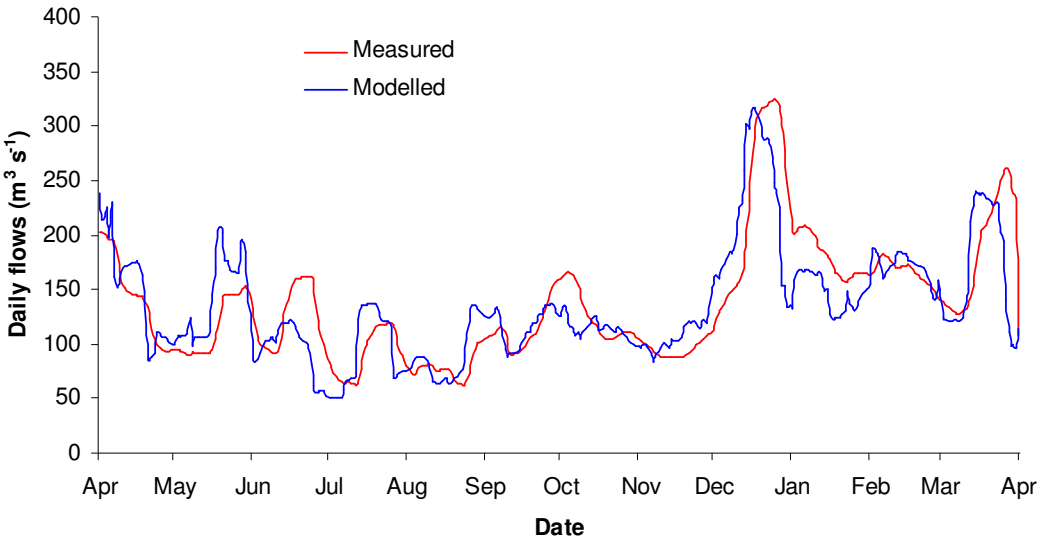

Figure 85. SnowSim (with new precipitation system) fourteen day running mean free water output compared to measured fourteen day running mean daily lake inflows during the verification period of 2000-2001.

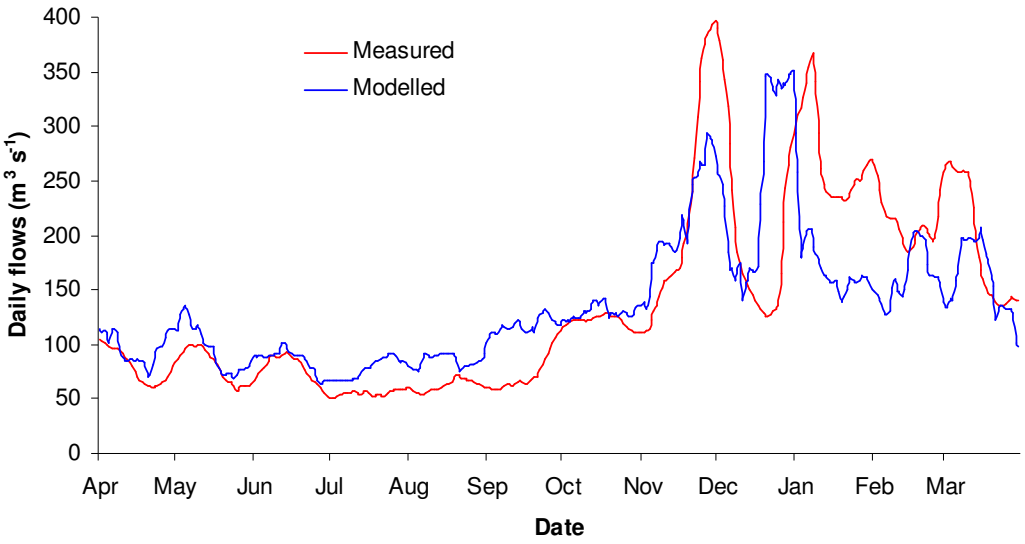

Figure 86. SnowSim (with new precipitation system) fourteen day running mean free water output compared to measured fourteen day running mean daily lake inflows during the verification period of 2001-2002.

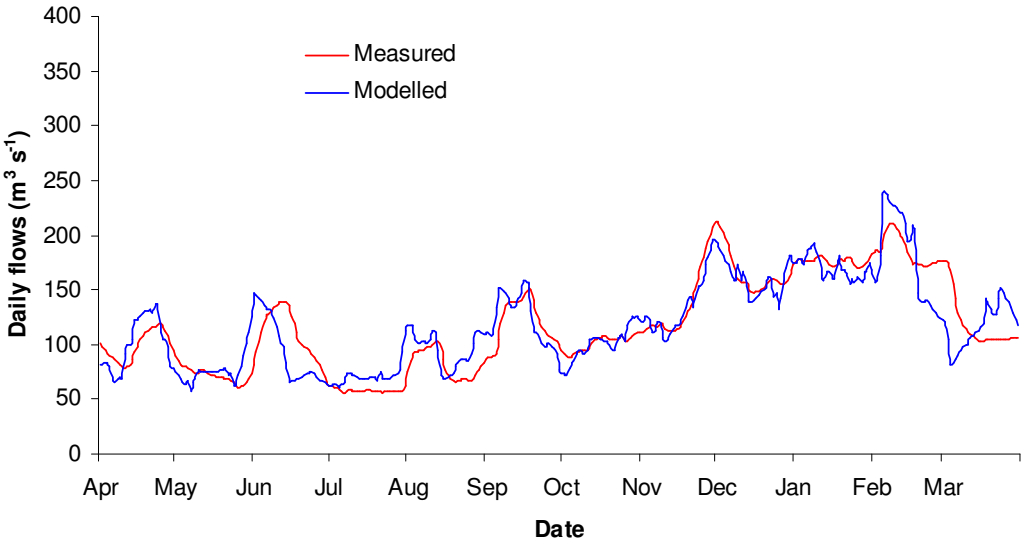

Figure 87. SnowSim (with new precipitation system) fourteen day running mean free water output compared to measured fourteen day running mean daily lake inflows during the calibration period of 2002-2003.

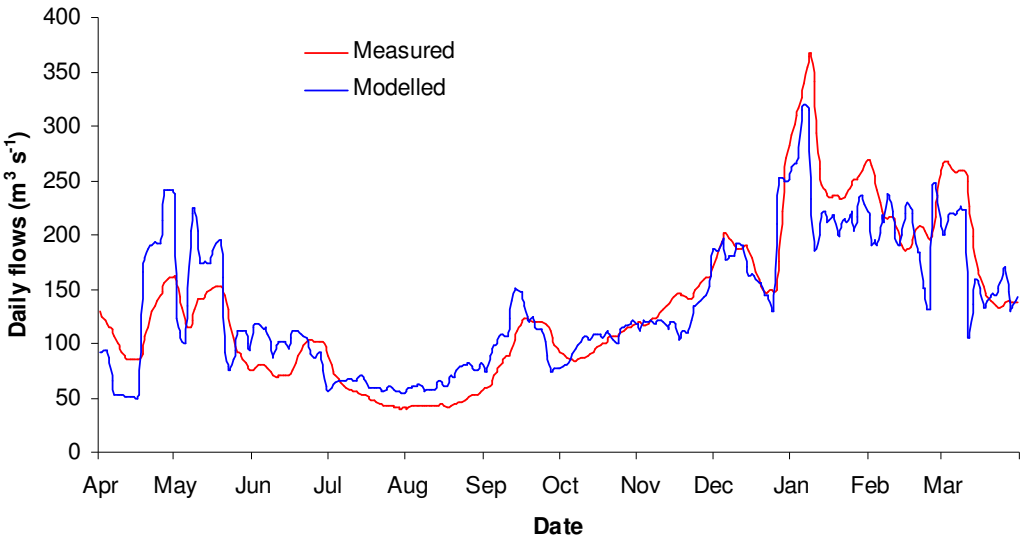

Figure 88. SnowSim (with new precipitation system) fourteen day running mean free water output compared to measured fourteen day running mean daily lake inflows during the verification period of 2003-2004.

The flow duration curves for the calibration and verification periods are shown in Figures 89 and 90.

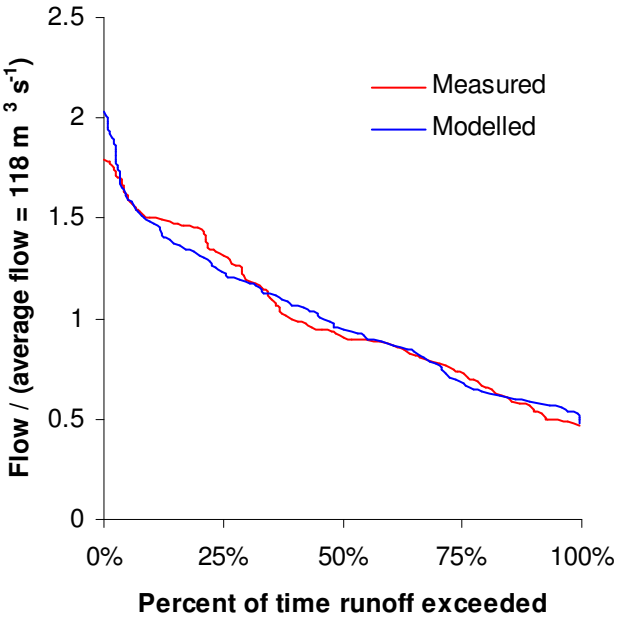

Figure 89. Flow duration curve for modelled free water and measured lake inflows during April 2002 until March 2003 (calibration period).

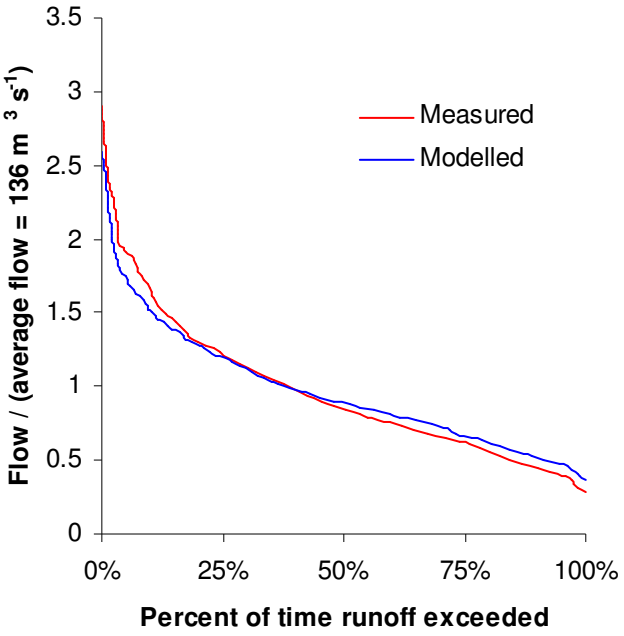

Figure 90. Flow duration curve for modelled free water and measured lake inflows during April 2000 until March 2002 and April 2003 until March 2004 (verification period).

Scatter diagrams of modelled maximum monthly free water versus measured monthly maximum lake inflows are shown for the calibration and verification periods in Figures 91 and 92.

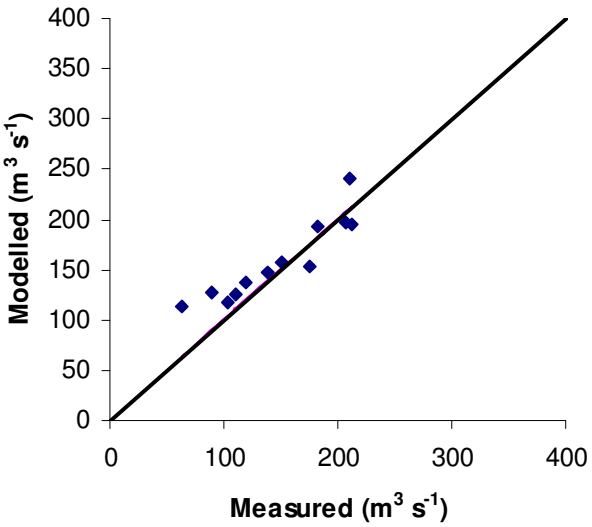

Figure 91. Scatter diagram of modelled monthly maximum free water against measured monthly maximum lake inflows for the calibration period from April 2002 until March 2003.

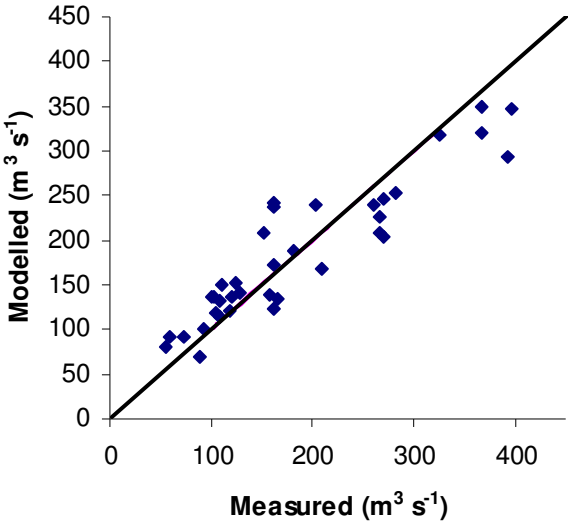

Figure 92. Scatter diagram of modelled monthly maximum free water against measured monthly maximum lake inflows for the verification period from April 2000 until March 2002 and April 2003 until March 2004.

The free water to lake inflow graphs show the variability in flow regimes from one year to the next. SnowSim captures the seasonal variation well in all years. The quality of magnitude of modelled flow peaks is variable with the 2001-2002 year being particularly poor towards the end of the season. The climate records from the new Meridian climate stations located in the Godley and Ohau rivers were not used in the 2000-2001 and 2001-2002 model runs. This is likely to have reduced the quality of the temperature and precipitation estimations and in turn influenced the poor model results for those years. The flow duration curves indicate the model depicts the variation in flow well, though underestimates peaks and over estimates low flows. This result follows from SnowSim being an empirical model which by its very nature is better at modelling average conditions than extreme events. The scatter diagrams of monthly maximum flows indicate that SnowSim may be a valuable tool for identifying peak flow conditions, so critical in flood flow determination. Once again a slight over estimation of the low values, and under estimation of the high values is apparent. Generally, SnowSim models well the variability of flow, the relative magnitudes of flow events, and the frequency of peak flows. Room for improvement exists in capturing extreme events for both low flow and high magnitude events. The average daily lake inflows, precipitation, modelled free water, estimated ice melt and offset to align modelled to measured outputs are shown in Table 17.

Table 17. Average daily flow quantities for catchment wide quantities during 2000 until 2004.

Snow Season	*Average measured lake inflows ($m^3 s^{-1}$)*	*Average modelled precipitation ($m^3 s^{-1}$)*	*Average modelled free water ($m^3 s^{-1}$)*	*Average estimated ice melt ($m^3 s^{-1}$)*	*Average free water offset ($m^3 s^{-1}$)*
April 2000 until March 2001	137.0	156.7	95.8	68.2	-1.2
April 2001 until March 2002	136.7	129.9	73.7	65.5	23.5
April 2002 until March 2003	118.1	106.2	72.6	40.9	28.1
April 2003 until March 2004	135.3	142.2	91.2	58.3	8.7

Of interest are the 2000-2001 and the 2003-2004 seasons when more precipitation was modelled to have fallen in the catchment than was measured flowing into the lake. The variability in the offset required each year indicates it is related to the method used to relate free water to lake inflows. The assumption that each year the catchment's glaciers are in a state of negative mass balance as set out in equation (16), is likely to be a source of this offset error. Low annual precipitation does not necessarily mean reduced melt of glacial ice. On the contrary, low precipitation is likely to mean increased melt because of the greater likelihood of ice being exposed to the atmosphere as measured in Bolivia (Wagnon et al. 2001). This points towards the inclusion of an ice melt component to SnowSim as being a valuable addition.

7.4.2 Numerical criteria

The numerical verification criteria obtained for SnowSim during the calibration and verification periods are shown in Table 18. The numerical criteria indicate the quality of modelling dropped from the calibration period to the verification period. This is backed up by the ratio of the quantity (1 - *NTD*) for the verification and calibration periods of 1.49. This indicates the model has been over tuned to the calibration year. This could be alleviated to some extent through further calibration to different years. The *CO* criterion value of 0.81 indicates the variation in lake inflows during the verification periods is greater than the

modelled free water. During the calibration period the *CO* criterion value was 0.96. The reduction in the *CO* criterion between the calibration and verification period may be related to the greater range in flow observed during the verification years with the model less able to capture these extreme events. The *NTD* criterion reduced from 0.74 for the calibration period to 0.61 for the verification period.

Table 18. Verification criteria results for SnowSim when applied to the calibration period from April 2002 until March 2003, and when applied to the verification period from April 2000 until March 2002 and April 2003 until March 2004.

Period	*CO*	*NTD*	$\frac{(1\text{-}NTD)VER}{(1\text{-}NTD)CAL}$	*NTM*	*S*	*R*	*A*	*PD*
Calibration	0.96	0.74	1.49	0.96	0.35	0.00	0.14	0.00
Verification	0.81	0.61		0.76	0.43	-0.01	0.22	0.01

For individual years it ranged from 0.53 for the 2001-2002 snow year, to 0.77 for the 2003-2004 snow year, higher than that obtained for the calibration year. This provides an indication of the variability of lake inflows from year to year, and the difficulty in capturing the average conditions through calibration to a single year. As noted earlier, more climate data was available from 2002, coinciding with the improved *NTD* values. At a monthly timescale SnowSim performs considerably better than at the daily level with a value of 0.76 returned for the *NTM* criterion during the verification period. This result is further evidence that the quality of output improves as the temporal resolution increases. Identifying what is an acceptable level of error of output for the desired application may enable selection of an optimum model time scale to ensure that the desired accuracy is achieved. The returned *S* criterion of 0.43 for the verification period indicates that on average, the standard deviation of the error between the modelled free water and the measured lake inflows is less than half the average inflow measurement. The *R* criterion value of -0.01 indicates there is almost no bias in the model to either over or under estimate the lake inflows. As the modelled free water was adjusted with an offset to bring it into line with the measured lake inflows this criterion merely confirms that the offset correction is optimal. This is confirmed by the very low *PD* criterion value of 0.01. The *A* criterion indicates that the absolute error between modelled free water and measured lake inflows is on average 0.3 of the mean measured daily inflows. This can be used to provide an accuracy measurement for the modelled free water output. The

modelled free water on any one day will on average be within 0.3 x 136 $m^3 s^{-1}$ = 41 $m^3 s^{-1}$ of the measured lake inflows.

When compared to the criteria values found for various models applied to the Polish Dunajec River (see Table 11) SnowSim returns comparable results. The *R* and *PD* criteria are much lower for SnowSim, but that follows from the artificial offset applied to the model output. The one criterion that consistently out performs the other models is the *S* criterion. This can be accounted for by the use of 14 day means to the model outputs and measured inflows. This effectively filters the output reducing extreme values and in turn reducing the variance in the modelled to measured errors. The *NTD* and *NTM* criteria of SnowSim when applied to the Lake Pukaki catchment fall within the range of values that the various models returned for the Dunajec River. While a direct comparison is impossible because of the different application catchments, the lack of a propagation component in SnowSim and the need to optimise the offset, the similarity of criteria values returned indicates that SnowSim is of a comparable standard to other snowmelt models used throughout the world in a variety of applications. The quality of the *NTM* criterion in particular is of interest as it provides confidence in the applicability of using SnowSim for providing monthly scale output. Such outputs are potentially valuable for water resource planning and research at a seasonal scale.

7.5 Summary

SnowSim is capable of providing a high quality of snow water equivalent quantity estimation when calibrated using site measurements. Rapid temperature changes cannot be modelled because of temporal scale limitations. This can result in incorrect phase estimation of precipitation. The cumulative nature of snow storage, results in an increase of model to measurement errors as the snow season progresses. Optimal model parameters from point site calibration are not optimal at the catchment scale, highlighting the spatial variability of snow storage processes. Model performance at the catchment scale, whilst not as high as obtained at the point scale, still returns reasonable results once optimised. This is further improved with the modified precipitation distribution system. Difficulty in comparing catchment scale model output to measured lake inflows limits the depth of model analysis. Short wave radiation may on occasion be a significant component of melt energies and on such occasions is capable of being well modelled. The frequency of such events throughout the year is too low for the inclusion of a radiation component in SnowSim to improve results. A magnitude offset between modelled and measured values indicates the model does not capture all hydrological processes in the catchment. Verification of SnowSim (with the new precipitation distribution

system) at the catchment scale over three years of new data suggests output at the monthly scale is of the highest quality.

8 Conclusion

8.1 Summary of main findings

SnowSim, a temperature-index snowmelt model, has been implemented on a GIS and applied to the Lake Pukaki catchment in New Zealand. SnowSim has been tuned independently to a point site within the catchment, and to the catchment as a whole. At the point site, the Rose Ridge climate station near the head of the Murchison valley in the catchment, a model accuracy of *NTD* = 0.93 was returned (where a value of 1 is a perfect model). A lapse rate of 0.005 ^{o}C m^{-1}, a snow/rain temperature threshold of 1.5 ^{o}C and a melt factor ranging from 1 to 5 mm ^{o}C^{-1} d^{-1} was considered optimal. At the catchment scale, a model accuracy of *NTD* = 0.71 was returned once the model was updated with a new precipitation distribution system. A lapse rate of 0.005 ^{o}C m^{-1}, a snow/rain temperature threshold of 2.5 ^{o}C and a melt factor ranging from 1 to 6 mm ^{o}C^{-1} d^{-1} was found to be optimal. These tuned melt factors are in line with those commonly found for other models in other catchments and are less than 50% of those used by SnowSim when applied to the whole of New Zealand by McAlevey (1998). The inclusion of daily measured lapse rates provided no improvement in temperature estimation within SnowSim. This result is considered to be because of the high spatial variability of lapse rates which deems it unlikely that a single lapse rate measurement is accurate for use across the entire catchment. Inclusion of a radiation component in SnowSim provided a slight improvement of model output at the point site, and a significant loss in model accuracy at the catchment scale. At the catchment scale, this result is contrary to that found in continental locations. A likely explanation is the diminished importance of solar radiation to snowmelt in the Lake Pukaki catchment compared to that measured in continental locations. An offset error between model output and measured lake inflows was identified and found to be variable from year to year. Inclusion of an ice melt component in SnowSim is therefore considered necessary to identify if this is the source of the error. Application of the tuned SnowSim to four years of input data returned a general output accuracy of *NTD* = 0.61. A noticeable improvement in model output was found for the years when data from new Meridian Energy climate stations were included in the input, highlighting the value of these stations. The variety of potential outputs from the model is considered valuable for operational and research applications especially when combined with a flow model.

8.2 Limitations

The accuracy of the outputs of an empirically based model is restricted by the inability to capture events and locations that differ from the average. This leads to a spatial and temporal resolution limitation of such a model. As the time scale reduces, the ability of the model to capture the increasing variations also reduces. This is an important consideration when applying SnowSim. The monthly SnowSim outputs can be considered to provide a good level of catchment modelling. At the daily level, severe inaccuracies may potentially occur especially during rapidly changing climatic conditions as commonly occur in the catchment. Even though calculations are performed at a daily level, the model accuracy is least at that resolution. The same is true on a spatial scale. Calculations occur on a 1 km x 1 km grid, but at any one grid the accuracy of the model is at as minimum. At the catchment scale, though, the model accuracy is greatest. These limitations should be considered when utilising model outputs. As far as model portability goes, this research has highlighted the importance of tuning SnowSim to the specific area of interest. The application of SnowSim, prepared at a national scale returns very poor results at either the catchment scale, or the grid square scale. Likewise, the catchment-optimised SnowSim returns poor results at the grid square scale. Applying SnowSim to other catchments or to other point locations without tuning is likely to return model outputs with greatly reduced accuracy. Indeed the accuracy of the application of SnowSim should, as a matter of course, be checked through comparison to river flow records. This leads to the limitation of applying SnowSim only to regions that are gauged.

8.3 Potential applications

SnowSim on a GIS platform provides the opportunity to provide a great deal of useful information not previously available in New Zealand. As well as daily snow storage information (the traditional use of SnowSim), output may include daily precipitation , daily snowfall, daily rainfall, daily temperature, daily sub-freezing regions, daily snow cover regions, daily melt water, daily snow-wetness data. This information may be described in spatial terms (showing regions of difference) as well as in total catchment values, though as discussed above, accuracy reduces as spatial and temporal scales reduce. All this information may be used in a variety of applications. These include the use of catchment snow storage volumes for hydro electric water resource planning. This is a particularly appropriate application as the output is at a catchment scale, maximising model accuracy. Use of time scales greater than daily may also be appropriate further improving available accuracy. The

absence of a need for flow propagation ensures use of output directly from SnowSim without the requirement of a runoff model.

In combination with a runoff model, daily flow rates for catchment can be ascertained. If this is further combined with temperature and precipitation forecasts, flow forecasts for Lake Pukaki can be provided. Such information would be immensely valuable because of the influence Lake Pukaki storage levels have on the electricity spot price market. The increasing value of infrastructure in the catchment because of growth in the tourist industry means that damage from flood events is becoming increasingly expensive. The ability to identify major runoff events, especially those caused by melt conditions, makes SnowSim useful for flood forecast applications, enabling improved flood planning and potentially, flood warnings. Snowmelt and rainfall in the mountains has been identified as primary components of the major September 1878 and December 1995 Waitaki floods (Waugh et al. 1997) suggesting that monitoring of these processes through SnowSim is prudent. For recreational safety, SnowSim may be used to identify a likely state of the mountain snow pack. The snow cover, snow depth, air temperature and snow wetness outputs would all be valuable for assisting with avalanche forecasting efforts currently carried out in the region. In a similar manner, these outputs may be used for the identification of preferential locations for recreational activities. During the ski season, identification of areas where snow is present, with an accompanying preferred air temperature may enable powder skiing opportunities to be identified. For agricultural applications, knowledge of likely depth and extent of the snow pack provides a basis for planning stock holding capacity and likelihood and extent of melt runoff. As well as operational applications, SnowSim provides a valuable tool for understanding snow related processes. The Tasman Glacier being the largest glacier in New Zealand, it presents a unique opportunity to study glacial processes on a large scale. Tuned to the catchment, SnowSim can be utilised as a component of a glacial flow model of the Tasman, not to mention the many other glaciers in the region. Another research application that has far reaching implications is the use of SnowSim to explore variations in snow storage both in the past and in the future. Such research assists with understanding the impacts of changes in climate especially that associated with global warming.

8.4 Future work

High in the list for future SnowSim research needs to be the inclusion of an ice melt component. The annually variable offset to bring the free water outputs in line with the measured lake inflows is currently the greatest failing of the model in the Lake Pukaki

catchment. Looking further afield, tuning SnowSim to other catchments is crucial in understanding the variability of snow processes. To that end, tuning of SnowSim to the Lake Pukaki catchment utilising further years of data and to a higher level of precision is worth undertaking to further improve snow storage modelling accuracy in this region. The identification that New Zealand snow processes are unique within the world provides an opportunity to explore interactions not highlighted in the more common continental studies. The importance of estimation of distribution of precipitation and temperature has been highlighted in this research and shows a clear direction for further investigation. Identifying the key contributors to variability in temperature may enable improved snow storage modelling at point sites. Determining the correct phase of precipitation is crucial, especially during major falls. At the catchment scale precipitation distribution becomes more important. The need to prepare a new precipitation surface for this study highlights the poor state of knowledge of precipitation in the catchment. While fitting a surface to match outputs is a valuable approach, extensive precipitation measurements, mirroring those taken in the 1970's in the Whitcombe and Rakaia catchments need to be obtained for the upper Lake Pukaki region. Lack of this data in such an economically important catchment is surprising and needs to be addressed as soon as possible. The assumption that daily precipitation distribution is related to the annual average precipitation distribution prevents accurate precipitation estimation during easterly and southerly conditions. A relationship between precipitation distribution and synoptic condition is likely to provide model outputs closer to reality. Such work would also enable the identification of the importance of southerly conditions to snow storage. Changing the timescale of the model calculations to hourly is likely to provide an improvement in modelling. The rapid change possible in precipitation and temperatures frequently resulted in the daily mean temperature being quite different to the temperature experienced during the periods of precipitation. The importance of turbulent fluxes to snowmelt may mean that consideration of wind flow in SnowSim could provide a step up in output accuracy. Use of large scale synoptic indices may be also be of value as they provide information about wind speed and direction, and air temperature and pressure, all significant components of the turbulent melt fluxes (Moore and Owens 1984a).

Of interest is the variety of lapse rates measured throughout the year. Consideration of air pressures should provide a means of establishing more accurate distributed air temperature estimation. Satellite derived imagery provides potential for both enhancing SnowSim and verifying output. Daily snow cover maps of the catchment are available from NASA providing a means of directly comparing SnowSim output to measured data. The results of

such a comparison may then be used to feedback into the model. Satellite imagery may also be used to investigate temperature distributions on both a temporal and spatial scale. This may be used either to determine an improved temperature distribution process, or be used directly as an input to the model.

9 References

Alam, F. C. K. (1972). Distribution of precipitation in mountainous areas of West Pakistan. In: Distribution of precipitation in mountainous areas, Geilo, Norway, World Meteorological Organisation **22**.

Anderson, B. (2004). Response of the Franz Josef Glacier to climate change. Unpub. Ph.D. thesis, Department of Geography, University of Canterbury, Christchurch.

Anderson, E. A. (1973). National Weather Service Forecast System - Snow accumulation and ablation model, NOAA Technical Memorandum NWS HYDRO-17.

Anderton, P. W. (1974). Estimation of snow storage and melt in the catchment of Lake Pukaki. In: New Zealand Hydrological Society Symposium Proceedings, Dunedin.

Anderton, P. W. (1975). Tasman Glacier 1971-73. Hydrological research: Annual report No 33, Ministry of Works and Development.

Archer, A. C. (1970). Studies of snow characteristics in the north-eastern Ben Ohau Mountains, New Zealand. Journal of Hydrology (NZ) **9**(1): 4-21.

Arnold, N. S., Willis, I. C., Sharp, M. J., Richards, K. S. and Lawson, W. J. (1996). A distributed surface energy-balance model for a small valley glacier. 1. Development and testing for Haut Glacier d'Arolla, Valais, Switzerland. Journal of Glaciology **42**(140): 77-89.

Baker, D., Escher-Vetter, H., Moser, H. and Oerter, H. (1982). A glacier discharge model based on results from field studies of energy balance, water storage and flow. In: Hydrological Aspects of Alpine and High Mountain Areas, Exeter, IAHS **138:** 103-112.

Barringer, J. R. F. (1989). A variable lapse rate snowline model for The Remarkables, Central Otago, New Zealand. Journal of Hydrology (NZ) **28**(1): 32-46.

Baumgartner, M. F., Spreafico, M. and Weiss, H. W. (2000). Operational snowmelt runoff forecasting in the Central Asian mountains. In: Remote sensing and hydrology, Santa Fe, New Mexico, USA, IAHS.

Bergström, D. (1975). The development of a snow routine for HBV-2 Model. Nordic Hydrology **6**(2).

Bintanja, R. and Reijmer, C. H. (2001). Meteorological conditions over Antarctic blue-ice areas and their influence on the local surface mass balance. Journal of Glaciology **47**(156): 37-50.

Bowden, D. T. (1994). Application of a snowmelt-runoff model to the Lake Pukaki basin, Mount Cook. Unpub. M.Sc. thesis, Department of Geography, University of Canterbury, Christchurch.

Braithwaite, R. J. (1990). A simple energy-balance model to calculate ice ablation at the margin of the Greenland ice sheet. Journal of Glaciology **36**(123): 222-228.

Braun, L. (1991). Modelling of the snow-water equivalent in the mountain environment. In: Snow, Hydrology and Forests in High Alpine Areas, Vienna, IAHS **205:** 3-17.

Broadbent, M. (1974). Seismic and gravity surveys on the Tasman Glacier: 1971-2. Geophysics division Report No. 91. Wellington, Department of Scientific and Industrial Research.

Brock, B. W., Willis, I. C. and Sharp, M. J. (2000a). Measurement and parameterization of albedo variations at Haut Glacier d'Arolla, Switzerland. Journal of Glaciology **46**(155): 675-688.

Brock, B. W., Willis, I. C., Sharp, M. J. and Arnold, N. S. (2000b). Modelling seasonal and spatial variations in the surface energy balance of Haut Glacier d'Arolla, Switzerland. Annals of Glaciology **31**: 53-62.

Broderick, T. N. (1891). Report on the Tasman Glacier. Appendix to the Journal of the House of Representatives of New Zealand, Session 2 **1**(C1-A, Appendix 4): 39-43.

Broderick, T. N. (1906). Glacier Movements. Appendix to the Journal of the House of Representatives of New Zealand, Session 2 **1**(C-1A, Appendix 2): 16-17.

Burnash, R. J. C., Ferral, R. L. and McGuire, R. A. (1973). A generalized streamflow simulation system. Sacramento, California, Joint Federal-State River Forecast Center**:** 204 pp.

Calver, A. (1988). Calibration, sensitivity and validation of a physically-based rainfall-runoff model. Journal of Hydrology **103**(1-2): 103-115.

Carter, B. and MacGibbon, J. (2003). Wool. A history of New Zealands wool industry. Wellington, Ngaio Press.

Cazorzi, F. and Dalla-Fonatana, G. (1986). Improved utilisation of maximum and minimum daily temperature in snowmelt modelling. In: Modelling Snowmelt-induced Processes, Budapest, Hungary, IAHS **155:** 141-150.

Cazorzi, F. and Dalla-Fontana, G. (1996). Snowmelt modeling by combining air temperature and a distributed radiation index. Journal of Hydrology **181**: 169-187.

Charbonneau, R., Fortin, J. P. and Morin, G. (1977). The CEQUEAU model: description and examples of its use in problems related to water resources management. Bulletin des sciences hydrologiques, AIHS **22**(1): 193-203.

Chinn, T. J. (2001). Distribution of the glacial water resources of New Zealand. Journal of Hydrology (NZ) **40**(2): 139-187.

Chinn, T. J. and Whitehouse, I. E. (1980). Glacier snow line variations in the Southern Alps, New Zealand. In: International workshop on the World Glacier Inventory, Rideralp, Switzerland, IAHS **126:** 219-228.

Claridge, D. (1983). A geophysical study of the termini of the Mount Cook National Park glaciers. Unpub. M.Sc. thesis, Geology, University of Auckland, Auckland.

Coates, G. (2002). The rise and fall of the Southern Alps. Christchurch, Canterbury University Press.

Cotton, W. R., Pielke Sr., R. A., Walko, R. L., Liston, G. E., Tremback, C. J., Jiang, H., McAnelly, R. L., Harrington, J. Y., Nicholls, M. E., Carrio, G. G. and McFadden, J. P. (2003). RAMS 2001: Current status and future directions. Meteorology and Atmospheric Physics **82**: 5-29.

Cutler, E. S. (2002). High elevation seasonal snow melt at the Tasman Glacier neve, Southern Alps, NZ. Unpub. M.Sc. thesis, Geography, University of Otago, Dunedin.

De Latour, S. M. A. (1999). Seasonal snow storage in hydro catchments and atmospheric circulations. Unpub. M.Sc. thesis, Geography, University of Otago, Dunedin.

DLS (1986). The Story of Mount Cook National Park. Wellington, Department of Lands and Survey.

Dozier, J. (1980). A clear-sky spectral solar radiation model for snow-covered mountainous terrain. Water Resources Research **16**(4): 709-718.

Dubayah, R. and Rich, P. M. (1995). Topographical solar radiation models for GIS. International Journal of Geographical Information Systems **9**(4): 405-419.

Duguay, C., R. (1993). Radiation modelling in mountainous terrain review and status. Mountain Research and Development **13**: 339-357.

Fitzharris, B. (1978). Problems in estimating snow accumulation with elevation on New Zealand mountains. Journal of Hydrology (NZ) **17**(2): 78-90.

Fitzharris, B. (1992). The 1992 electricity crisis and the role of climate and hydrology. New Zealand Geographer **48**(2): 79-83.

Fitzharris, B. (1997). Snowing the new electricity market. New Zealand Geographical Society Conference Series **19**: 410-412.

Fitzharris, B. (2004). Snow accounts for New Zealand. Report prepared for NIWA, Ministry for the Environment, and Statistics New Zealand, Climate Management Centre, Department of Geography, University of Otago.

Fitzharris, B. and Garr, G. E. (1995). Simulation of past variability in seasonal snow in the Southern Alps, New Zealand. Annals of Glaciology **21**: 377-382.

Fitzharris, B. B. and McAlevey, B. (1999). Remote sensing of seasonal snow cover in the mountains of New Zealand using satellite imagery. Geocarto International **14**(3): 33-42.

Givone, C. and Meignien, X. (1990). Influence of topography on spatial distribution of rain. In: Hydrology of mountainous areas, Czechoslovakia, IAHS **190:** 57-65.

Goldthwaite, R. P. and McKellar, I. C. (1962). New Zealand glaciology. In: Antarctic Research. Washington, American Geophysical Union**:** 209-216.

Gómez-Landsea, E. and Rango, A. (2002). Operational snowmelt runoff forecasting in the Spanish Pyrenees using the snowmelt runoff model. Hydrological Processes **16**: 1583-1591.

Gotleib, L. (1980). A general runoff model for snowcovered and glacierized basins. In: 6th Nordic Hydrological Conference Proceedings, Vemdalen, Sweden.

Griffiths, G. A. and McSaveney, M. J. (1983). Distribution of mean annual precipitation across some steepland regions of New Zealand. New Zealand Journal of Science **26**: 197-209.

Halstead, I., Tuck, E. and Curry, B. (2003). Waitaki catchment snow report 2002/03 season, NIWA.

Hay, J. E. and Fizharris, B. B. (1988). A comparison of the energy-balance and bulk-aerodynamic approaches for estimating glacier melt. Journal of Glaciology **34**(117): 145-153.

Heather, B. D. and Robertson, H. A. (1996). The field guide to the birds of New Zealand. Auckland, Viking.

Henderson, R. D. and Thompson, S. M. (1999). Extreme rainfalls in the Southern Alps of New Zealand. Journal of Hydrology (NZ) **38**(2): 309-330.

Hochstein, M. P., Watson, M. I., Malengeau, B., Nobes, D. C. and Owens, I. F. (1998). Rapid melting of the terminal section of the Hooker Glacier (Mt Cook National Park, New Zealand). N.Z. Journal of Geology and Geophysics **41**: 203-218.

Hock, R. (1999). A distributed temperature-index ice- and snow melt model including potential direct solar radiation. Journal of Glaciology **45**(149): 101-111.

Hock, R. (2003). Temperature index melt modelling in mountain areas. Journal of Hydrology **282**: 104–115.

Hock, R. (2004). Glacier melt and discharge: A review of processes and their modelling (in preparation).

Hock, R. and Noetzli, C. (1997). Areal melt and discharge modelling of Storglaciären, Sweden. Annals of Glaciology **24**: 211-216.

Hogg, I. (1982). Summer heat and ice balances on Hodges Glacier, South Georgia, Falkland Islands Dependencies. Journal of Glaciology **28**(99): 221-239.

Ishikawa, N., Owens, I. F. and Sturman, A. P. (1992). Heat balance characteristics during fine periods on the lower parts of the Franz Josef Glacier, South Westland, New Zealand. International Journal of Climatology **12**: 397-410.

Islam, M. N. (2001). Hydrological modelling of glacierized mountain watersheds in the Southern Alps, New Zealand. Unpub. Ph.d. thesis, Environmental Management and Design Division, Lincoln University, Lincoln.

Kelliher, F., Owens, I. F., Sturman, A. P., Byers, J. N., Hunt, J. E. and McSeveny, T. M. (1996). Radiation and ablation on the neve of Franz Josef. Journal of Hydrology (NZ) **35**(1): 131-150.

Kelliher, F. M. and Jackson, R. (2001). Evaporation and the water balance. In: The physical environment. A New Zealand perspective. A. Sturman and R. Spronken-Smith. Victoria, Oxford University Press**:** 206-217.

King, M. (2003). The Penguin history of New Zealand. Auckland, The Penguin Group.

Kirkbride, M. P. (1995). Relationships between temperature and ablation on the Tasman Glacier, Mount Cook National Park, New Zealand. New Zealand Journal of Geology and Geophysics **38**: 17-27.

Kumar, L., Skidmore, A. K. and Knowles, E. (1997). Modelling topographic variation in solar radiation in a GIS environment. International Journal of Geographical Information Science **11**(5): 475-497.

Kustas, W. P. and Rango, A. (1994). A simple energy budget algorithm for the snowmelt runoff model. Water Resources Research **30**(5): 1515-1527.

Lang, H. and Braun, L. (1988). On the information content of air temperature in the context of snow melt estimation. In: Hydrology of mountainous areas, Czechoslovakia, IAHS **190:** 347-354.

Leathwick, J. R., Wilson, G. and Stephens, R. T. T. (1998). Climate surfaces for New Zealand. Hamilton, Manaki Whenua - Landcare Research.

Leavesley, G. H., Lichty, R. W., Troutman, B. M. and Saindon, L. G. (1983). Precipitation-runoff modelling system: User's manual., U.S. Geological Survey Water Resources Investigations Report B3-4238.

Marr, C. (2001). James MacKenzie. In: Rural Canterbury. G. Cant and R. Kirkpatrick. Wellington, Daphne Brasell Associates Ltd.

Marsh (1999). Snowcover formation and melt: recent advances and future prospects. Hydrological Processes **13**: 2117-2134.

Martin, J. E., Ed. (1998). People, Politics and Power Stations. Electric power generation in New Zealand 1880 - 1998. Wellington, Electricity Corporation of New Zealand.

Martinec, J. (1975). Snowmelt-runoff model for streamflow forecasts. Nordic Hydrology **6**: 145-154.

Martinec, J. and Rango, A. (1986). Parameter values for snowmelt runoff modelling. Journal of Hydrology **84**: 197-219.

McAlevey, B. (1998). A distributed seasonal snow model for New Zealand. Unpub. M.Sc. thesis, Geography, University of Otago, Dunedin.

McKerchar, A. I. and Pearson, C. P. (1997). Quality of long flow records for New Zealand rivers. Journal of Hydrology (NZ) **36**(2): 15-41.

McKinnon, M., Ed. (1997). New Zealand Historical Atlas. Auckland, Bateman.

McSaveney, M. J., Chinn, T. J., Horrell, G. A. and Longson, C. K. (1978). The measured distribution of precipitation across the Southern Alps. Report No WS 71. Christchurch, Ministry of Works and Development.

Moon, G. (1992). A field guide to New Zealand birds. Auckland, Reed Books.

Moore, R. D. and Owens, I. F. (1984a). Controls on advective snowmelt in a maritime alpine basin. Journal of Climate and Applied Meteorology **23**(4): 135-142.

Moore, R. D. and Owens, I. F. (1984b). Modelling alpine snow accumulation and ablation using daily climate observations. Journal of Hydrology (NZ) **23**(2): 73-83.

Morgenstern, U. and Thomson, J. (2003). Ice core drilling on Tasman Glacier. New Zealand Alpine Journal **55**: 128-129.

Munro, D. S. and Young, G. J. (1982). An operational net shortwave radiation model for glacier basins. Water Resources Research **18**(2): 220-203.

Neale, S. (1996). Measuring and modelling snow melt in a New Zealand alpine environment. Unpub. M.Sc. thesis, Geography, University of Otago, Dunedin.

Neale, S. M. and Fitzharris, B. (1997). Energy balance and synoptic climatology of a melting snowpack in the Southern Alps, New Zealand. International Journal of Climatology **17**: 1595-1609.

Ngai Tahu Report (1991). Wellington, Waitangi Tribunal. **2**.

NZMS (1985). New Zealand Annual Rainfall: Normals 1951-1980. New Zealand Meteorological Service Miscellaneous Publication. Wellington, N.Z., New Zealand Meteorological Service. **175:** part 6(i).

Oerlemans, J. and Klok, E. J. (2002). Energy balance of a glacier surface: analysis of automatic weather station data from the Morteratschgletscher, Switzerland. Arctic and Alpine research **34**(2): 477-485.

Owens, I., McGregor, G. and Prowse, T. (1983). Snow avalanche hazards in the Canterbury high country. In: Canterbury at the crossroads. R. D. Bedford and A. P. Sturman. Christchurch, New Zealand Geographical Society**:** 166-181.

Paterson, W. S. B. (1994). The Physics of Glaciers. Oxford, Butterworth-Heinemann.

Pawson, E. (2001). Transforming the environment. In: Rural Canterbury: celebrating its history. G. Cant and R. Kirkpatrick. Wellington, Daphne Brasell Associates Ltd**:** 121-139.

Payer, T., Leber, D., Haeusler, H., Brauner, M. and Wangda, D. (2003). Snow/ice melt precipitation runoff modelling of glaciers in the Bhutan Himilaya. Geophysical Research Abstracts **5**(10227).

Pellicciotti, F. (2004). Glacial melt modelling (in preparation). Unpub. Ph.d. thesis, Department of Geography, University of Cambridge, Cambridge.

Peters, E. J. (1996). An integrated approach to inflow forecasting for reservoir management: The upper Waitaki. Unpub. Ph.d. thesis, Department of national resources engineering, Lincoln University, Lincoln.

Pomeroy, J. W., Gray, D. M., Shook, K. R., Toth, B., Essery, R. L. H., Pietroniro, A. and Hedstrom, N. (1998). An evaluation of snow accumulation and ablation processes for land surface modelling. Hydrological Processes **12**: 2339-2367.

Prowse, T. D. and Owens, I. F. (1982). Energy balance over melting snow, Craigeburn Range. Journal of Hydrology (NZ) **21 no2**: 133-147.

Purdie, J. (1996). Ice loss at the terminus of the Tasman Glacier. Unpub. M.Sc. thesis, Department of Geography, University of Otago, Dunedin.

Purdie, J. and Fitzharris, B. (1999). Processes and rates of ice loss at the terminus of Tasman Glacier, New Zealand. Global and Planetary Change **22**: 79-91.

Qobilov, T., Pertziger, F., Vasilina, L. and Baumgartner, M. F. (2000). Operational technology for snow-cover mapping in the Central Asian mountains using NOAA-AVHRR data. In: Remote sensing and hydrology, Santa Fe, New Mexico, USA, IAHS **267:** 76-80.

Quick, M. C. and Pipes, A. (1976). A combined snowmelt and rainfall runoff model. Canadian Journal of Civil Engineering **3**(3): 449-460.

Reed, A. W. and Calman, R. (2004). Reed book of Maori mythology. Auckland, Reed Publishing Ltd.

Ruddell, A. R. (1995). Recent glacier and climate change in the New Zealand Alps. Unpub. Ph.D. thesis, School of Earth Sciences, University of Melbourne, Melbourne.

Ryan, A. P. (1987). The climate and weather of Canterbury (including Aorangi). Wellington, New Zealand Meteorological Service.

Salinger, M. J. (1979). Climatic regions of New Zealand based on cluster techniques. New Zealand Statistician **14**: 26-34.

Seidel, K. and Martinec, J. (2004). Remote sensing in snow hydrology. Runoff modelling, effect of climate change. Chichester, UK, Praxis Publishing Ltd.

Sheridan, M. (1995). Dam dwellers - end of an era - living with hydro-electricity development in the Waitaki Valley and MacKenzie Country. Twizel, Sheridan Press.

Sinclair, M. (1994). A diagnostic model for estimating orographic precipitation. Journal of applied meteorology **33**: 1163-1175.

Skaar, E. (1972). Distribution of precipitation in the Sognefjord region. In: Distribution of precipitation in mountainous areas, Geilo, Norway, World Meteorological Organisation **2:** 171-185.

Skinner, B. E. (1964). Measurement of twentieth century ice loss on the Tasman Glacier, New Zealand. N.Z. Journal of Geology and Geophysics **7**(4): 796-803.

Sturman, A. P. (1986). Atmospheric circulation and monthly precipitation distribution in Canterbury, New Zealand. Weather and Climate **6**: 7-14.

Sugawara, M. (1979). Automatic calibration of the TANK Model. Hydrological Sciences Bulletin **24**(3).

Suggate, R. P., Ed. (1978). The Geology of New Zealand. Wellington, E.C.Keating.

Swanson, R. H. (1970). Local snow distribution is not a function of local topography under continuous tree cover. Journal of Hydrology (NZ) **9**(2): 292-298.

Swift, L. W. (1976). Algorithm for solar radiation on mountain slopes. Water Resources Research **12**(1): 108-112.

Thompson, C. S. (1985). Maps of rainfall parameters for New Zealand. N.Z.M.S. misc. pub. No 187. Wellington, New Zealand Meteorological Service.

Thompson, S. M. (1997). Snow storage estimation for hydro-electricity catchments from monitored rainfall and river flow. Wellington, NIWA.

Thompson, S. M. and Adams, J. E. (1979). Suspended load in some major rivers of New Zealand. In: Physical Hydrology. New Zealand Experience. D. L. Murray and P. Ackroyd, New Zealand Hydrological Society.

Tomlinson, A. and Sanson, J. (1994). Rainfall normals for New Zealand 1961 - 1990. NIWA science and technology series No. 3. Wellington, NIWA.

Turcan, J. (1981). Empirical-Regressive Forecasting Runoff Model. In: Proceedings of Conference VUVH, Bratislava.

Varley, M. J., Beven, K. J. and Oliver, H. R. (1996). Modelling solar radiation in steeply sloping terrain. International Journal of climatology **16**: 93-104.

Von Haast, H. F. (1948). The life and times of Sir Julius von Haast. Wellington, H.F. von Haast.

Von Lendenfeld, R. (1884). der Tasman-Glestscher und seine Umrandung. Mitteilungen aus justus perthes' geographischer anstalt **16**.

Wagnon, P., Ribstein, P., Francou, B. and Sicart, J. E. (2001). Anomolous heat and mass budget of Glacier Zongo, Bolivia, during the 1997/98 El Nino year. Journal of Glaciology **47**(156): 21-28.

Wallace, S. J. (2001). Mapping glacial landforms in the Pukaki and Tekapo lake basins. Unpub. P.G.Dip.Sc. thesis, Geography, University of Otago, Dunedin.

Waugh, J., Freestone, H. and Lew, D. (1997). Historic floods and droughts in New Zealand. In: Floods and droughts: the New Zealand experience. M. P. Mosley and C. P. Pearson. Wellington, New Zealand Hydrological Society**:** 29-50.

Whitehouse, I. E. (1988). Geomorphology of the central Southern Alps, New Zealand: the interaction of plate collision and atmospheric circulation. Zeitschrift fur Geomorphologie. Supplementband **69**: 105-116.

Wigley, H. (1979). The Mount Cook way - the first fifty years of the Mount Cook Company. Auckland, Collins.

Willis, I. C., Arnold, N. S. and Brock, B. W. (2002). Effect of snowpack removal on energy balance, melt and runoff in a small supraglacial catchment. Hydrological Processes **16**: 2721-2749.

WMO (1982). WMO project for the intercomparison of conceptual models of snowmelt runoff. In: Hydrological aspects of alpine and high mountain areas, Exeter, IAHS **138:** 193-202.

WMO (1986). Intercomparison of models of snowmelt runoff, WMO-No.646. Geneva, World Meteorological Organization.

Woo, M.-k. and Dubreuil, M.-A. (1985). Empirical relationships between dust content and arctic snow albedo. Cold region science and technology **10**: 125-132.

Zimmermann, N. (2001). Arc/Info - AMLs. Birmensdorf, Swiss Federal Research Institute WSL.http://www.wsl.ch/staff/niklaus.zimmermann/programs/aml.html#1